Journal of Human Evolution 206 (2025) 103730

Contents lists available at ScienceDirect

Journal of Human Evolution

journal homepage: www.elsevier.com/locate/jhevol

Reconstruction of the locomotor repertoire of early primates in the light of astragalar and calcaneal shape

Oriol Monclús-Gonzalo [a, *], David M. Alba [a], Anne-Claire Fabre [b, c, d], Judit Marigó [e, a, *]

[a] Institut Català de Paleontologia Miquel Crusafont (ICP-CERCA), Universitat Autònoma de Barcelona, Edifici ICTA-ICP, c/ Columnes s/n, 08193 Cerdanyola del Vallès, Barcelona, Spain
[b] Naturhistorisches Museum Bern, 3005 Bern, Switzerland
[c] Institute of Ecology and Evolution, University of Bern, 3012 Bern, Switzerland
[d] Life Sciences Department, Vertebrates Division, Natural History Museum, London SW7 5BD, UK
[e] Universitat Autònoma de Barcelona, Departament de Geologia, 08193 Cerdanyola del Vallès, Barcelona, Spain

ARTICLE INFO

Article history:
Received 7 June 2024
Accepted 23 June 2025
Available online xxx

Keywords:
Early euprimates
Plesiadapiforms
Astragalus
Calcaneus
Functional morphology
Locomotion

ABSTRACT

The locomotor behavior of the earliest euprimates is key to our understanding of the origin and early diversification of the group. Postcranial traits suggest that major locomotor shifts occurred during the early evolution of this clade. Two tarsal bones, the astragalus and the calcaneus, have been extensively studied because of their functional importance. To provide further insights into early primate evolution, we use a three-dimensional high-density sliding semilandmark geometric morphometric approach to quantify tarsal shape on an extensive (936) sample of astragali and calcanei from extant and extinct primates as well as other euarchontans. We reconstruct the locomotor repertoire for a total of 37 extinct taxa, representing all major Paleogene primate groups, using a partial least squares regression between astragalar/calcaneal shape and locomotor percentages compiled from the literature. Our results concur with previous studies and confirm that the astragalar/calcaneal shape exhibits a strong functional signal, allowing to accurately estimate the locomotor repertoire of extinct species. Locomotor estimates based on fossils indicate that early euprimates displayed a diverse array of locomotor repertoires comparable to extant species, highlighting cases of convergent evolution among distantly related groups. Locomotor differences between plesiadapiforms and early euprimates include a greater use of leaping by the latter, suggesting that the origin and early diversification of euprimates involved an important locomotor shift. Based on tarsal shape, this study improves our understanding of early primate locomotion and evolution, providing the most extensive taxonomic scope to date.

1. Introduction

Primates of modern aspect (or euprimates, sensu Hoffstetter, 1977) are characterized by a group of distinct traits associated with grasping (e.g., nails instead of claws, opposable hallux, and pollex), improvement in the visual apparatus (e.g., postorbital bar, convergent orbits, and larger and more complex brains than other mammals), leaping (e.g., elongation of the tarsus), and frugivory (bunodont cusps and broad taloned basins; Cartmill, 1974, 1992; Szalay et al., 1987; reviewed in Silcox et al., 2015). The earliest euprimates, first recorded at the beginning of the Eocene (excluding the enigmatic *Altiatlasius* from the late Paleocene; Sigé et al., 1990), are represented by adapiforms and omomyiforms, which rapidly expanded across Eurasia and North America (Smith et al., 2006; Beard, 2008; Rose et al., 2011; Morse et al., 2019). Adapiforms are regarded as a paraphyletic assemblage of stem strepsirrhines (Godinot, 1998; Marigó et al., 2016; Ni et al., 2016). Compared with omomyiforms, adapiforms are generally larger and have longer snouts, smaller eye sockets (indicating a diurnal lifestyle), and dentitions suggesting mainly folivorous or frugivorous diets (Gunnell et al., 2008). Based on available partial skeletons and abundant isolated postcranial remains, most adapiforms are considered to have been generalized arboreal quadrupeds with some resemblances to extant lemurs (e.g. Gregory, 1920; Decker and Szalay, 1974; Dagosto, 1983; Rose and Walker, 1985; Covert, 1988; Gebo et al., 1991; Marigó et al., 2016, 2020; Llera Martín

* Corresponding authors.
E-mail addresses: oriol.monclus@icp.cat (O. Monclús-Gonzalo), judit.marigo@uab.cat (J. Marigó).

https://doi.org/10.1016/j.jhevol.2025.103730

et al., 2022; Monclús-Gonzalo et al., 2023). Omomyiforms, on the other hand, are an extinct assemblage of stem haplorhines or stem tarsiiformes whose exact relationships with either tarsiers or anthropoids are still a matter of debate (Rosenberger and Preuschoft, 2012; Ni et al., 2013, 2016). They are usually referred to as 'tarsier-like', but current evidence indicates that omomyiforms differed substantially from tarsiers in their postcranial skeleton and likely occupied an ecological niche more similar to that of extant cheirogaleids and some galagids (Godinot and Dagosto, 1983; Gebo, 1988; Dagosto et al., 1999; Dunn et al., 2006; Gunnell et al., 2008).

Anthropoids are also first recorded during the Eocene. The oldest group, eosimiids, from the middle Eocene of Asia (and probably afrotarsiids; Chaimanee et al., 2012, 2024), are usually regarded as the most basal stem anthropoids, exhibiting a mixture of primitive haplorrhine features together with more derived anthropoid ones (Beard et al., 1994, 1996; Gebo et al., 2000, 2001; Beard and Wang, 2004; Chaimanee et al., 2012, 2024; but see Gunnell and Miller, 2001; Miller et al., 2005). Another group of likely stem anthropoids, the amphipithecids, also exhibit a combination of primitive and derived traits, as well as some resemblances to adapiforms, which have raised doubts on their inclusion within the Anthropoidea (Gunnell and Ciochcon, 2008), despite being favored by most authors (Kay et al., 2004; Beard et al., 2009; Marivaux et al., 2010; Coster et al., 2013; Jaeger et al., 2020; Chaimanee et al., 2024). Conversely, early anthropoids from the late Eocene and early Oligocene of Afro-Arabia (e.g., parapithecids and proteopithecids) display more clear-cut anthropoid synapomorphies (Fleagle and Kay, 1988; Simons and Seiffert, 1999; Seiffert et al., 2000, 2004, 2005). Early anthropoids generally differ from omomyiforms and most adapiforms in possessing adaptations for a more quadrupedal locomotion with higher utilization of larger and more horizontal substrates, thus departing from the more active grasp-leaping behavior exhibited by extant lemuriforms and tarsiers (Gebo, 1986; Dagosto, 1990; Kay et al., 1997).

There is a relatively diverse group of placentals, from the Paleocene and Eocene, which are usually regarded either as broadly ancestral to or as a paraphyletic assemblage of stem primates: plesiadapiforms (Silcox et al., 2007). Despite their considerable taxonomic diversity (including more than 120 species classified into 10 families; Silcox et al., 2017; Crowell et al., 2024), relatively little is known about the postcranial anatomy of these animals, except for a few partial skeletons (Bloch and Boyer, 2002, 2007; Bloch et al., 2007; Chester et al., 2017, 2019, 2025; Boyer and Gingerich, 2019) and some isolated bones (Chester et al., 2015), thus hampering efforts to reach a comprehensive understanding of their locomotor diversity. Although most authors agree that plesiadapiforms were arboreal (Szalay and Decker, 1974; Szalay and Dagosto, 1980; Szalay and Drawhorn, 1980; Beard, 1989; Godinot and Beard, 1991; Rose, 1994; Kirk et al., 2008; Chester et al., 2015, 2017, 2019), given that they lack most euprimate-like traits associated with locomotor behavior, their locomotor repertoire has been inferred to differ substantially from that of euprimates. Only *Carpolestes simpsoni* has been shown to exhibit adaptations related to grasping small branches, such as an opposable hallux with a nail instead of a claw (Bloch and Boyer, 2002). Altogether, the current evidence suggests that plesiadapiforms were probably as ecologically diverse as they were taxonomically, occupying a wide array of ecological niches, as defined by divergent dietary and locomotor adaptations (Bloch and Boyer, 2007; Prufrock et al., 2016; López-Torres et al., 2017; Silcox et al., 2017).

To explain the acquisition of euprimate distinct traits, several (not mutually exclusive) adaptive hypotheses have been proposed. These include the visual predation hypothesis (Cartmill, 1974, 1992), the angiosperm coevolution hypothesis (Sussman and Raven, 1978; Sussman, 1991; Sussman et al., 2012), and the grasp-leaping hypothesis (Szalay and Delson, 1979; Szalay and Dagosto, 1980; Kemp, 2024a, 2024b). Both the visual predation and the angiosperm coevolution hypotheses focus on selective pressures derived from the utilization of the fine branch milieu to access food resources, either small animal prey or angiosperm products. This led to their unification by Rasmussen (1990) based on the didelphid *Caluromys* as an extant analogue of the earliest euprimates. Conversely, the grasp-leaping hypothesis proposes that the modern primate morphotype, including the features related to the visual apparatus, is explained by the ability of the last common ancestor (LCA) of euprimates to engage in active leaping behavior (Szalay and Delson, 1979; Szalay and Dagosto, 1980). Increasing evidence from the last two decades (e.g., Bloch and Boyer, 2002; Bloch et al., 2007; Chester et al., 2015) indicates that distinctive euprimate traits did not appear simultaneously but in a stepwise manner. Accordingly, the origin of euprimates should be considered a protracted process rather than an abrupt event, allowing for the former adaptive hypotheses to fit into different stages along early primate (and euprimate) evolution (Gebo, 2004; Dagosto, 2007; Sargis et al., 2007; Silcox and López-Torres, 2017). Therefore, inferences about plesiadapiform locomotor abilities, irrespective of their exact phylogenetic position, are necessary to better understand the origin and early diversification of euprimates.

Among other elements of the postcranial skeleton, the hindfoot, composed by two tarsal bones (the astragalus and the calcaneus), has been extensively studied. This is because many astragalar and calcaneal features are informative about the locomotor adaptations of extinct species, given their critical role in important functional aspects of the foot. These include the leverage of many muscles and the mobility at the ankle joint and more distal tarsal joints, where most of the inversion and eversion of the foot, as well as its supination and pronation, occurs (Su and Zeiniger, 2022). In addition, the type of foot posture, defined by the location of the fulcrum of the foot (i.e., the position in which the lever comprised by the foot pivots), also influences the morphology of these two bones, particularly the calcaneus (Morton, 1924; Moyà-Solà et al., 2012). Tarsi-fulcrumators, including extant strepsirrhines and tarsiers, are characterized by a fulcrum located more proximally, at the distal part of the tarsus, resulting in increased grasping capabilities. However, the load arm of the lever is reduced and must be compensated via elongation of the midtarsal region. Conversely, metatarsi-fulcrumators, comprising extant anthropoids and most nonprimate mammals, exhibit a fulcrum that is placed more distally, in the metatarsal heads or the phalanges, and thus they do not require further elongation of the tarsus (Morton, 1924).

The relationship between the shape of these two bones and locomotor behavior, as a result of the strong functional signal embedded in their morphology, has been extensively addressed, mostly from a descriptive and qualitative perspective (e.g., Gregory, 1920; Decker and Szalay, 1974; Szalay and Decker, 1974; Walker, 1974; Conroy and Rose, 1983; Rose and Walker, 1985; Gebo, 1986, 1988; Covert, 1988; Dagosto, 1988, 1990; Gebo et al., 2000; Pina et al., 2011) or using morphometric approaches based on linear measurements and indices (e.g., Gebo and Simons, 1987; Gebo et al., 1991, 2001, 2012; Marivaux et al., 2003, 2010, 2011; Boyer et al., 2010, 2015; Moyà-Solà et al., 2012; Boyer and Seiffert, 2013; Seiffert et al., 2015; Dunn et al., 2016; Marigó et al., 2016; Yapuncich et al., 2017, 2019; Yapuncich and Granatosky, 2021). Only a handful of studies have tackled this question utilizing multivariate methods (Parr et al., 2014; Boyer et al., 2017a; Püschel et al., 2017, 2018, 2020; Llera Martín et al., 2022), albeit employing simplified locomotor categories that do not adequately represent

the complex spectrum of primate locomotor repertoires. Here, we quantitatively investigate the correlation between astragalar/calcaneal shape and locomotor behavior in extant primates to identify the main morphological correlates that span the extensive behavioral spectrum exhibited by this group (Bock and Von Wahlert, 1965). In particular, we use a three-dimensional (3D) high-density sliding semilandmark geometric morphometric approach to quantify the shape of the astragalus and the calcaneus. In addition, we use percentages of locomotor behaviors in extant primate species to quantify their locomotor repertoires and infer the locomotor repertoire of extinct primate species, which enables us to discuss the locomotor behavior exhibited by primates in the context of their early evolutionary history. As shown by previous studies (see references mentioned previously), we hypothesize that the shape of these two tarsal bones exhibits a strong correlation with locomotion so that they can be used as predictors to reconstruct the locomotor behavior of extinct primate species. Both the astragalus and the calcaneus are relatively well known for several Paleogene primate species (Yapuncich et al., 2022: Fig. 12.1) and hence are important as potential indicators of their locomotor behavior. In line with previous studies, we predict that the locomotor repertoire estimated for early primates will be substantially diverse, as evinced by previous studies carried out on the available postcranial remains (e.g., Walker, 1974; Conroy and Rose, 1983; Gebo, 1988; Covert, 1995; Bloch et al., 2007; Boyer et al., 2013a; Marigó et al., 2016, 2020; Monclús-Gonzalo et al., 2023; Monclús-Gonzalo et al., 2025). In addition, we also expect that locomotor estimates for euprimates will considerably differ from those for plesiadapiforms, emphasizing behaviors such as frequent leaping, which have been correlated with the morphological features that distinguish the euprimate ancestral morphotype from plesiadapiforms (Dagosto, 1988, 2007).

2. Materials and methods

2.1. Sample composition and data collection

Osteological sample The analyzed astragalar and calcaneal extant samples are composed of 440 and 412 specimens, respectively, representing nearly the entire diversity of the superorder Euarchonta at the family rank. In addition, we compiled surface models of astragali (38) and calcanei (46) of extinct specimens representing all major Paleogene primate groups (Table 1). Most adapine postcranial remains are referred to *Adapis parisiensis*. However, the lack of stratigraphic information for some of the oldest specimens, coupled with geochronological and morphological evidence, suggests that there are several species included within *A. parisiensis* (Godinot, 1998; Marigó et al., 2019). For this reason, apart from the slightly older and larger *Leptadapis magnus*, we informally refer the material previously assigned to *A. parisiensis* to the '*Adapis* group' (e.g., Marigó et al., 2019). All these surface models were downloaded from MorphoSource (www.morphosource.org; Boyer et al., 2017b), except for a right astragalus of *Djebelemur martinezi* (CBI-1-545), which was downloaded from MorphoMuseuM (www.morphomuseum.com; Lebrun and Orliac, 2016; Marivaux et al., 2018). The list of the specimens is provided in Supplementary Online Material (SOM) Table S1 (see Figs. 1–4 for a representative sample of extant and extinct astragali and calcanei). A phylogenetic tree (SOM Fig. S1) comprising all extant primates in our study was downloaded from the 10kTrees Project v. 3 (Arnold et al., 2010). The criteria used to place the extinct taxa are explained in SOM S1.

Locomotor data collection Behavioral data consist of percentages of locomotor behaviors compiled from the literature (SOM Table S2), divided into five categories based on Hunt et al.'s (1996) descriptions for standardized primate locomotor and postural modes (for more information on how the five locomotor categories were compiled, see SOM S1): quadrupedalism (Q), climbing (C), leaping (L), suspension (S), and clawed clinging/climbing (CC). To standardize the data, the minimum number of studies (provided that more than one study was available for a given extant species) was considered when compiling the locomotor percentages (SOM S1). Because of the lack of behavioral information for some categories in several extant species, data from closely related species were sometimes used (see SOM Table S2 for details). An arcsine square root transformation was applied to the locomotor percentages; this is a standard procedure for analyzing proportional ecological data that makes the variances more homogeneous throughout the sample and approximates the data to a more normal distribution (Sokal and Rohlf, 1995).

2.2. Quantification of shape, astragalar/calcaneal shape variation, and influence of size

Quantification of shape using three-dimensional geometric morphometrics A 3D high-density sliding semilandmark procedure (Bookstein, 1997; Gunz et al., 2005) was used to quantify the shape of the two tarsal bones (Fig. 5; Tables 2 and 3), following the pipeline presented in Bardua et al. (2019). This methodology allows semilandmarks to slide along the curves and the surfaces, previously predefined using a template, while minimizing the bending energy. As a result, semilandmarks, which are inherently

Table 1
List of the extinct primate species and astragali/calcanei included in this study.

Family	Species	Astragalus	Calcaneus
Plesiadapiformes:			
Purgatoriidae	*Purgatorius* sp.	1	1
Micromomyidae	*Tinimomys graybulliensis*	0	1
Paromomyidae	*Ignacius graybullianus*	1	0
Paromomyidae	*Phenacolemur* sp.	0	1
Plesiadapidae	*Nannodectes gidleyi*	1	0
Plesiadapidae	*Plesiadapis cookei*	1	1
Plesiadapidae	*Plesiadapis rex*	1	0
Carpolestidae	*Carpolestes simpsoni*	0	1
Omomyiformes:			
Incertae sedis	*Teilhardina belgica*	1	1
Incertae sedis	*Vastanomys major*	1	0
Omomyidae	*Absarokius* sp.	0	1
Omomyidae	*Arapahovius gazini*	1	1
Omomyidae	*Necrolemur* sp.	1	0
Omomyidae	*Hemiacodon gracilis*	2	0
Omomyidae	*Omomys carteri*	2	4
Omomyidae	*Ourayia uintensis*	0	1
Omomyidae	*Shoshonius cooperi*	2	1
Omomyidae	*Washakius insignis*	1	1
Adapiformes:			
Notharctidae	*Marcgodinotius indicus*	1	3
Notharctidae	*Cantius* sp.	1	3
Notharctidae	*Copelemur tutus*	0	1
Notharctidae	*Notharctus* sp.	4	5
Notharctidae	*Smilodectes* sp.	1	2
Notharctidae	*Anchomomys frontanyensis*	1	1
Adapidae	'*Adapis* group'	5	5
Adapidae	*Leptadapis magnus*	1	3
Adapidae	*Caenopithecus lemuroides*	0	1
Stem Lemuriformes:			
Djebelemuridae	*Djebelemur martinezi*	1	0
Stem Anthropoidea:			
Eosimiidae	*Eosimias* sp.	2	3
Amphipithecidae	*Ganlea* sp.	1	0
Parapithecidae	*Apidium* sp.	3	0
Parapithecidae	*Simonsius grangeri*	1	0
Parapithecidae	Parapithecidae indet.	0	3
Proteopithecidae	*Proteopithecus sylviae*	0	1

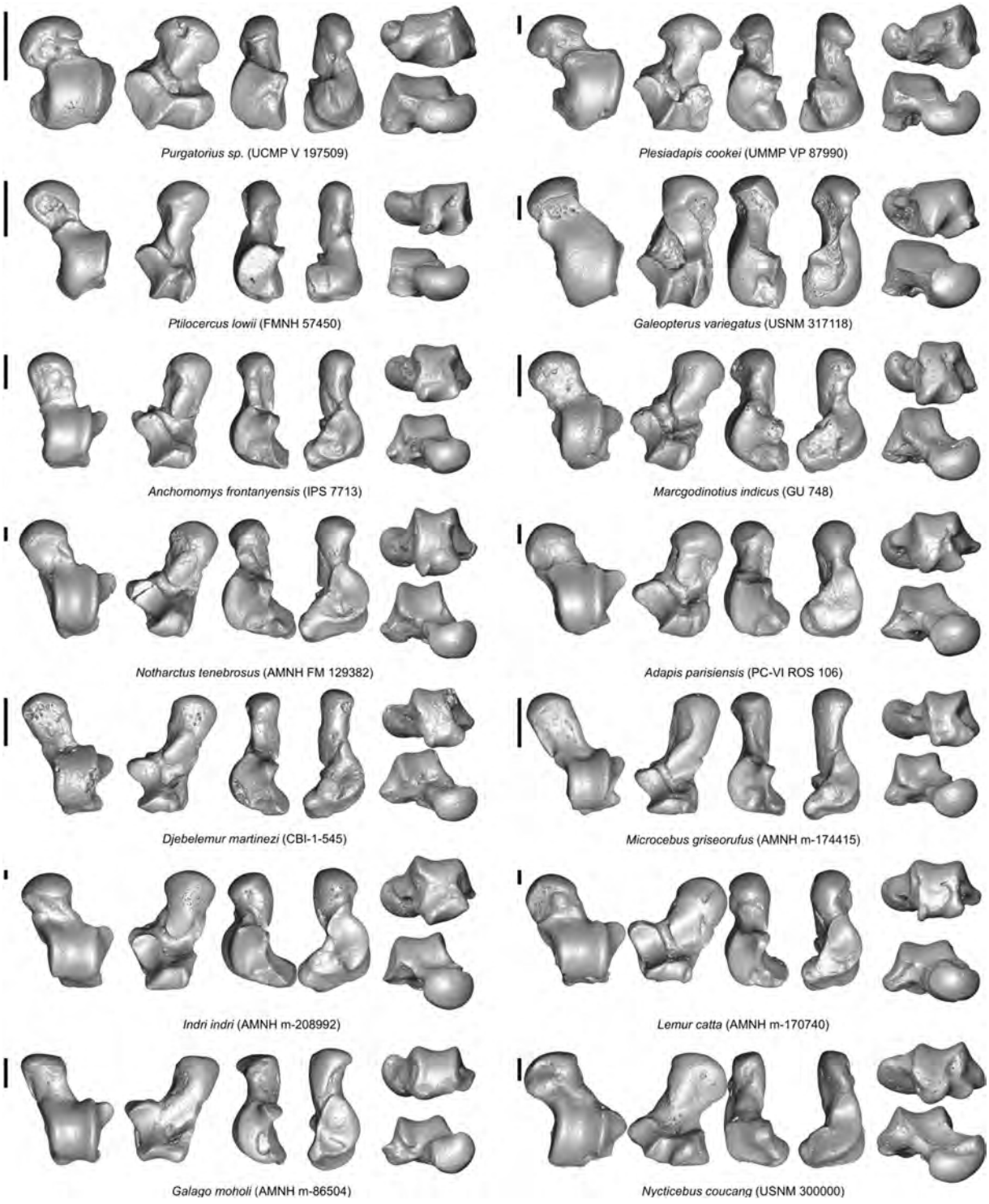

Figure 1. Selected sample of astragali belonging to plesiadapiforms, scandentians, dermopterans, adapiforms, and extant strepsirrhines. Scale bars = 2 mm.

nonhomologous, are consequently transformed into geometrically homologous landmarks and can be used to compare shapes (Gunz and Mitteroecker, 2013). Specimens from the left foot were mirrored before placing the landmarks. Anatomical landmarks and sliding semilandmarks of curves were placed manually on each 3D surface using the software Landmark v. 3.0.0.6 (Wiley, 2006), while the remaining analyses were performed in R v. 4.3.0 (R Core Team, 2023). To carry out the sliding-semilandmark procedure, the R package morpho v.2.11 (Schlager, 2017) was used. To do so, it is first required to create a template for each bone, following the pipeline presented in Cornette et al. (2013), with 25 anatomical landmarks, 195 sliding semilandmarks on curves, and 130 sliding semilandmarks on surfaces for the astragalus and 20 anatomical landmarks, 100 sliding semilandmarks on curves, and 49 sliding semilandmarks on surfaces for the calcaneus. All the sliding semilandmarks of each template,

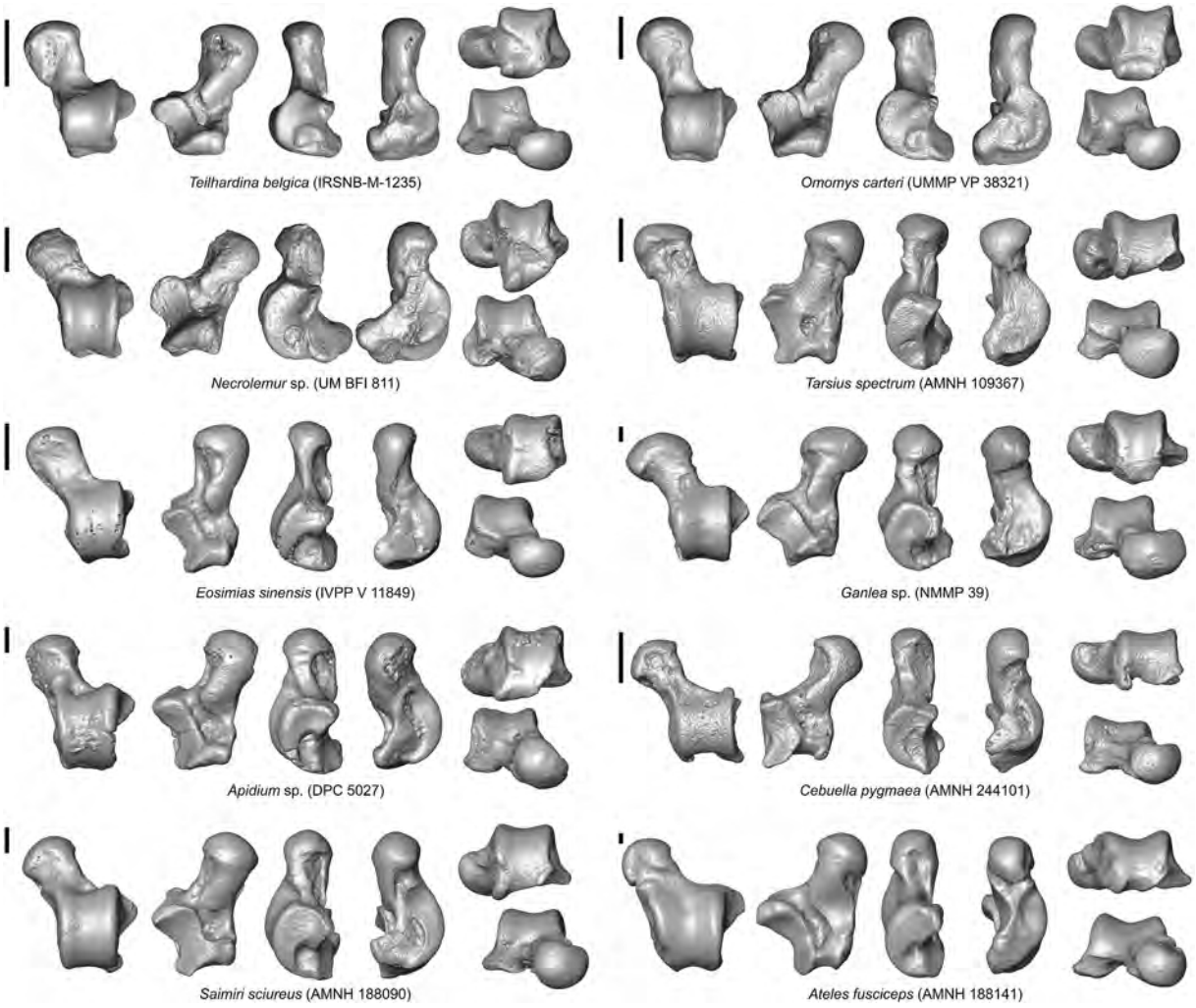

Figure 2. Selected sample of astragali belonging to extant and extinct haplorhines. Scale bars = 2 mm.

based on the homology between the anatomical landmarks and the curves, are projected onto the specimens using a thin-plate spline deformation (Gunz and Mitteroecker, 2013) using the function 'placePatch' of the package morpho. Before this step, all specimens were decimated to a maximum of 50,000 faces using the software Avizo v. 8.1.1 (Visualization Sciences Group, Merignac) to facilitate the projection and sliding procedures, as well as their visualization in the subsequent analyses. After projecting the sliding semilandmarks on surfaces, four thin-plate spline relaxation procedures were performed using the function 'slider3d' of the package morpho. The first relaxation was performed against the template, whereas the other three were performed against the Procrustes consensus obtained from the previous iteration. After the relaxation procedure, a generalized Procrustes superimposition (Rohlf and Slice, 1990) was performed using the function 'gpagen' of the package geomorph v. 4.0.6 (Adams and Otarola and Castillo, 2013).

Astragalar/calcaneal shape variation To assess astragalar and calcaneal shape variation across the sample, a principal component analysis (PCA) was performed on the species-mean Procrustes shape coordinates using the 'gm.prcomp' function of the package 'geomorph'. To decide how many principal components (PCs) should be considered as relevant for the analysis, a barplot depicting the variance explained by each PC was built following Hammer and Harper (2024). Phylogenetic signal was calculated employing two different methods, Blomberg's K (Blomberg et al., 2003) and Pagel's lambda (Pagel, 1999), using the 'phylosig' function of the package 'phytools' v. 2.1–1 (Revell, 2012). Additionally, a phylogenetic PCA (Revell, 2009; Polly et al., 2013) was also performed on the species-mean Procrustes shape coordinates using the 'gm.prcomp' function of the package 'geomorph'. Compared to a standard PCA, a phylogenetic PCA allows us to calculate PCs that are oriented by the nonphylogenetic component of variation, allowing us to take into account the phylogenetic nonindependence among species. Therefore, differences between PCA and phylogenetic PCA scatterplots might indicate that factors other than the phylogenetic structure of the sample account for phenotypic variation. Principal components obtained from the phylogenetic PCA will be used as shape data to calculate branch-specific evolutionary rates to address the evolution of astragalar and calcaneal morphology across the primate phylogenetic tree (see subsection 2.5).

Influence of size and foot type on astragalar/calcaneal shape The correlation between tarsal size, defined as the natural log-transformed (ln) centroid size (CS), and ln body mass (BM) was first examined to identify the presence of allometric effects

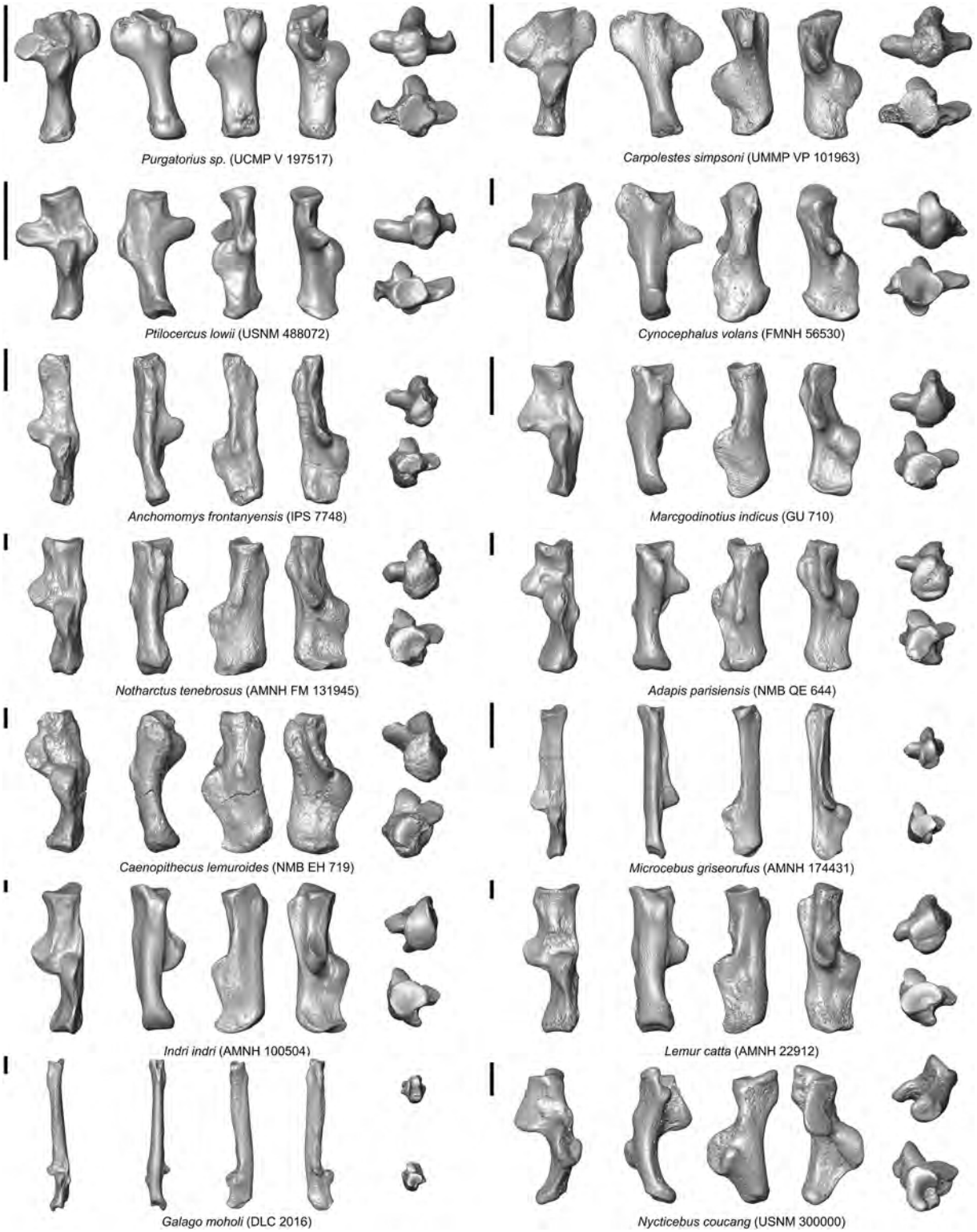

Figure 3. Selected sample of different calcanei belonging to plesiadapiforms, scandentians, dermopterans, adapiforms, and extant strepsirrhines. Scale bars = 3 mm.

between these two variables (see SOM Table S3 for details on the BM). For the calcaneus, this analysis was repeated without galagids and tarsiers as they are clear outliers in the linear regression. After that, a series of allometric regressions of the resulting PCs vs. ln CS or ln BM were calculated using a phylogenetic generalized least squares analysis with the 'pgls' function in the package 'caper' v. 1.0.3 (Orme et al., 2023). Shape differences based on the PCs between tarsi-fulcrumators and metatarsi-fulcrumators and the interaction term between size and foot type variables were also examined.

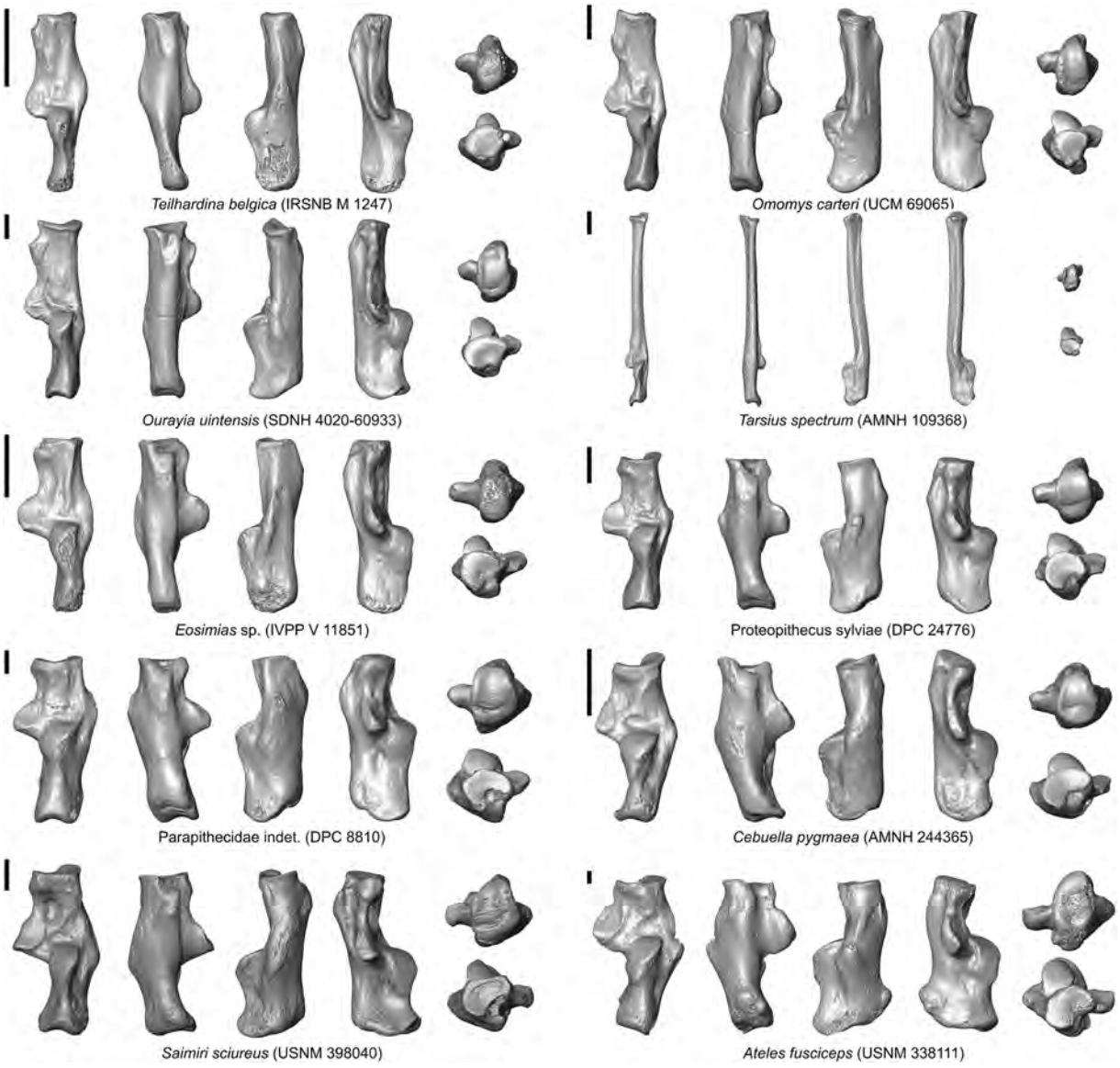

Figure 4. Selected sample of different calcanei belonging to extant and extinct haplorhines. Scale bars = 3 mm.

2.3. Covariation between astragalar/calcaneal shape and locomotor behavior in extant euprimates

To study the covariance between astragalar/calcaneal shape and locomotor behavior, a two-block partial least squares (PLS) analysis (Rohlf and Corti, 2000) was implemented using the functions 'two.b.pls' of the package geomorph and 'pls2b' of the package morpho. This type of analysis uses 3D landmark data and performs a singular value decomposition, which decomposes the covariance matrix of the two blocks of variables into two matrices of eigenvectors (one for each block of data) and a matrix of eigenvalues (the square roots of eigenvectors; Rohlf and Corti, 2000; Bookstein et al., 2003). The two blocks of data consisted of (1) the astragalar/calcaneal shape (Procrustes shape coordinates) averaged by species and (2) locomotor percentages for the 78 species included in the extant comparative sample. The significance of each linear combination is assessed by comparing the singular value to those obtained after resampling. If the PLS covariation coefficient is higher than the ones obtained from permutated blocks, its associated p value is significant. (The α level of significance was set at <0.05).

2.4. Reconstruction of extinct primate locomotor behavior

Prediction of locomotor percentages Although the standard version of two-block PLS is conceptualized as a symmetric analysis that does not allow for predictive outcomes (Zelditch et al., 2012), there is another version of this analysis more comparable to a regression, known as PLS regression, which allows the generation of predictive models (Wold et al., 2001). Similar approaches have already been applied in archaeology and paleoanthropology (e.g., Archer et al., 2018; Bastir et al., 2019; Torres-Tamayo et al., 2020) and in the reconstruction of extinct primate locomotion, using the navicular bone (Monclús-Gonzalo et al., 2023), the astragalus (Monclús-Gonzalo et al., 2025), or the ulna (Raventós-Izard et al., 2025) as a predictor. Therefore, a PLS regression approach was applied to estimate the locomotor behavior of the 37 Paleogene taxa based on their astragalar/calcaneal shape. To do so, the two

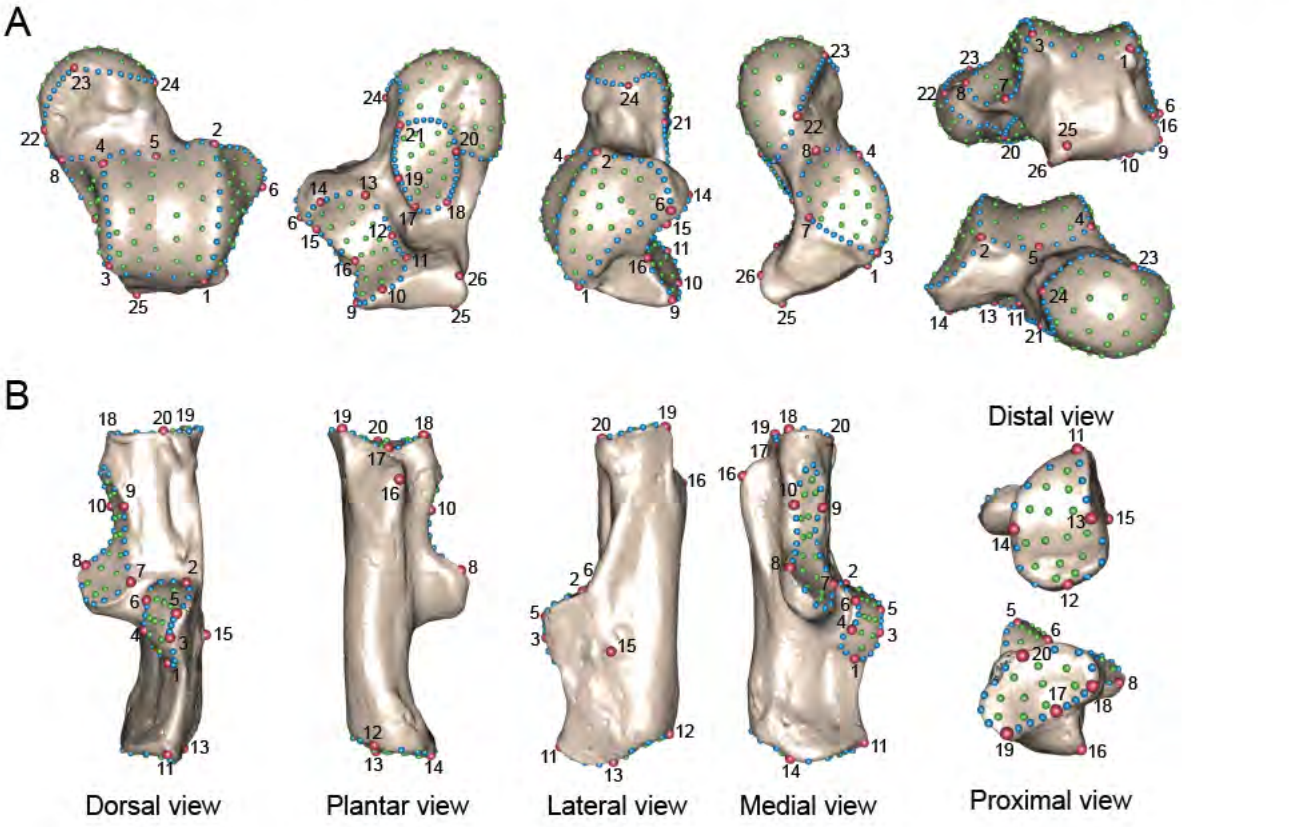

Figure 5. Landmark configuration of the astragalus (A) and the calcaneus (B). Red points represent anatomical landmarks (see Tables 2 and 3), blue points represent curve semilandmarks, and light green points represent surface semilandmarks. Views for both bones are indicated in the calcaneus. The two specimens used as a reference are right-sided and belong to the species *Lemur catta*: DLC 6848 (A) and AMNH 170739 (B). (For interpretation of the references to color in this figure legend, the reader is referred to the web version of this article.)

Table 2
Definition of the 26 anatomical landmarks (LMs) used for the astragalus.

LM	Definition
1	Proximalmost point of the lateral trochlear rim
2	Distalmost point of the lateral trochlear rim
3	Proximalmost point of the medial trochlear rim
4	Distalmost point of the medial trochlear rim
5	Point of maximum concavity on the lateral side of the junction between the astragalar body and the astragalar neck
6	Tip of the lateral astragalar process
7	Point of maximum concavity between LM3 and LM8
8	Distalmost point of the plantar aspect of the medial tibial facet
9	Proximalmost point of the ectal facet
10	Point of maximum curvature between LM9 and LM11
11	Proximomedialmost point of the ectal facet
12	Point of maximum curvature between LM11 and LM13
13	Distalmost point of the ectal facet
14	Point of maximum curvature between LM13 and LM15
15	Proximolateralmost point of the ectal facet
16	Point of maximum curvature between LM15 and LM9
17	Proximalmost point of the sustentacular facet
18	Proximomedialmost point of the sustentacular facet
19	Proximolateralmost point of the sustentacular facet
20	Medialmost joint of the sustentacular and the navicular facets
21	Lateralmost joint of the sustentacular and navicular facets
22	Proximalmost point of the navicular facet on the medial side of the astragalar neck
23	Proximodorsalmost point of the navicular facet
24	Proximalmost point of the navicular facet on the lateral side of the astragalar neck
25	Point of maximum curvature on the proximalmost point of the medial side of the astragalus
26	Plantarmost point of the m. Flexor Hallucis Longus groove on the medial side of the astragalus, below LM25

To visualize placement of the LMs on the bone, see Figure 5.

Table 3
Definition of the 20 anatomical landmarks (LMs) used for the calcaneus.

LM	Definition
1	Proximalmost point of the ectal facet
2	Distalmost point of the ectal facet
3	Proximolateralmost point of the ectal facet
4	Proximomedialmost point of the ectal facet
5	Dorsalmost point of the ectal facet
6	Medialmost point of the ectal facet
7	Proximolateralmost point of the sustentacular facet
8	Proximomedialmost point of the sustentacular facet
9	Distolateralmost point of the sustentacular facet
10	Distomedialmost point of the sustentacular facet
11	Dorsalmost point of the proximal facet
12	Plantarmost point of the proximal facet
13	Lateralmost point of the proximal facet
14	Medialmost point of the proximal facet
15	Lateralmost point of the peroneal tubercle
16	Plantarmost point of the calcaneal tubercle
17	Most concave point of the cuboid facet
18	Dorsomedialmost point of the cuboid facet
19	Plantolateralmost point of the cuboid facet
20	Dorsalmost point of the cuboid facet

To visualize placement of the LMs on the bone, see Figure 5. Landmarks includsed in the restricted configuration (see Material and Methods section) are denoted with an asterisk.

sets of eigenvectors generated by the singular warp analysis performed on each covariance analysis were used. The species-mean Procrustes shape coordinates of every extinct taxon are projected onto the latent space generated after the singular warp analysis. After that, the coefficients obtained from the linear regression of the original latent variables can be used to estimate the variables corresponding to the second block of data. The resulting new latent variables can be projected back to obtain the scores of each behavioral category. To calculate the locomotor percentages, the arcsin square root transformation must be reverted and the resulting values normalized to ensure that their total sum is equal to 100. To check the accuracy of this method, a leave-one-out cross-validation approach was applied on the extant species set. The leave-one-out subsampling approach removes each extant individual one by one from the original sample and performs the analysis again with the remaining extant species to compare the original behavioral data compiled from the literature with the predictions and assess the error generated during the estimation procedure (Kuhn and Johnson, 2013). Based on the cross-validated results, the mean absolute error (i.e., the arithmetic average of the absolute errors) was computed to assess our prediction results using the extant sample (Willmott and Matsuura, 2005).

Ancestral reconstruction Ancestral states of the locomotor repertoire for each node of the phylogenetic tree were estimated with the function 'mvgls' and 'estim' of the package 'mvMORPH' v. 1.1.6 (Clavel et al., 2015). Four evolutionary models (Brownian motion, Ornstein-Uhlenbeck, Early Burst, and Pagel's lambda transformation) were computed and compared using the Generalized Information Criterion with the function 'GIC' of the package 'mvMORPH,' selecting the evolutionary model with the lowest GIC to calculate the ancestral locomotor reconstruction (Konishi and Kitagawa, 1996).

2.5. Rates of morphological evolution

To investigate the morphological evolution of the astragalus and the calcaneus, branch-specific evolutionary rates were estimated using the variable rates model in BayesTraits v3 (http://www.evolution.rdg.ac.uk/). The first 36 PCs from the phylogenetic PCA of species-mean Procrustes shape coordinates for the astragalus and the first 25 PCs for the calcaneus were used as input. These PCs accounted for >95% of the total variation in astragalar/calcaneal shape. Five independent chains for 200 million interactions were ran, sampling every 10,000 iterations and discarding the first 25 million iterations as burn-in. Trace plots were examined to ensure stationarity and retain only chains that stabilized after burn-in. Effective sample sizes of the posterior distributions (effective sample size < 100) and chain convergence were assessed using Gelman and Rubin's diagnostic, using the functions 'effectiveSize' and 'Gelman.diag' in the package 'coda' v0.19-41 (Plummer et al., 2005). The verification of chain convergence is crucial to detect large deviations and ensuring similar between-chain variances (Gelman and Rubin, 1992). Results were visualized on the phylogeny using the 'mytreebybranch' function (https://github.com/anjgoswami/salamanders/blob/master/mytreerateplotter.R). Branch-specific average rates were obtained using the 'rjpp' function in the package 'btrtools' v0.0.0.9000 (https://github.com/hferg/btrtools/tree/master/R).

2.6. Shape visualization

To visualize the shape differences in astragalar and calcaneal shape between the extremes of the PC and PLS axes, a thin-plate spline deformation of the 3D models of an astragalus and a calcaneus was carried out using the functions 'shape.predictor' and 'plotRefToTarget' of the package geomorph and 'shade3d' of the package rgl 1.1.3 (Adler and Murdoch, 2020). Displacement heatmaps were calculated to illustrate mesh distances between extreme landmark configurations using the function 'mehsdist' of the package morpho. This function first calculates the distances between the vertices of the reference mesh and that of the target mesh. Then, distances are given a negative value if inside the reference mesh or a positive value if outside (Bærentzen and Aanæs, 2002). The functions 'mshape' and 'findMeanSpec' of the package geomorph were used to find the most suitable astragalar and calcaneal specimens to use as reference. The specimens selected were an astragalus of *Plecturocebus moloch* (AMNH 244363) and a calcaneus of *Eulemur albifrons* (AMNH 170717).

3. Results

3.1. Astragalar shape variation

The first four PCs of the standard PCA performed on the species-mean Procrustes shape coordinates of the astragalus were chosen as the most meaningful and accounted for up to 59% of the total variance (SOM Fig. S2), differentiating species by phylogenetic group, locomotor behavior, and foot type.

The PC1 (accounting for 18% of the total variance, Fig. 6A) indicates differences in astragalar body shape (mediolaterally broader and dorsoplantarly lower toward negative scores and narrower and higher toward positive scores), trochlear wedging (broader distally than proximally in negative scores and more parallel rims in positive scores), development of a posterior trochlear shelf (PTS; more developed in positive than in negative scores), fibular facet shape (steeper in negative scores and more sloping in positive ones), relative size of the medial tibial facet (smaller and without reaching the plantar edge toward negative scores and larger and reaching the plantar edge in positive scores), proximodistal elongation of the neck (more elongated in positive scores than in negative scores), and head shape (smaller and more spherical in negative scores and larger and mediolaterally extended toward positive scores; Fig. 7). This axis separates extant haplorhines (negative scores) from extant strepsirrhines, scandentians, and dermopterans (intermediate to positive scores). As expected by the clear phylogenetic structure of PC1, a strong

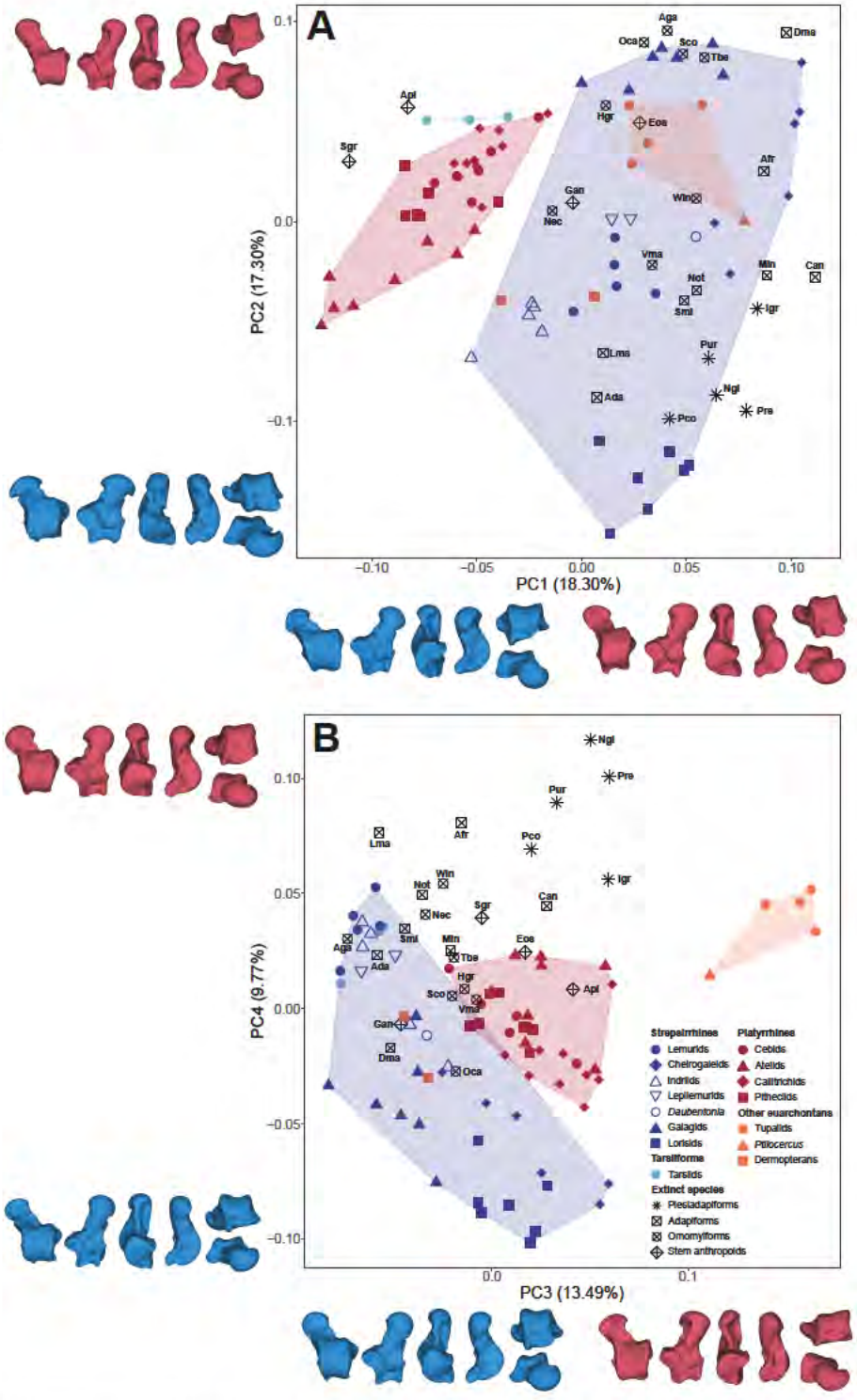

Figure 6. Results of the principal component analysis (PCA) performed on the species-mean Procrustes shape coordinates of the astragalus as depicted by bivariate plots of PC2 vs. PC1 (A) and PC4 vs. PC3 (B). Taxonomic groups are coded by color and symbol, as indicated in the legend. The percentage of variance explained by each PC is reported within parentheses. Astragalar shapes associated with minimum (blue) and maximum (red) values of each PC axis are plotted below each scatterplot (dorsal, plantar, lateral, medial, proximal, and distal views are shown, from left to right). Thin-plate splines correspond to an astragalus of *Plecturocebus moloch* (AMNH 244363). Abbreviations: Api = *Apidium*; Sgr = *Simonsius grangeri*; Gan = *Ganlea*; Eos = *Eosimias*; Nec = *Necrolemur*; Hgr = *Hemiacodon gracilis*; Sco = *Shoshonius cooperi*; Win = *Washakius insignis*; Oca = *Omomys carteri*; Aga = *Arapahovius gazini*; Vma = *Vastanomys major*; Tbe = *Teilhardina belgica*; Dma = *Djebelemur martinezi*; Afr = *Anchomomys frontanyensis*; Ada = *Adapis* group; Lma = *Leptadapis magnus*; Smi = *Smilodectes*; Not = *Notharctus*; Can = *Cantius*; Min = *Marcgodinotius indicus*; Ngi = *Nanodectes gidleyi*; Pre = *Plesiadapis rex*; Pco = *Plesiadapis cookei*; Igr = *Ignacius graybullianus*; Pur = *Purgatorius*; PC = principal component. (For interpretation of the references to color in this figure legend, the reader is referred to the web version of this article.)

phylogenetic signal is found for this axis (Table 4). Along PC1, most fossil species are projected onto slight to moderate negative scores and overlap with extant strepsirrhines, scandentians, and dermopterans, with only the Afro-Arabian anthropoids (*Apidium* and *Simonsius grangeri*) overlapping with extant haplorhines. Compared to the standard PC1, the phylogenetic PC1 (accounting for 18% of the total variance; SOM Fig. S3A) emphasizes changes in the trochlear and neck shape (a larger and broader trochlea relative to the neck toward negative scores and a smaller and more square-shaped trochlea relative to the neck in positive scores) and does not discriminate haplorhines from the other groups. Astragalar size and BM are significantly correlated (r^2 = 0.909; p < 0.001; SOM Fig. S4), although they exhibit a slight positive allometric slope. A significant allometric relationship is found between PC1 and either ln CS or ln BM, indicating a moderate negative correlation that accounts for 17–19% of the total variance (Table 5, SOM Figs. S5A–6A). Neither significant differences in PC1 were found between tarsi-fulcrumators and metatarsi-fulcrumators nor a significant interaction was found between either size variable and foot type.

The PC2 (accounting for 17% of the total variance, Fig. 6A) reflects differences in trochlear shape (more proximodistally elongated and less grooved toward negative scores and shorter and more grooved toward positive scores), fibular facet shape (more sloping in negative scores and steeper in positive scores), ectal facet shape (less concave in negative scores than in positive scores), neck shape (proximodistally abbreviated and mediolaterally broader in negative scores and more elongated and narrower in positive scores), and head shape (larger and mediolaterally broader toward negative scores and smaller and more spherical toward positive scores; Fig. 7). Within each group—nonprimates, strepsirrhines, and haplorhines—PC2 differentiates those species with better climbing and/or suspensory abilities (lorisids, dermopterans, and atelids) from those that engage in more quadrupedal or leaping behaviors. Therefore, a lower (albeit still significant) phylogenetic signal is found for this axis (Table 4). Plesiadapiforms and adapines are projected onto negative scores, between lorisids and the other extant groups. Notharctines, *Marcgodinotius indicus* and *Vastanomys major* are located in intermediate scores, overlapping with atelids, most extant strepsirrhines (excluding galagids and some cheirogaleids), and dermopterans. Conversely, fossil anthropoids, the remaining omomyiforms, *Anchomomys frontanyensis* and *D. martinezi* are projected onto positive scores. Given the lower phylogenetic component of the standard PC2, the phylogenetic PC2 (accounting for 11% of the total variation; SOM Fig. S3A) similarly discriminates more climbing and/or suspensory species (positive scores) from leapers and quadrupeds (negative scores). The PC2 is significantly correlated with both ln CS and ln BM (Table 5; SOM Figs. S5B–6B), suggesting a slight negative allometric correlation explaining up to 8–9% of the total variation. Significant differences in PC2 are found between tarsi-fulcrumators and metatarsi-fulcrumators, but the interaction between either size variable and foot type remains nonsignificant.

Table 4
Phylogenetic signal computed for the most explanatory principal components (PCs) derived from the species-mean Procrustes shape coordinates of each bone.

PC	Statistic	Astragalus	p	Calcaneus	p
		Phylogenetic signal		Phylogenetic signal	
1	K	1.854	**<0.001**	2.891	**<0.001**
	λ	0.975	**<0.001**	1.000	**<0.001**
2	K	1.035	**<0.001**	1.211	**<0.001**
	λ	0.993	**<0.001**	0.948	**<0.001**
3	K	0.867	**<0.001**	–	–
	λ	0.939	**<0.001**	–	–
4	K	1.369	**<0.001**	–	–
	λ	0.963	**<0.001**	–	–

Abbreviations: K = Blomberg's K; λ = Pagel's lambda.
Significant results (p <0.05) are indicated in bold.

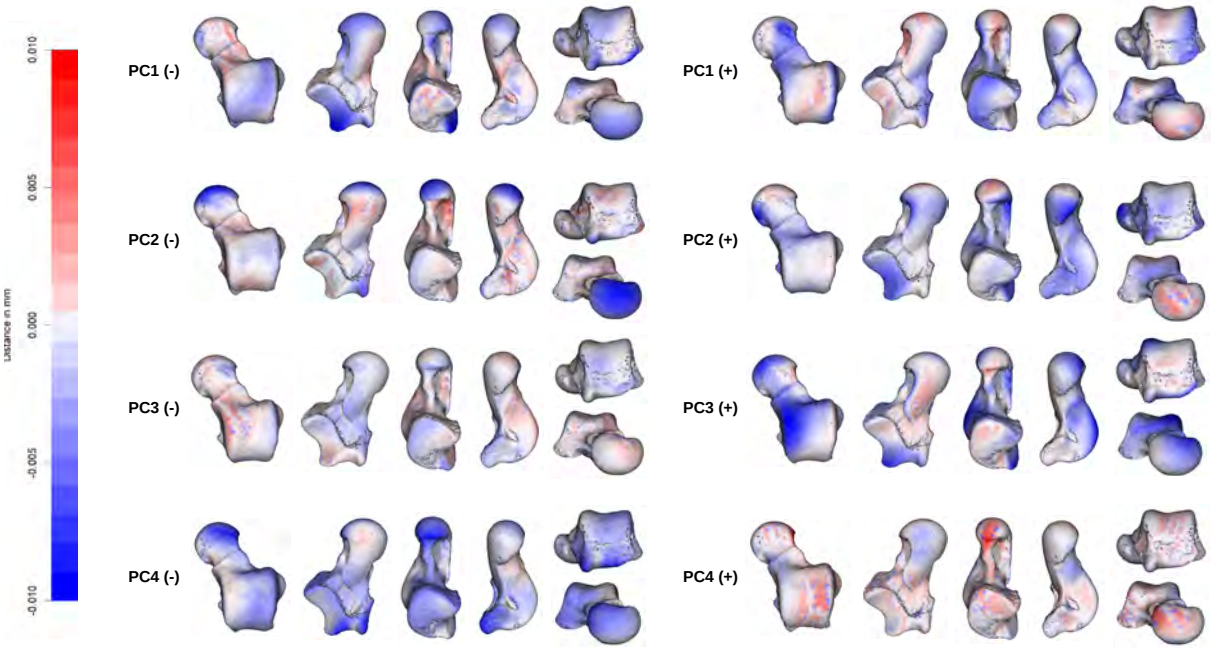

Figure 7. Displacement heatmaps illustrating mesh distances between the mean astragalar shape of each PC axis depicted in Figure 6 against the shapes associated with the minimum (–) and maximum (+) values. Blue and red indicate regions of contraction and expansion, respectively, based on the position of the extreme astragalar shapes (minimum or maximum values) relative to the mean shape along each PC axis. Abbreviation: PC = principal component. (For interpretation of the references to color in this figure legend, the reader is referred to the web version of this article.)

Table 5
Results of the phylogenetic generalized least squares (PGLS) analyses between astragalar/calcaneal shape and natural log-transformed (ln) centroid size (CS) or body mass (BM).

PC	Model	Astragalus		F	*p*	Calcaneus		F	*p*
		R^2	Df			R^2	Df		
1	ln CS	0.174	97	21.640	**<0.001**	−0.010	96	0.004	0.608
	ln BM	0.186	97	23.320	**<0.001**	0.082	96	9.694	**0.002**
	Foot type	−0.006	97	0.461	0.499	0.099	96	11.670	**0.001**
	ln CS × foot type	0.166	95	7.503	0.992	0.084	94	3.955	0.924
	ln BM × foot type	0.183	95	8.331	0.366	0.269	94	12.900	**0.006**
2	ln CS	0.088	97	10.480	**0.002**	0.107	96	12.630	**0.001**
	ln BM	0.084	97	9.980	**0.002**	0.005	96	1.451	0.231
	Foot type	0.049	97	6.037	**0.016**	−0.009	96	0.110	0.741
	ln CS × foot type	0.158	95	7.140	0.166	0.111	94	5.031	0.370
	ln BM × foot type	0.144	95	6.509	0.333	−0.004	94	0.870	0.303
3	ln CS	0.019	97	2.921	0.091	–		–	–
	ln BM	0.039	97	5.021	**0.027**	–		–	–
	Foot type	0.104	97	12.420	**0.001**	–		–	–
	ln CS × foot type	0.134	95	6.037	0.242	–		–	–
	ln BM × foot type	0.155	95	6.987	0.247	–		–	–
4	ln CS	−0.009	97	0.129	0.720	–		–	–
	ln BM	−0.006	97	0.402	0.528	–		–	–
	Foot type	0.036	97	4.662	**0.033**	–		–	–
	ln CS × foot type	0.063	95	3.187	**0.037**	–		–	–
	ln BM × foot type	0.050	95	2.719	0.094	–		–	–

Abbreviations: F = Fischer's F; Df = degrees of freedom; R^2 = adjusted coefficient of determination.
Astragalar and calcaneal shape are represented by the principal components (PCs) derived from the species-mean Procrustes shape coordinates of each bone. Additionally, the interaction between ln CS or ln BM and foot type was assessed too.[a]
[a] Significant results ($p < 0.05$) are indicated in bold.

The PC3 (accounting for 13% of the total variance, Fig. 6B) separates scandentians (very positive scores) from the other extant groups (slightly positive to negative scores). Shape differences associated with this axis are related to astragalar body shape (proximodistally shorter and lower medial side in positive scores than in negative scores), development of the trochlear rims (less developed in positive scores than in negative ones), and head shape (more dorsoplantarly compressed and laterally extended in positive scores than in negative scores; Fig. 7). A moderate phylogenetic signal, similar to that of PC2, is found for PC3 (Table 4). Fossil species are located in negative to slightly positive scores, thus overlapping with extant euprimates and dermopterans. Among fossil species, plesiadapiforms are the ones projected onto more positive scores, closer to scandentians. Unlike standard PC3, phylogenetic PC3 (accounting for 8% of the total variation; SOM Fig. S3B) discriminates plesiadapiforms (except for *Plesiadapis cookei*) from the other extant and extinct groups, resembling standard PC4. Only significant allometric relationship is found between PC3 and ln BM (Table 5; SOM Figs. S5C–S6C), although it is likely an artifact derived from the markedly different scores of scandentians. Conversely, strong significant differences in PC3 are found between tarsi-fulcrumators and metatarsi-fulcrumators, although the interaction between either size variable and foot type is nonsignificant.

The PC4 (accounting for 10% of the total variance, Fig. 6B) indicates differences between astragalar body (lower toward negative scores and higher toward positive ones), trochlear shape (more grooved and distally abbreviated in positive scores and shallower and more distally elongated in negative scores), fibular facet shape (more sloping in negative scores and steeper in positive ones), neck (narrower and more elongated in negative scores than in positive ones), and head shape (smaller relative to neck in negative scores than in positive ones; Fig. 7). The PC4 separates plesiadapiformes (very positive scores) from the extant groups (negative to slightly positive scores), with most adapiforms, omomyiforms, and early anthropoids being also projected onto slightly to moderately positive scores. A strong phylogenetic signal is found for this axis, indicating that phylogeny highly influences the distribution of species along PC4 (Table 4). Phylogenetic PC4 (accounting for 6% of the total variation; SOM Fig. S3B) resembles standard PC4, but it places greater emphasis on distal trochlear elongation, a feature that distinguishes notharctids (positive scores) due to their extreme development of the PTS. No significant correlation between PC4 and either ln CS or ln BM is found (Table 5; SOM Figs. S5D–S6D). Conversely, significant differences in PC4 are found between tarsi-fulcrumators and metatarsi-fulcrumators, as well as the interaction between ln CS and foot type, although this result is likely an artifact derived from the moderately positive scores of scandentians.

3.2. Calcaneal shape variation

The first two PCs of the standard PCA performed on the species-mean Procrustes shape coordinates of the calcaneus were chosen as the most meaningful and account for up to 82% of the total variance (SOM Fig. S7), differentiating species by phylogenetic group, locomotor behavior, and foot type.

The PC1 (accounting for 76% of the total variance; Fig. 8) is mostly associated with distal calcaneal elongation (abbreviated distal calcaneus toward negative scores and very elongated distal calcaneus toward positive scores; Fig. 9). This axis separates extant species depending on their degree of calcaneal elongation: scandentians, dermopterans, platyrrhines, lorisids, indriids, and *Daubentonia madagascariensis* are all projected in negative scores; lemurids, cheirogaleids, and lepilemurids are located along intermediate to slightly positive scores; and galagids and tarsiids are in the most positive scores of the axis. A strong phylogenetic signal is found for this axis, as evinced by the clear phylogenetic distribution of species along PC1 (Table 4). Plesiadapiforms (except for *C. simpsoni*) and adapines are projected onto very negative scores, outside the distribution of extant groups. Most adapiforms (except for *An. frontanyensis*), the Afro-Arabian anthropoids, and *C. simpsoni* are in slightly negative scores, overlapping with lorisids, indriids, *Da. madagascariensis*, platyrrhines, and nonprimate euarchontans. Omomyiforms, *Eosimias* and *An. frontanyensis* are projected onto slightly

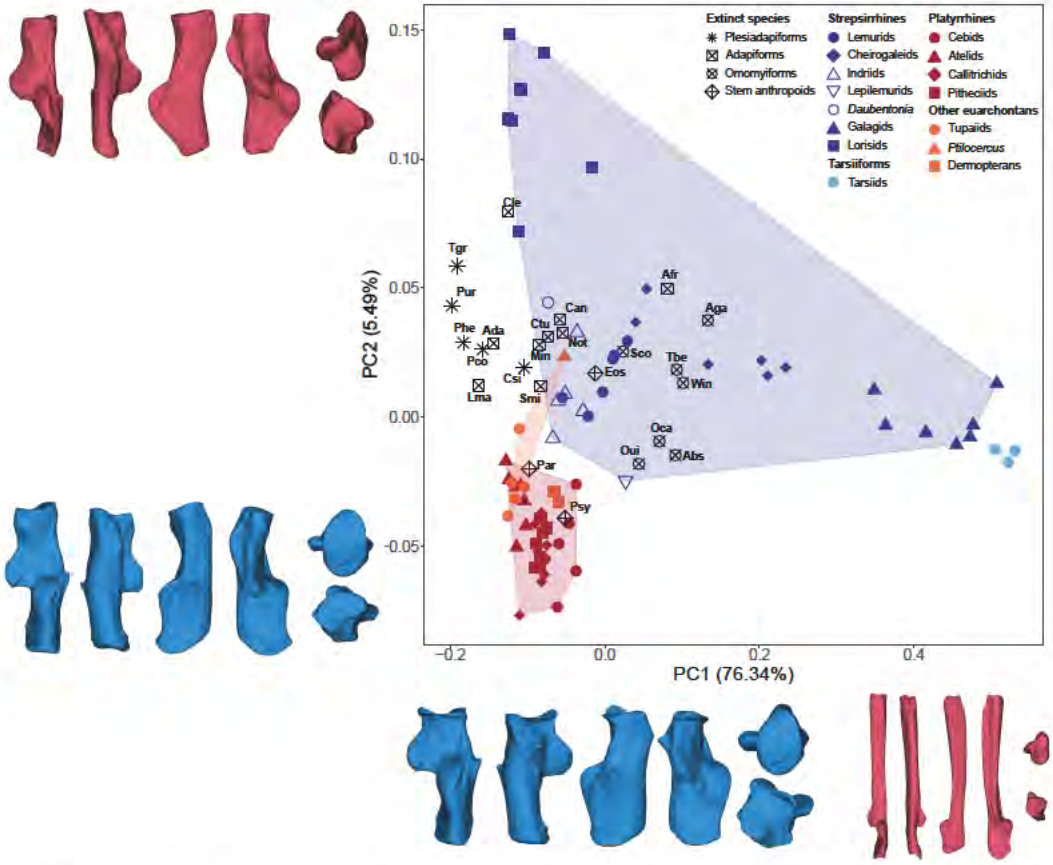

Figure 8. Results of the principal component analysis (PCA) performed on the species-mean Procrustes shape coordinates of the calcaneus as depicted by bivariate plots of PC2 vs. PC1. Taxonomic groups are coded by color and symbol, as indicated in the legend. The percentage of variance explained by each PC is reported within parentheses. Calcaneal shapes associated with minimum (blue) and maximum (red) values of each PC axis are plotted below each scatterplot (dorsal, plantar, lateral, medial, proximal, and distal views are shown, from left to right). Thin-plate splines correspond to a calcaneus of *Eulemur albifrons* (AMNH 170717). Abbreviations: Par = Parapithecidae indet; Psy = *Proteopithecus sylviae*; Eos = *Eosimias*; Oui = *Ourayia uintensis*; Sco = *Shoshonius cooperi*; Win = *Washakius insignis*; Oca = *Omomys carteri*; Abs = *Absarokius*; Aga = *Arapahovius gazini*; Tbe = *Teilhardina belgica*; Afr = *Anchomomys frontanyensis*; Ada = *Adapis* group; Lma = *Leptadapis magnus*; Cle = *Caenopithecus lemuroides*; Ctu = *Copelemur tutus*; Smi = *Smilodectes*; Not = *Notharctus*; Can = *Cantius*; Min = *Marcgodinotius indicus*; Csi = *Carpolestes simpsoni*; Pco = *Plesiadapis cookei*; Phe = *Phenacolemur*; Tgr = *Tinimomys graybulliensis*; Pur = *Purgatorius*; PC = principal component. (For interpretation of the references to color in this figure legend, the reader is referred to the web version of this article.)

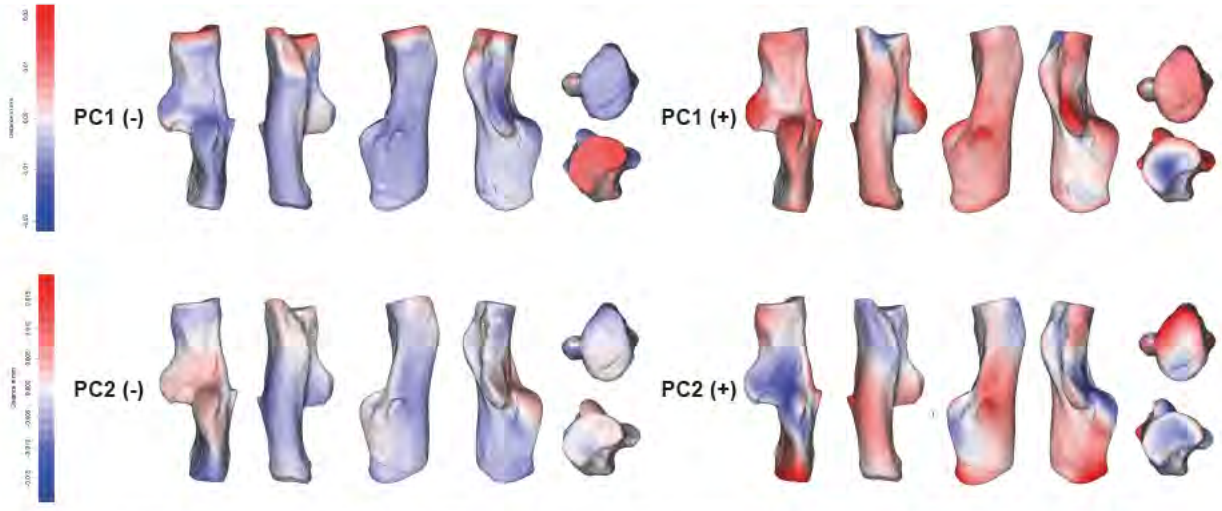

Figure 9. Displacement heatmaps illustrating mesh distances between the mean calcaneal shape of each PC axis depicted in Figure 8 against the shapes associated with the minimum (−) and maximum (+) values. Blue and red indicate regions of contraction and expansion, respectively, based on the position of the extreme calcaneal shapes (minimum or maximum values) relative to the mean shape along each PC axis. Abbreviation: PC = principal component. (For interpretation of the references to color in this figure legend, the reader is referred to the web version of this article.)

positive scores, overlying with lemurids and cheirogaleids. Despite the strong phylogenetic signal found for the standard PC1, the phylogenetic PC1 (accounting for 41% of the total variation; SOM Fig. S8) reflects the same distribution as proximodistal elongation is still the main source of variation for this bone even when the phylogenetic structure of the sample is considered. Nevertheless, it is remarkable that the amount of variance explained by this axis is only slightly more than half (41%) than that in the standard PCA (76%), suggesting that considering phylogenetic nonindependence among species improves the resolution for assessing aspects of calcaneal shape variation beyond distal elongation. Calcaneal size and BM are significantly correlated ($r^2 = 0.667$; $p < 0.001$; SOM Fig. S9). However, it is evident from the visualization of the scatterplot that galagids and tarsiers, which engage in a specialized locomotor behavior called vertical clinging and leaping (VCL), are outliers from the common trend exhibited by the rest of the sample. If galagids and tarsiers are removed from the analysis, the determination coefficient improves substantially ($r^2 = 0.919$; $p < 0.001$; SOM Fig. S10). A significant allometric relationship is found between PC1 and ln BM, but not with ln CS as the size variable (Table 5; SOM Fig. S11A, B). Significant differences are also found in PC1 between tarsi-fulcrumators and metatarsi-fulcrumators, and the interaction between ln BM and foot type is significant as well, explaining up to 27% of the total variance.

The PC2 (accounting for 5% of the total variance; Fig. 8) reflects changes in the shape and orientation of the ectal facet (more saddle shaped toward negative scores and more rounded and oblique toward positive scores), shape and orientation of the sustentacular facet (narrower and more dorsally oriented in negative scores and mediolaterally broader and medially oriented toward positive scores), position of the peroneal tubercle (more distally in negative scores than in positive ones), shape and orientation of the tuber calcanei (straighter, mediolaterally broader, and dorsoplantarly higher in negative scores and medially oriented and dorsoplantarly lower in positive scores), shape of the cuboid facet (flatter in negative scores and more concave in positive scores), and plantar edge shape (straighter in negative scores and more concave toward positive scores; Fig. 9). The PC2 separates lorisids (very positive scores) from extant anthropoids, tarsiids, and nonprimate euarchontans (negative scores). The remaining extant strepsirrhines are located between these groups in slightly positive scores. Most fossil species are projected onto slightly positive scores as well, largely overlapping with extant lemuroids and galagids. *Caenopithecus lemuroides* overlies with lorisids in more positive scores than any other fossil species, and the Afro-Arabian anthropoids fall within platyrrhine variation in negative scores. Compared to PC1, this axis has a weaker (albeit significant) phylogenetic signal (Table 4). As expected from the only moderately strong phylogenetic signal, the phylogenetic PC1 (accounting for 10% of the total variation; SOM Fig. S8) depicts a similar distribution of the species, separating the most climbing and/or suspensory species of each group—lorisids, atelids, and *Ptilocercus lowii*—from the most quadrupedal ones. Remarkably, the phylogenetic PC2 differs from the standard PC2 by associating distal calcaneal elongation with positive scores too. This association may explain the greater amount of variance explained by this axis than the standard PC2. Unlike PC1, the only significant allometric relationship is found between PC2 and ln CS (Table 5; SOM Figs. S11C, D), explaining up to 11% of the total variance. Neither significant differences in PC2 were found between tarsi-fulcrumators and metatarsi-fulcrumators nor a significant interaction was found between either size variable and foot type.

3.3. Astragalar shape as a predictor for locomotion

The covariation between astragalar shape and locomotor behavior is significant and explains up to 92% of covariance in the first two PLS axes (Table 6). Mean absolute error resulting from the cross-validated results performed on the extant species set reveals that the analysis accurately predicted all five locomotor variables (Table 7; SOM Fig. S12; SOM Table S4).

The first axis (PLS1; Fig. 10A) resembles PC2 (Fig. 6A) and discriminates between the more suspensory lorisids, atelids, dermopterans, and *Da. madagascariensis*, with more positive scores of the shape axis, and specialized VCL species (i.e., tarsiers, galagids, lepilemurids, and indriids). The group of more suspensory primates is characterized by a dorsoplantarly low astragalar body, a proximodistally elongated and slightly grooved trochlea, a laterally sloping fibular facet, a flat and slightly laterally oriented ectal facet, a proximodistally short and mediolaterally broad neck, and a relatively large and mediolaterally expanded head (Fig. 11). Conversely, the specialized leaping species possess a dorsoplantarly high astragalar body, a proximodistally abbreviated trochlea, a relatively deep trochlear groove, a comparatively steep fibular facet, a concave and plantarly oriented ectal facet, a proximodistally elongated and mediolaterally narrow astragalar neck, and a spherical astragalar head (Fig. 11). Plesiadapiforms display positive scores, suggesting that suspensory behaviors were an important component of their locomotor repertoire. Among fossil euprimates, the *Adapis* group exhibits the most positive scores, followed by *V. major* and *M. indicus*, indicating that suspension was also an important component of their locomotor repertoires. Notharctines, *L. magnus* and *Ganlea* are projected onto slightly positive scores, overlapping with more generalized species. The remaining species (*Eosimias*, the parapithecids, *An. frontanyensis*, *D. martinezi*, and most omomyiforms in exclusion of *V. major*) are plotted toward more negative values of the shape axis, indicating higher percentages of leaping behavior.

The second axis (PLS2; Fig. 10B) exhibits a clear phylogenetic pattern that nevertheless is also correlated with different

Table 6
Results of the two-block partial least squares (2B-PLS) between species-mean Procrustes shape coordinates of astragalar and calcaneal shape and quantified locomotor data.[a]

Bone	Latent variables	Singular value	% covariation	r-PLS	*p*
Astragalus	PLS1*	0.017	63.298	0.790	**<0.001**
	PLS2*	0.011	28.410	0.731	**<0.001**
	PLS3	0.006	7.371	0.666	**<0.001**
	PLS4	0.002	0.696	0.489	0.164
	PLS5	0.001	0.224	0.497	**0.026**
Calcaneus	PLS1*	0.039	88.463	0.565	**<0.001**
	PLS2*	0.012	8.964	0.753	**<0.001**
	PLS3	0.006	2.397	0.713	**<0.001**
	PLS4	0.001	0.125	0.413	0.177
	PLS5	0.001	0.051	0.467	0.015

Abbreviations: r-PLS = correlation coefficient between PLS scores.
[a] Significant results ($p < 0.05$) are indicated in bold, while the most explanatory PLS axes are denoted with asterisks.

Table 7
Mean absolute error (MAE)[a] calculated for the entire comparative sample after comparing the original locomotor values compiled for each extant species with the predicted ones using a leave-one-out cross-validation approach.

	Astragalus	Calcaneus
Q	0.172	0.184
C	0.101	0.095
L	0.174	0.162
S	0.138	0.134
CC	0.136	0.122

Abbreviations: Q = quadrupedalism; C = climbing; L = leaping; S = suspension; CC = clawed clinging/climbing.
[a] MAE is defined as the arithmetic average of the absolute errors.

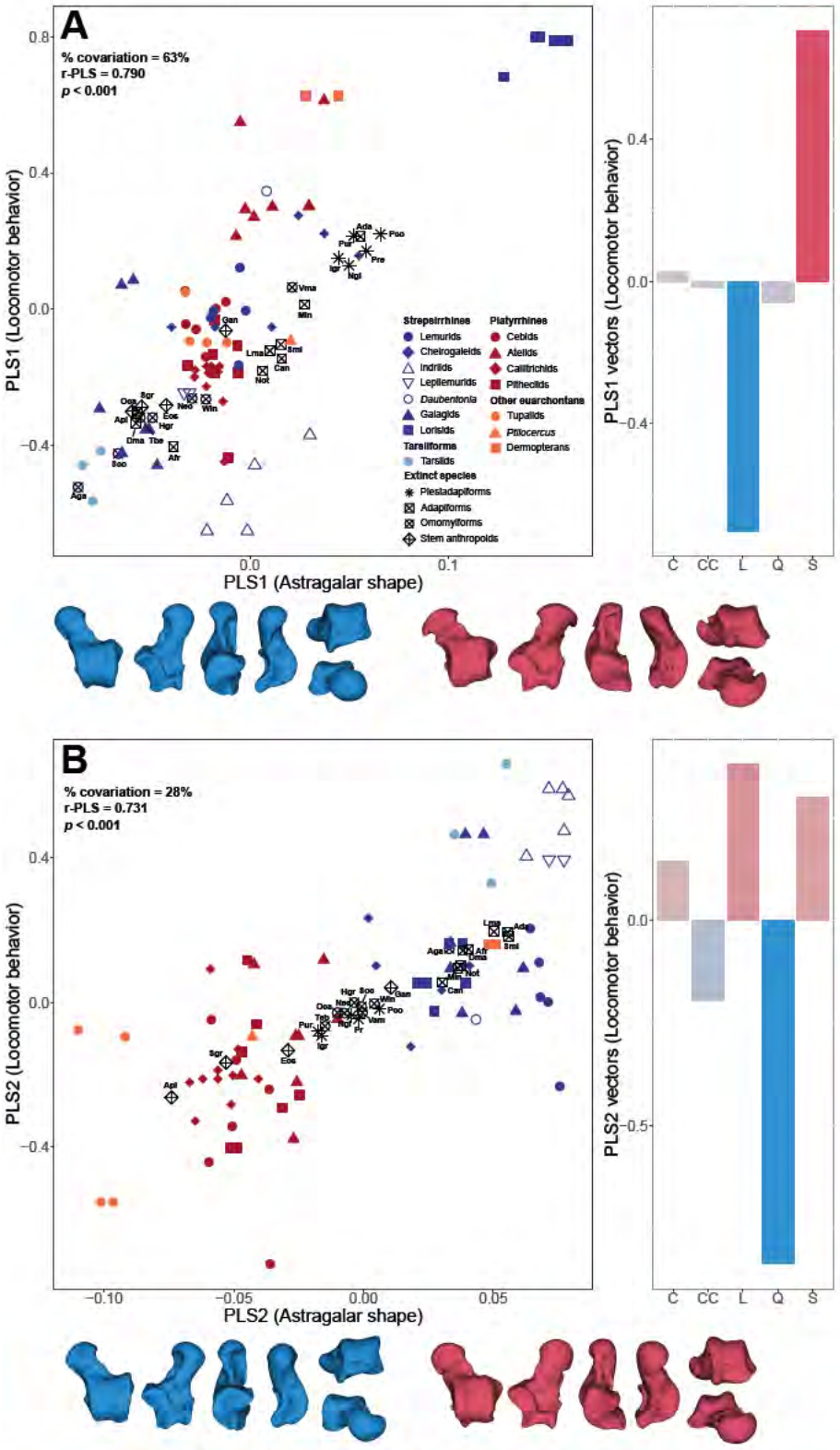

Figure 10. Results of the partial least squares regression (PLSR) for the first (PLS1; A) and second (PLS2; B) sets of linear combinations between the species-mean Procrustes shape coordinates (astragalar shape) and quantified locomotor data. The vectors of the first (A) or second (B) PLS axis of the locomotor variables are plotted to the right of each scatterplot. Taxonomic groups are coded by color and symbol, as indicated in the legend. Astragalar shapes associated with minimum (blue) and maximum (red) values of covariation are plotted below each scatterplot (dorsal, plantar, lateral, medial, proximal, and distal views are shown, from left to right). Thin-plate splines correspond to an astragalus of *Plecturocebus moloch* (AMNH 244363). Abbreviations: Q = quadrupedalism; C = climbing; L = leaping; S = suspension; CC = clawed clinging/climbing; Api = *Apidium*; Sgr = *Simonsius grangeri*; Gan = *Ganlea*; Eos = *Eosimias*; Nec = *Necrolemur*; Hgr = *Hemiacodon_gracilis*; Sco = *Shoshonius cooperi*; Win = *Washakius insignis*; Oca = *Omomys carteri*; Aga = *Arapahovius gazini*; Vma = *Vastanomys major*; Tbe = *Teilhardina belgica*; Dma = *Djebelemur martinezi*; Afr = *Anchomomys frontanyensis*; Ada = *Adapis* group; Lma = *Leptadapis magnus*; Smi = *Smilodectes*; Not = *Notharctus*; Can = *Cantius*; Min = *Marcgodinotius indicus*; Ngi = *Nanodectes gidleyi*; Pre = *Plesiadapis rex*; Pco = *Plesiadapis cookei*; Igr = *Ignacius graybullianus*; Pur = *Purgatorius*; PLS = partial least squares; r-PLS = correlation coefficient between PLS scores. (For interpretation of the references to color in this figure legend, the reader is referred to the web version of this article.)

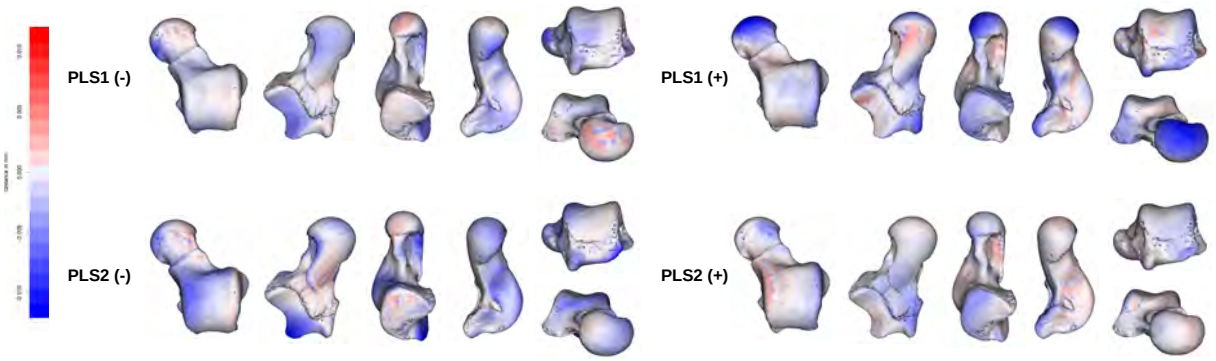

Figure 11. Displacement heatmaps illustrating mesh distances between the mean astragalar shape of each PLS shape axis depicted in Figure 10 against the shapes associated with the minimum (−) and maximum (+) values. Blue and red indicate regions of contraction and expansion, respectively, based on the position of the extreme astragalar shapes (minimum or maximum values) relative to the mean shape along each PLS shape axis. PLS = partial least squares. (For interpretation of the references to color in this figure legend, the reader is referred to the web version of this article.)

locomotor behaviors, resembling PC3 (Fig. 6B). Species with higher percentages of quadrupedalism, such as tree shrews and most platyrrhines, exhibit the most negative values along the shape axis, associated with a dorsoplantarly low astragalar body, a flat and slightly wedged trochlea (wider distally than proximally) with an elevated lateral rim, a steep fibular facet, a restricted medial tibial facet, an only slightly concave ectal facet, and a laterally tilted head (Fig. 11). In contrast, those species (strepsirrhines, dermopterans, and tarsiids) with a higher proportion of suspensory behaviors, leaping, and climbing, which can be interpreted as an emphasis in a 'grasp-leaping' behavior in euprimates, display the most positive scores and exhibit a dorsoplantarly high astragalar body, a moderately grooved trochlea with equally high parallel rims, a sloping fibular facet, a broad and dorsoplantarly extended medial tibial facet, a moderately concave ectal facet, and a head comparably oriented in the horizontal plane (Fig. 11). Plesiadapiforms, *Ganlea*, and most omomyiforms are projected onto intermediate scores between the two clusters formed by platyrrhines (negative scores) and strepsirrhines and tarsiers (positive scores). This indicates no predominance in their locomotor behavior of neither quadrupedalism nor a combination of suspensory and climbing and/or leaping behaviors typical of most extant prosimians. Conversely, *Eosimias* and the parapithecids are projected onto negative scores, overlapping with platyrrhines and suggesting an important quadrupedal component in their locomotor repertoire, whereas adapiforms and *Arapahovius gazini* fall with the extant strepsirrhine/tarsier cluster, indicating greater frequencies of suspensory, leaping, and climbing behaviors.

3.4. Calcaneal shape as a predictor for locomotion

There is significant covariation between calcaneal shape and locomotor behavior and explains 97% of the total covariance in the first two PLS axes (Fig. 12; Table 6). Mean absolute error resulting from the cross-validated results performed on the extant species set reveals that the analysis accurately predicted all five locomotor variables (Table 7; SOM Fig. S13; SOM Table S5).

The first axis (PLS1; Fig. 12A) is primarily related to distal calcaneal elongation, resembling PC1 (Fig. 8A). Species associated with high percentages of either quadrupedalism or suspension, in positive scores, are characterized by a proximodistally short distal calcaneus with mediolaterally wide ectal and sustentacular facets and a dorsoplantarly high and concave cuboid facet with a comparatively deep cuboid pit (Fig. 13). Conversely, leaping behaviors, exhibited by galagids and tarsiers (small VCL species), in negative scores, are associated with an extreme proximodistal elongation of the distal part of the calcaneus and mediolaterally narrow and restricted ectal and sustentacular facets (Fig. 13). Larger-bodied specialized VCL species, namely indriids and *Lepilemur*, are clear outliers of the trend observed in the scatterplot, displaying relatively positive scores in the shape axis and negative scores in the locomotor axis. Neither indriids nor lepilemurids exhibit extreme proximodistal elongation of the distal calcaneus. Plesiadapiforms display very positive scores, indicating that quadrupedalism and suspension were frequent behaviors in their locomotor repertoire. Omomyiforms and the small-sized adapiform *An. frontanyensis* overlap between cheirogaleids and non-indriid lemuroids, suggesting moderate use of climbing and leaping behaviors, without reaching the extremes exhibited by galagids and tarsiers. In contrast, the remaining adapiforms fall among anthropoids, indicating a higher frequency of quadrupedalism in their locomotion. *Caenopithecus lemuroides* is located very close to lorisids, denoting a similar type of locomotion. Early anthropoids are projected closer to adapiforms, except for *Eosimias*, which overlaps with omomyiforms.

The second axis (PLS2; Fig. 12B) resembles PC2 (Fig. 8) and phylogenetic PC2 (SOM Fig. S8), separating the most suspensory species (lorisids, atelids, and dermopterans) from the most quadrupeds (tupaiids, pitheciids, and cebids), as well as clawed clingers (callitrichids). Suspensory species, in most positive scores, are associated with a rounded and oblique ectal facet, mediolaterally broad and medially oriented sustentacular facet, a very proximally located peroneal tubercle, a medially oriented and dorsoplantarly low tuber calcanei, a very concave cuboid facet, and a concave plantar edge (Fig. 13). Conversely, quadrupedal species, in negative scores, exhibit a saddle-shaped ectal facet, a narrow and dorsally oriented sustentacular facet, a distally positioned peroneal tubercle, a straight, stout, and mediolaterally broad tuber calcanei, a flat cuboid facet, and a straight plantar edge (Fig. 13). Plesiadapiforms are distributed along the shape axis in a gradient, ranging from *Purgatorius* (negative scores) to *C. simpsoni* (positive scores), indicating distinct proportions of quadrupedal and suspensory behaviors within their locomotor repertoire depending on the species. Most adapiforms and omomyiforms are projected onto slightly negative to slightly positive scores, indicating a predominance of quadrupedalism over suspension, albeit some species like *Ca. lemuroides*, *M. indicus*, *Ar. gazini*, and *An. frontanyensis* are in more positive scores, suggesting a greater reliance in suspensory locomotion. Within anthropoids, the Afro-Arabian anthropoids are distinguished by their very negative scores, whereas *Eosimias* overlaps with adapiforms and omomyiforms in slightly positive scores. This result suggests that while the former probably

engaged in mostly quadrupedal locomotion with little to no suspension, *Eosimias* exhibited a more versatile locomotor behavior that included some degree of suspensory locomotion.

3.5. Variation in the locomotor behavior of Paleogene primates

Variation in the predicted percentages of locomotion in Paleogene primates not only supports the existence of a diverse array of locomotor behaviors among the various primate groups represented in this study but, in some cases, also denotes different estimates for some locomotor categories depending on the bone used as a predictor (Figs. 14–16; Tables 8 and 9).

When astragalar shape is used as a predictor, all plesiadapiform species are reconstructed displaying a very similar locomotor repertoire, with an important quadrupedal component (42–47%), and moderate amounts of climbing (14–22%), leaping (15–24%), and suspension (15–20%). No clawed clinging/climbing behavior is inferred for plesiadapiforms when astragalar shape is utilized as a predictor. This locomotor profile approaches the condition exhibited by *Cheirogaleus*, as well as that of the most arboreal tree shrews (*P. lowii* and *Tupaia minor*). Contrarily, when calcaneal shape is used as a predictor, plesiadapiforms reveal a different picture: on the one hand, *Purgatorius*, *Tinimomys graybulliensis*, and *Phenacolemur* (i.e., nonplesiadapoid plesiadapiforms) are characterized by relatively high amounts of quadrupedalism (60–67%) followed by small amounts of the other behaviors (>15%), except for clawed clinging/climbing. The only exception to this is *T. graybulliensis*, which is inferred to suspend more than the other two (19%). On the other hand, the locomotor repertoire of *Pl. cookei* and *C. simpsoni* (i.e., plesiadapoids) is dominated by quadrupedalism (42–49%) and suspension (26–32%), with only moderate amounts of climbing (15%) and traces of leaping (2–4%). Contrasting with nonplesiadapoid species, both *Pl. cookei* and *C. simpsoni* are inferred to participate in some degree of scansorial behavior as well (6–9%). The former nonplesiadapoid species mostly resembles extant tupaiids in their inferred locomotor repertoire. In contrast, plesiadapoids (particularly *C. simpsoni*) approach the locomotor profile of lorisids and other suspensory species (e.g., dermopterans and *Da. madagascariensis*).

Among early euprimates, adapiforms are the group exhibiting the most diverse locomotor behavior. Overall, three different main locomotor repertoires can be inferred from their estimated locomotion. The first one, exhibited by most species, is that of an arboreal quadruped and leaper, characterized by higher percentages (mostly above 30%) for both locomotor behaviors. When astragalar shape is used as a predictor, most notharctines, *M. indicus, L. magnus,* as well as *An. frontanyensis* and *D. martinezi* for both bones, concur with this locomotor profile. Remarkably, when astragalar shape is used as the predictor, higher values for leaping behavior are recovered (40–58%), whereas when calcaneal shape is utilized, comparatively higher percentages for suspension (up to 16%) are obtained for these species. Compared to extant species, they are better analogized to lemurids (in the case of notharctines and *L. magnus*) and to *Mirza* and *Microcebus* (*M. indicus*, *An. frontanyensis*, and *D. martinezi*). The second locomotor profile, characterized by a high quadrupedal component (49–55%), is represented by the *Adapis* group, *L. magnus*, and *Copelemur tutus* when calcaneal shape is used as the predictor. In this case, they are better analogized to small quadrupedal anthropoids (e.g., *Saimiri*, *Cebus*, and *Callicebus*), which participate in different arboreal behaviors (climbing, leaping, and suspension) but mainly move quadrupedally above relatively large supports. Lastly, the third locomotor profile is characterized by a high proportion of suspension (28–30%) and relatively low values for the other behaviors, particularly leaping. *Marcgodinotius indicus* and *Ca. lemuroides* fit this locomotor profile when calcaneal shape is used as a predictor and the *Adapis* group, when astragalar shape is used as a predictor. They resemble extant lorisids, *Daubentonia*, and *Cheirogaleus* due to their inferred emphasis on suspension.

Omomyiforms consistently exhibit a very homogeneous locomotor repertoire when either astragalar or calcaneal shape is used as the predictor. All omomyiforms display high percentages of leaping behavior (39–64%), followed by moderate amounts of quadrupedalism (20–39%) and climbing (12–23%). Compared with extant species, omomyiforms most closely resemble *Microcebus* and the most generalized galagids (i.e., those that more rarely engage in VCL behaviors). The only exception is *V. major*, which is inferred to have relied more on quadrupedalism (41%) and to have been a less frequent leaper (27%). In addition, moderate amounts of climbing (20%) and suspension (12%) indicate a more generalized behavior for this species, approaching that of *Otolemur*.

Anthropoids are reconstructed as mostly relying on quadrupedalism (43–55%) and leaping (30–42%), with small amounts of climbing in their locomotor repertoire as well (12–15%). Remarkably, they are inferred not to participate in suspensory behaviors at all. This locomotor profile is exhibited by parapithecids, *Proteopithecus sylviae*, and *Eosimias* when astragalar shape is used as the predictor, resembling the locomotor repertoire exhibited by extant small platyrrhines (e.g., *Saimiri*, *Cebus*, and *Callicebus*). Contrarily, when calcaneal shape is used as the predictor, *Ganlea* and *Eosimias* display less emphasis on quadrupedalism (28–31%), higher amounts of leaping (36–39%), and moderate frequency of climbing (19–20%). In addition, they are inferred to have moved using suspension as well (6–13%). This results in *Eosimias* (as predicted from calcaneal shape) approaching the condition exhibited by extant cheirogaleids, whereas *Ganlea* is better analogized to extant lemurids and *Otolemur*.

3.6. The evolution of astragalar and calcaneal shape in relation to locomotor changes among early primates

Branch-specific rate reconstructions (Fig. 17A, B) indicate that the transition from plesiadapiforms to euprimates exhibits very high evolutionary rates, the highest across the entire tree in the case of the calcaneus. Plesiadapiform branches are also characterized by very high evolutionary rates, particularly plesiadapoids. Similarly, adapiforms and omomyiforms display high evolutionary rates. Among the former, *Ca. lemuroides* and adapines exhibit particularly high evolutionary rates for the calcaneus, while the other species do not show increased rates compared to the branch leading from the euprimate LCA, suggesting less morphological change. In contrast, evolutionary rates for the astragalus remain consistently high across all adapiform species. Omomyiforms display increased evolutionary rates for both bones, with further increases in the branch leading to crown tarsiiforms. Remarkably, evolutionary rates in the branch leading to anthropoids are consistently low, indicating little morphological change between the euprimate/haplorrhine and anthropoid LCAs. However, in both bones, the lineage leading to the clade comprised by crown anthropoids and Afro-Arabian parapithecids and proteopithecids—to the exclusion of *Eosimias* and *Ganlea*—is characterized by increased evolutionary rates, suggesting significant morphological changes were occurring along this branch. Additionally, extant groups that exhibit specialized locomotor behaviors—such as lorisids, galagids, atelids, and tarsiids—display higher evolutionary rates at the base of their clades than other groups. This pinpoints that evolutionary rates of astragalar and calcaneal morphology are informative about locomotor transitions.

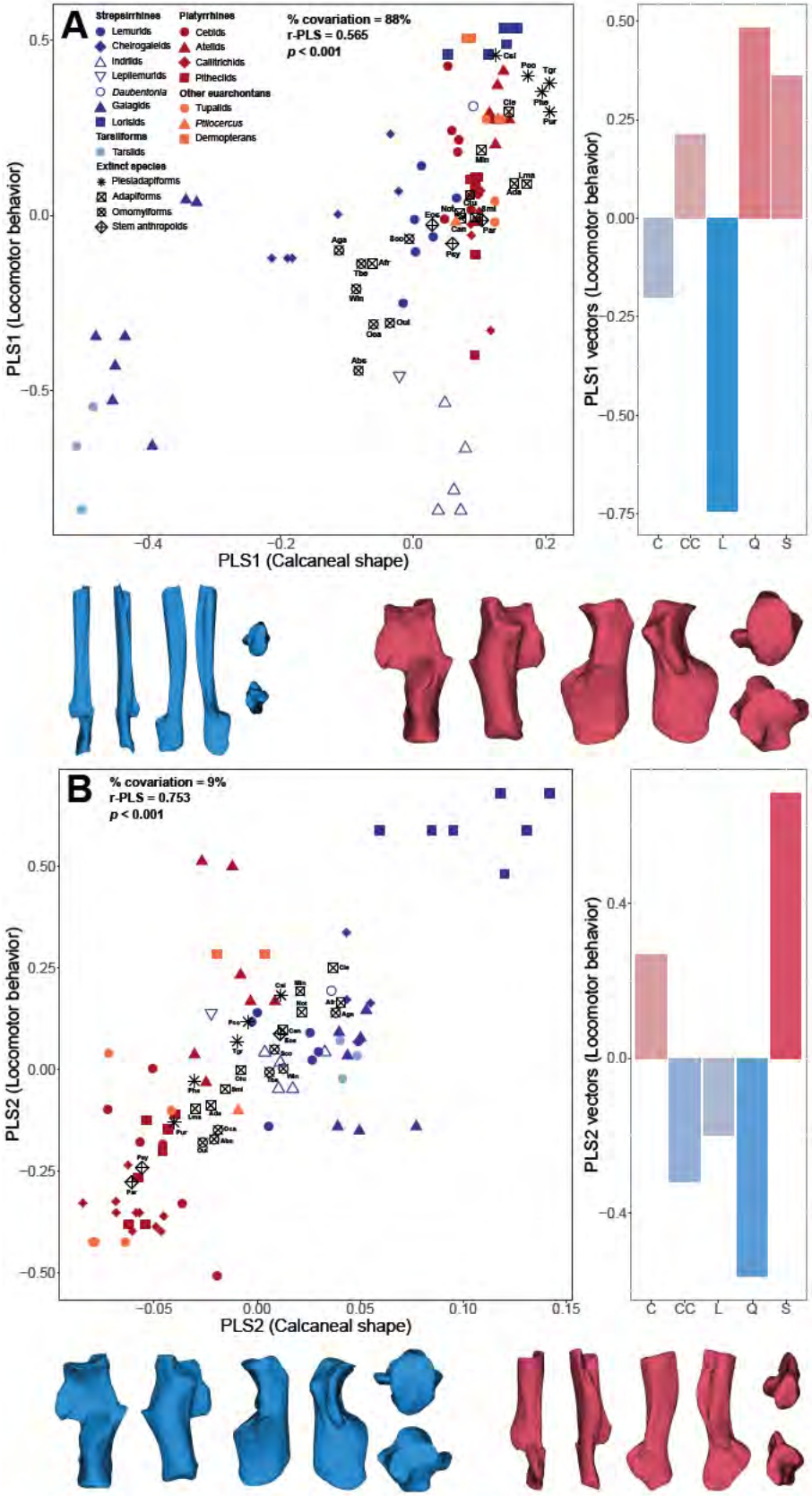

Figure 12. Results of the partial least squares regression (PLSR) for the first (PLS1; A) and second (PLS2; B) sets of linear combinations between the species-mean Procrustes shape coordinates (calcaneal shape) and quantified locomotor data. The vectors of the first (A) or second (B) PLS axis of the locomotor variables are plotted to the right of each scatterplot. Taxonomic groups are coded by color and symbol, as indicated in the legend. Calcaneal shapes associated with minimum (blue) and maximum (red) values of covariation are plotted below each scatterplot (dorsal, plantar, lateral, medial, and proximal views are shown, from left to right). *Eulemur albifrons* (AMNH 170717). Abbreviations: Q = quadrupedalism; C = climbing; L = leaping; S = suspension; CC = clawed clinging/climbing; Par = Parapithecidae indet; Psy = *Proteopithecus sylviae*; Eos = *Eosimias*;

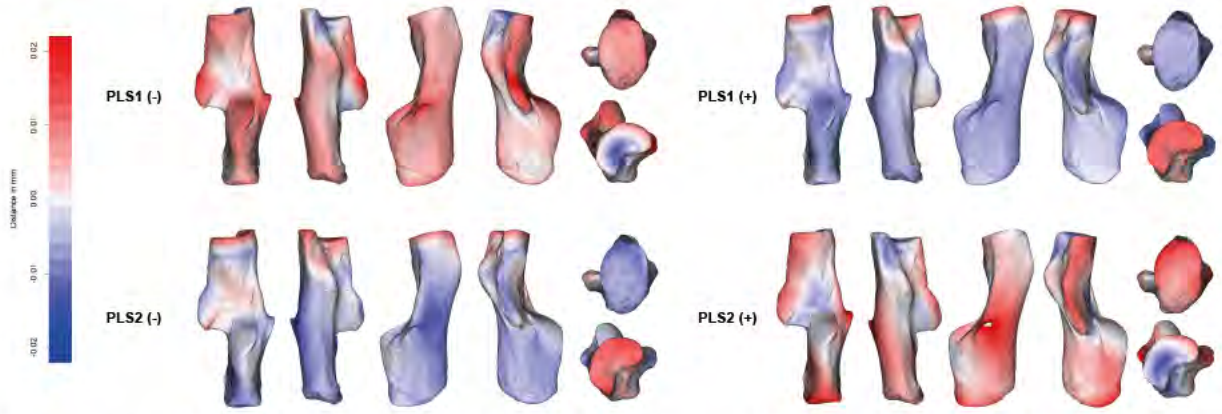

Figure 13. Displacement heatmaps illustrating mesh distances between the mean calcaneal shape of each PLS shape axis depicted in Figure 12 against the shapes associated with the minimum (−) and maximum (+) values. Blue and red indicate regions of contraction and expansion, respectively, based on the position of the extreme calcaneal shapes (minimum or maximum values) relative to the mean shape along each PLS shape axis. PLS = partial least squares. (For interpretation of the references to color in this figure legend, the reader is referred to the web version of this article.)

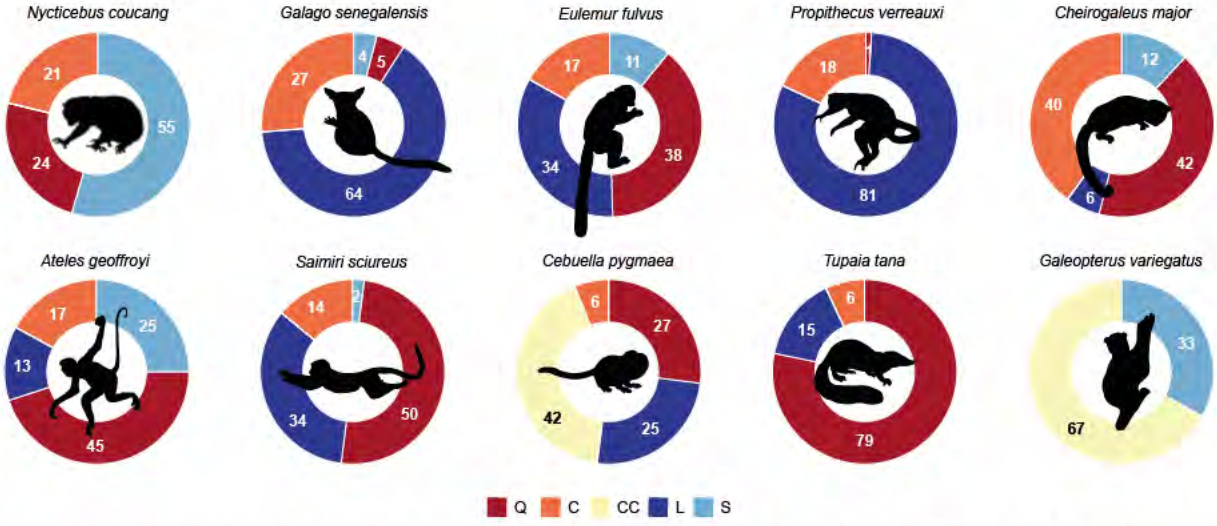

Figure 14. Donut charts summarizing the locomotor repertoire of a representative sample of the main primate groups (and close relatives) from the extant comparative sample. Abbreviations: Q = quadrupedalism; C = climbing; L = leaping; S = suspension; CC = clawed clinging/climbing. (For interpretation of the references to color in this figure, the reader is referred to the web version of this article.)

Increases in the rates of morphological evolution in both bones are reflected by the ancestral locomotor reconstructions (Fig. 17C, D; Table 10). The locomotor repertoires of the euarchont and primate LCAs are estimated to be very similar, dominated by quadrupedalism (39–49%) and lower amounts of the other locomotor variables (<26%). Conversely, the euprimate LCA shows an important increase in leaping behavior (22–32%). The strepsirrhine, tarsiiform, and anthropoid LCAs are reconstructed as more habitual leapers (24–43%) than the euprimate LCA, suggesting further increases in leaping behavior occurring in the different euprimate lineages. More specifically, the tarsiiform LCA shows the highest percentages of leaping behavior, whereas the anthropoid LCA exhibits comparatively higher percentages of quadrupedal locomotion (39–40%). Lastly, the strepsirrhine LCA is reconstructed as engaging in substantially higher suspension (12–17%) than either the tarsiiform or anthropoid LCAs.

4. Discussion

4.1. Functional morphology of the astragalocalcaneal complex

Comparative anatomy is a powerful tool to elucidate the relationship between the shape of a given structure (e.g., the hindfoot) and function (which might provide hints of the 'biological role', sensu Bock and von Wahlert, 1965). If this correlation is found to be strong, it allows us to provide reliable morphofunctional inferences—as it may be expected that similar selective pressures lead to similar anatomical adaptations (Lauder, 1986).

Oui = *Ourayia uintensis*; Sco = *Shoshonius cooperi*; Win = *Washakius insignis*; Oca = *Omomys carteri*; Abs = *Absarokius*; Aga = *Arapahovius gazini*; Tbe = *Teilhardina belgica*; Afr = *Anchomomys frontanyensis*; Ada = *Adapis* group; Lma = *Leptadapis magnus*; Cle = *Caenopithecus lemuroides*; Ctu = *Copelemur tutus*; Smi = *Smilodectes*; Not = *Notharctus*; Can = *Cantius*; Min = *Marcgodinotius indicus*; Csi = *Carpolestes simpsoni*; Pco = *Plesiadapis cookei*; Phe = *Phenacolemur*; Tgr = *Tinimomys graybulliensis*; Pur = *Purgatorius*; PLS = partial least squares; r-PLS = correlation coefficient between PLS scores. (For interpretation of the references to color in this figure legend, the reader is referred to the web version of this article.)

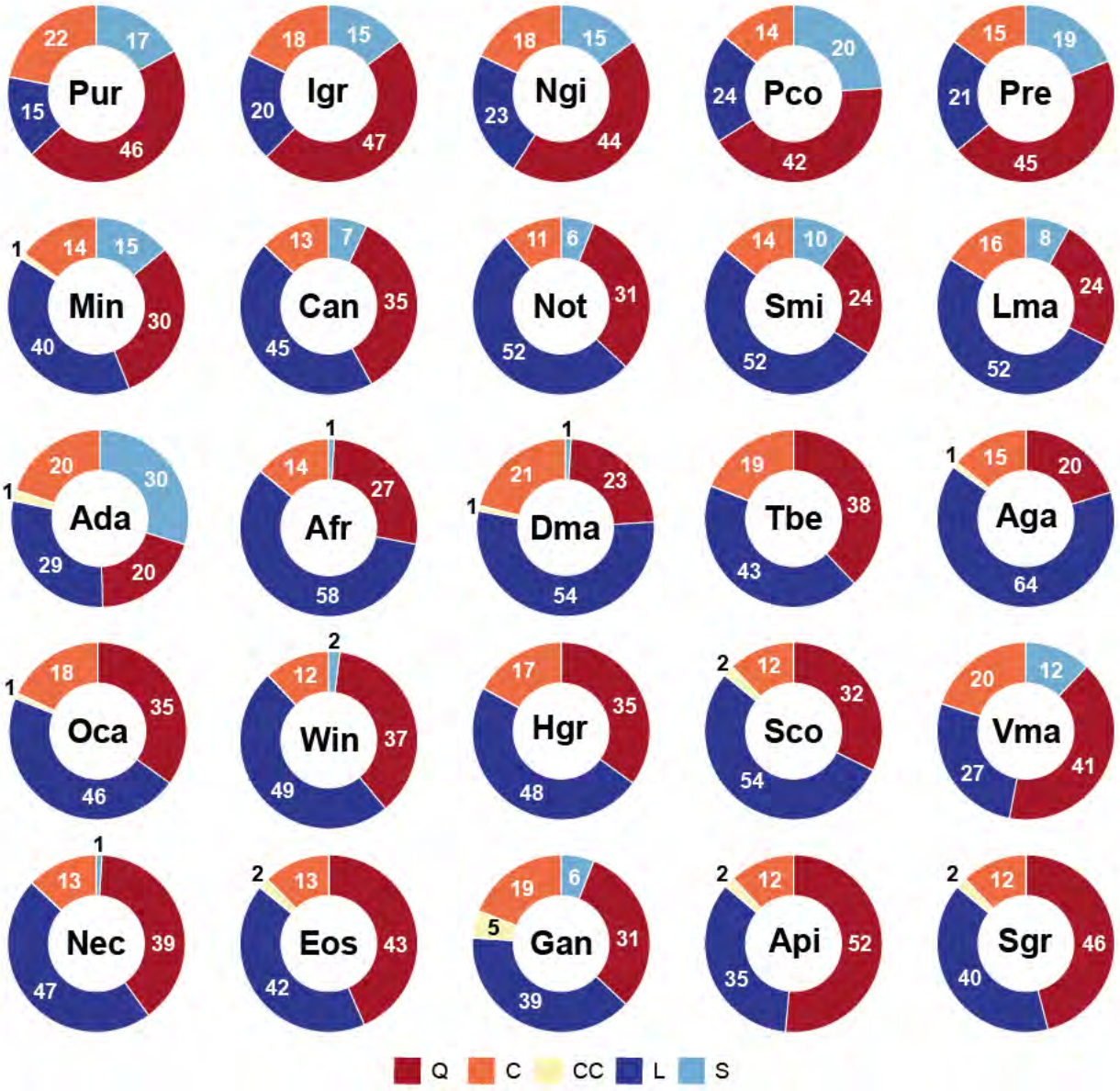

Figure 15. Donut charts summarizing the estimated locomotor repertoires of the extinct Paleogene taxa based on astragalar shape. Abbreviations: Q = quadrupedalism; C = climbing; L = leaping; S = suspension; CC = clawed clinging/climbing. Api = *Apidium*; Sgr = *Simonsius grangeri*; Gan = *Ganlea*; Eos = *Eosimias*; Nec = *Necrolemur*; Hgr = *Hemiacodon_gracilis*; Sco = *Shoshonius cooperi*; Win = *Washakius insignis*; Oca = *Omomys carteri*; Aga = *Arapahovius gazini*; Vma = *Vastanomys major*; Tbe = *Teilhardina belgica*; Dma = *Djebelemur martinezi*; Afr = *Anchomomys frontanyensis*; Ada = *Adapis* group; Lma = *Leptadapis magnus*; Smi = *Smilodectes*; Not = *Notharctus*; Can = *Cantius*; Min = *Marcgodinotius indicus*; Ngi = *Nanodectes gidleyi*; Pre = *Plesiadapis rex*; Pco = *Plesiadapis cookei*; Igr = *Ignacius graybullianus*; Pur = *Purgatorius*. (For interpretation of the references to color in this figure, the reader is referred to the web version of this article.)

Below, the main morphofunctional relationships between the hindfoot and locomotor behavior among primates (and their closest relatives) are discussed on the basis of both the correlations observed between tarsal shape and function and their relevance regarding plesiadapiform and early euprimate locomotor behavior.

In line with previous studies, our results indicate that the shape of the facets that conform the different joints constituting the ankle and tarsal elongation encompasses most functional information to reliably predict the locomotor behavior in extinct species (e.g., Szalay and Decker, 1974; Conroy and Rose, 1983; Moyà-Solà et al., 2012; Boyer and Seiffert, 2013; Boyer et al., 2013b, 2015; Parr et al., 2014; Yapuncich et al., 2017, 2019; Yapuncich and Granatosky, 2021). Our analyses show a strong correlation between astragalar/calcaneal shape and suspensory behaviors, such as a dorsoplantarly low astragalar body, a proximodistally elongated and slightly grooved trochlea, a laterally sloping fibular facet, a flat and slightly laterally oriented ectal facet, a proximodistally short and mediolaterally broad neck, a relatively large and mediolaterally expanded head (for the astragalus), a rounded an oblique ectal facet, mediolaterally broad and medially oriented sustentacular facet, a very proximally located peroneal tubercle, a medially oriented and dorsoplantarly low tuber calcanei, a very concave cuboid facet, and a concave plantar edge (for the calcaneus). Previous studies have shown that suspensory species (lorisids, atelids, dermopterans, *Daubentonia*, and *Cheirogaleus*) exhibit many to all of these features to some degree (Sarmiento, 1983; Gebo, 1989a; Boyer and Seiffert, 2013; Yapuncich and Granatosky, 2021), resulting in increased foot mobility that allows them to engage in different types of slow locomotion dominated by cautious climbing along with other types of progression, such as bridging movements to cross spatial gaps in

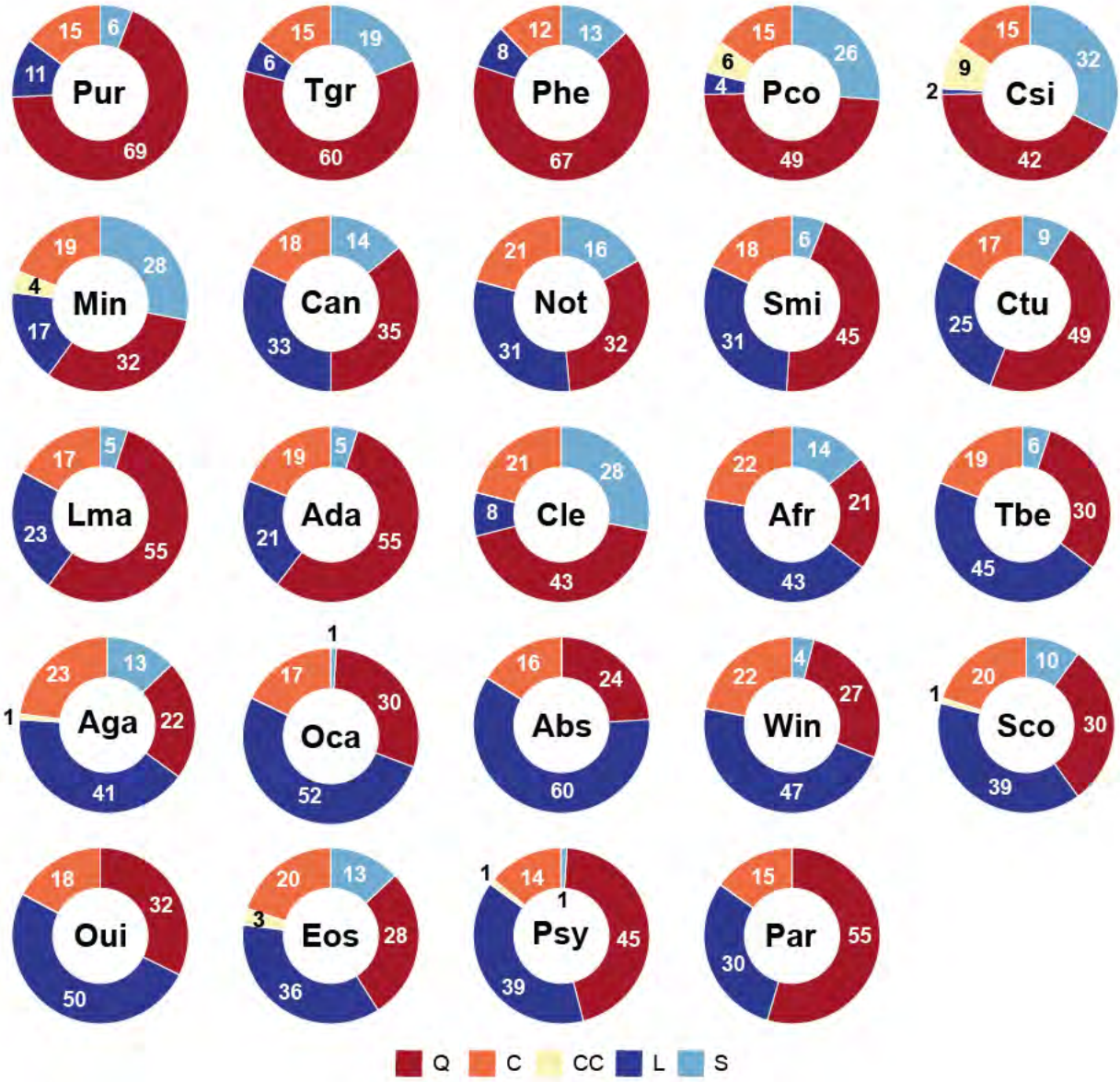

Figure 16. Donut charts summarizing the estimated locomotor repertoires of the extinct Paleogene taxa based on calcaneal shape. Abbreviations: Q = quadrupedalism; C = climbing; L = leaping; S = suspension; CC = clawed clinging/climbing. Par = Parapithecidae indet; Psy = *Proteopithecus sylviae*; Eos = *Eosimias*; Oui = *Ourayia uintensis*; Sco = *Shoshonius cooperi*; Win = *Washakius insignis*; Oca = *Omomys carteri*; Abs = *Absarokius*; Aga = *Arapahovius gazini*; Tbe = *Teilhardina belgica*; Afr = *Anchomomys frontanyensis*; Ada = *Adapis* group; Lma = *Leptadapis magnus*; Cle = *Caenopithecus lemuroides*; Ctu = *Copelemur tutus*; Smi = *Smilodectes*; Not = *Notharctus*; Can = *Cantius*; Min = *Marcgodinotius indicus*; Csi = *Carpolestes simpsoni*; Pco = *Plesiadapis cookei*; Phe = *Phenacolemur*; Tgr = *Tinimomys graybulliensis*; Pur = *Purgatorius*. (For interpretation of the references to color in this figure, the reader is referred to the web version of this article.)

the canopy and below-branch suspension (Gebo, 1987a; Oxnard et al., 1990; Youlatos and Meldrum, 2011; Youlatos et al., 2018). Some of these features (such as the medial bending of the tuber calcanei or a mediolaterally broader trochlea and calcaneal ectal facets) are found in some extinct species, including, *M. indicus*, *Ca. lemuroides*, and the *Adapis* group (Godinot, 1991; Seiffert et al., 2015; Dunn et al., 2016; Llera Martín et al., 2022). Additionally, as indicated by the allometric regressions, body size appears to influence certain climbing-related features, particularly in the astragalus (e.g., lower astragalar body and relatively larger facet areas than in fast-leaping and quadrupedal species). This pattern may stem from the distinct biomechanical constraints faced by larger-bodied species (Demes and Günther, 1989; Preuschoft et al., 1996), as exemplified by atelids and indriids compared to smaller platyrrhines and strepsirrhines, respectively (Fleagle and Mittermeier, 1980; Gebo and Dagosto, 1988). Lorisids are outliers from this allometric regression, representing the most extreme morphology for these features irrespective of their body size (Gebo, 1989a).

Conversely, specialized leapers display the opposite condition, characterized by features functionally related to foot stability (Gebo, 1987b, 1988; Boyer et al., 2013b), such as a dorsoplantarly high astragalar body, a proximodistally abbreviated trochlea, a relatively deep trochlear groove, a comparatively steep fibular facet, a concave and plantarly oriented ectal facet, a proximodistally elongated and mediolaterally narrow astragalar neck, a spherical astragalar head (in the astragalus), mediolaterally narrow and restricted calcaneal ectal and sustentacular facets, and a straight calcaneal plantar edge (in the calcaneus). However, as climbing and clinging on vertical substrates is interwoven with leaping behavior in the case of VCL species (tarsiers, galagids, and

Table 8
Estimated locomotor percentages using species-mean Procrustes shape coordinates of astragalar shape as a predictor.

Family	Species	Q	C	L	S	CC
Plesiadapiformes:						
Purgatoriidae	*Purgatorius* sp.	46	22	15	17	0
Paromomyidae	*Ignacius graybullianus*	48	18	20	15	0
Plesiadapidae	*Nannodectes gidleyi*	44	18	23	15	0
Plesiadapidae	*Plesiadapis cookei*	42	14	20	24	0
Plesiadapidae	*Plesiadapis rex*	45	15	21	19	0
Omomyiformes:						
Incertae sedis	*Teilhardina belgica*	38	19	43	0	0
Incertae sedis	*Vastanomys major*	41	20	27	12	0
Omomyidae	*Arapahovius gazini*	20	14	64	0	1
Omomyidae	*Necrolemur* sp.	39	13	47	1	0
Omomyidae	*Hemiacodon gracilis*	35	17	48	0	0
Omomyidae	*Omomys carteri*	35	18	46	0	1
Omomyidae	*Shoshonius cooperi*	32	12	53	0	2
Omomyidae	*Washakius insignis*	37	12	49	2	0
Adapiformes:						
Notharctidae	*Marcgodinotius indicus*	30	15	40	14	1
Notharctidae	*Cantius* sp.	35	13	45	7	0
Notharctidae	*Notharctus* sp.	31	11	52	6	0
Notharctidae	*Smilodectes* sp.	24	14	52	10	0
Notharctidae	*Anchomomys frontanyensis*	27	14	58	1	0
Adapidae	*'Adapis* group'	20	20	29	30	2
Adapidae	*Leptadapis magnus*	24	16	51	8	0
Stem Lemuriformes:						
Djebelemuridae	*Djebelemur martinezi*	23	21	54	1	1
Anthropoidea:						
Eosimiidae	*Eosimias* sp.	43	12	42	0	2
Amphipitheciidae	*Ganlea* sp.	31	19	39	6	5
Parapithecidae	*Apidium* sp.	52	12	35	0	2
Parapithecidae	*Simonsius grangeri*	46	12	40	0	2

Abbreviations: Q = quadrupedalism; C = climbing; L = leaping; S = suspension; CC = clawed clinging/climbing.

Table 9
Estimated locomotor percentages using species-mean Procrustes shape coordinates of calcaneal shape as a predictor.

Family	Species	Q	C	L	S	CC
Plesiadapiformes:						
Purgatoriidae	*Purgatorius* sp.	69	15	11	6	0
Micromomyidae	*Tinimomys graybulliensis*	60	15	6	19	0
Paromomyidae	*Phenacolemur* sp.	67	12	8	13	0
Plesiadapidae	*Plesiadapis cookei*	48	15	4	26	6
Carpolestidae	*Carpolestes simpsoni*	42	15	1	32	9
Omomyiformes:						
Incertae sedis	*Teilhardina belgica*	30	19	45	5	0
Omomyidae	*Absarokius* sp.	24	16	60	0	0
Omomyidae	*Arapahovius gazini*	22	23	41	13	1
Omomyidae	*Omomys carteri*	30	18	52	1	0
Omomyidae	*Ourayia uintensis*	32	17	50	0	0
Omomyidae	*Shoshonius cooperi*	30	20	39	10	1
Omomyidae	*Washakius insignis*	27	22	47	4	0
Adapiformes:						
Notharctidae	*Marcgodinotius indicus*	32	19	17	28	4
Notharctidae	*Cantius* sp.	35	18	33	14	0
Notharctidae	*Copelemur tutus*	47	17	27	9	0
Notharctidae	*Notharctus* sp.	32	21	31	17	0
Notharctidae	*Smilodectes* sp.	45	18	31	6	0
Notharctidae	*Anchomomys frontanyensis*	21	22	42	14	0
Adapidae	*'Adapis* group'	56	19	21	5	0
Adapidae	*Leptadapis magnus*	55	17	23	5	0
Adapidae	*Caenopithecus lemuroides*	43	21	8	28	0
Anthropoidea:						
Eosimiidae	*Eosimias* sp.	28	20	36	13	3
Parapithecidae	*Parapithecidae* indet.	54	15	30	0	0
Proteopithecidae	*Proteopithecus sylviae*	45	14	39	1	1

Abbreviations: Q = quadrupedalism; C = climbing; L = leaping; S = suspension; CC = clawed clinging/climbing.

indriids) and clawed clinging callitrichids (Gebo, 1987a; Oxnard et al., 1990; Youlatos, 1999), this results in an admixture of morphological features associated with leaping (functionally linked to increasing the lever arm or the stability of the tarsal joints) and climbing (increasing the mobility of the foot). More precisely, strepsirrhines that engage in specialized VCL behavior, such as galagids and indriids (excluding more 'occasional' leapers such as cheirogaleids and some lemurids), exhibit clear adaptations for climbing vertical substrates (e.g., a sloping fibular facet, contrasting with the steeper shape found in haplorhines), which paradoxically contribute to greater foot mobility (Beard et al., 1988; Gebo and Dagosto, 1988; Gebo, 2011).

Generalized arboreal quadrupeds (e.g., lemurids, cheirogaleids, and many nonatelid platyrrhines) lack the extreme morphological adaptations found in either slow climbing/suspensory or specialized VCL species (Gebo, 1988). Our analyses show that quadrupedal species exhibit a dorsoplantarly low astragalar body, a flat and slightly wedged trochlea (wider distally than proximally) with an elevated lateral rim, a steep fibular facet, a restricted medial tibial facet, an only slightly concave ectal facet, a laterally tilted head (in the astragalus), a saddle-shaped ectal facet, a narrow and dorsally oriented sustentacular facet, a distally positioned peroneal tubercle, a straight, stout, and mediolaterally broad tuber calcanei, a flat cuboid facet, and a straight plantar edge (in the calcaneus). This set of features provides stability at the ankle (less concomitant mediolateral movements during plantarflexion or dorsiflexion) and increases the power arm of the triceps surae (facilitating force transmission, which is greater in the context of quadrupedal locomotion on large substrates; Conroy and Rose, 1983; Gebo, 1986, 1989b; Strasser, 1988). Early anthropoids and some adapiforms exhibit many of these features, suggesting that above-branch quadrupedal running on large and horizontal substrates was an important component of their locomotor behavior (Fleagle, 1980; Conroy and Rose, 1983; Gebo and Simons, 1987; Gebo, 1989b; Godinot, 1991; Fleagle and Simons, 1995). In addition, scandentians, regardless of their locomotor repertoire, that grade from mainly arboreal to more terrestrial forms, exhibit much reduced foot mobility and grasping capabilities, resembling some of those found in small quadrupedal primates (Sargis, 2001, 2002a, 2002b; Youlatos et al., 2017; Granatosky et al., 2022). As already suggested, astragalar and calcaneal shape of the most primitive (nonplesiadapoid) plesiadapiforms match some of the features exhibited by scandentians, evincing the potential of tree shrews as extant analogues of the ancestral euarchontan positional behavior (Sargis, 2001; Gebo, 2004; Bloch et al., 2007; Godinot, 2007; Sargis et al., 2007).

As previously stated, an elongated calcaneus is associated to habitual leaping behavior (Hall-Craggs, 1965; Decker and Szalay, 1974; Gebo, 1988; Dagosto, 1988, 2007; Moyà-Solà et al., 2012; Boyer et al., 2013b; Marigó et al., 2016; Monclús-Gonzalo et al., 2023). Proximodistal elongation of the distal calcaneus results in an increase of the lever arm of the foot, which is required to generate enough force to leap efficiently (Morton, 1924; Gebo, 1988). However, because of the different biomechanical constraints associated with distinct BMs, different anatomical solutions are exhibited by taxa (Demes and Günther, 1989). Small-bodied leapers (considered 'foot-powered leapers') exhibit elongation of the distal segments of the hind limb (the tarsus), whereas larger-bodied leapers (regarded 'thigh-powered leapers') display a more elongated proximal hind limb segment and use the foot solely as a force transducer (Gebo and Dagosto, 1988; Demes and Günther, 1989; Demes et al., 1996). Additionally, the type of foot (in relation to the location of the fulcrum; Morton, 1924) also

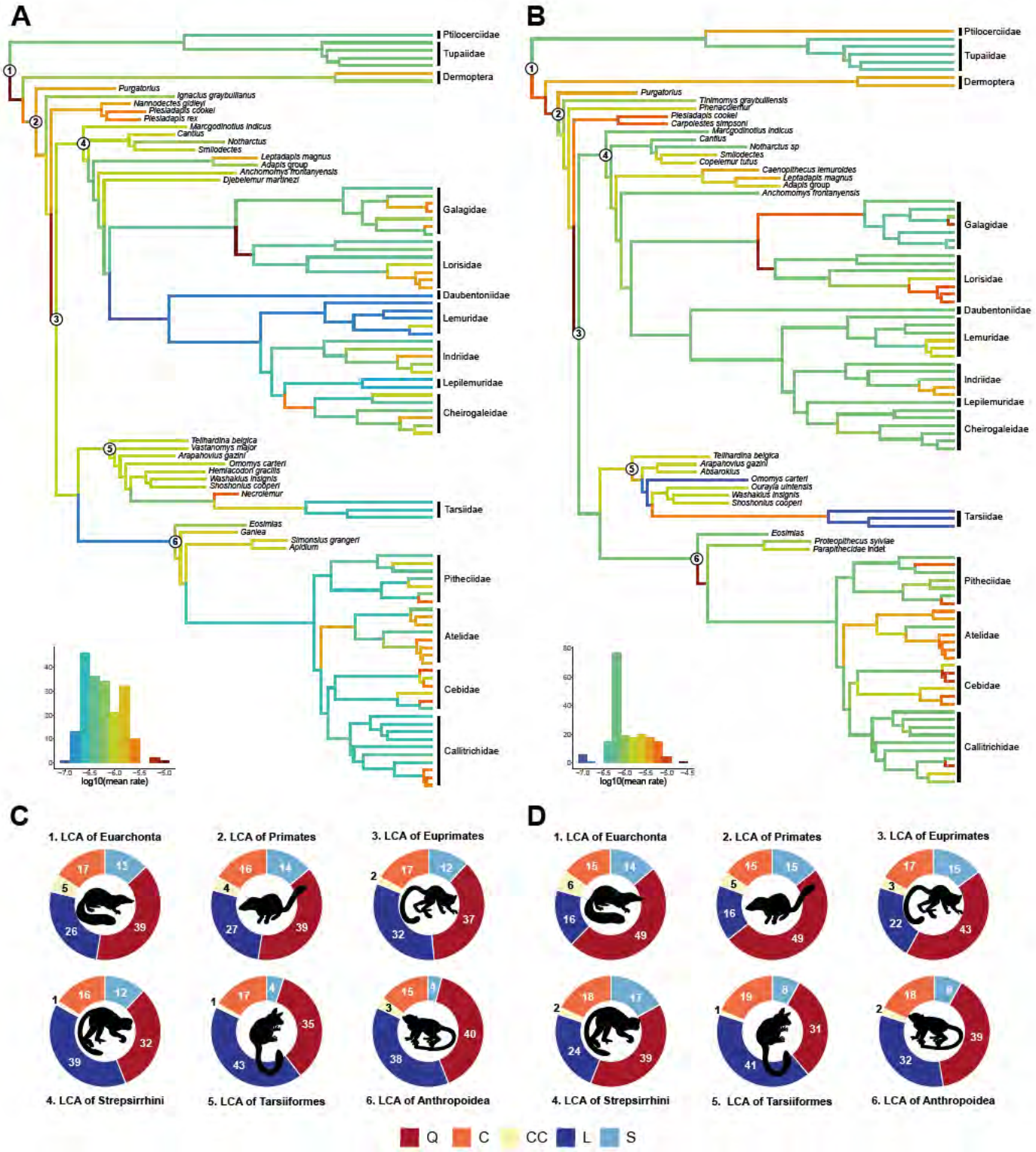

Figure 17. Branch-specific evolutionary rates for astragalar (A) and calcaneal (B) shape in extant and extinct primates. Branch rates are coded by color. (Warmer colors indicate faster evolutionary rates, while cooler colors represent slower evolutionary rates.) Below, each phylogenetic tree donut charts summarizes the estimated locomotor repertoires for each last common ancestor (LCA) based on astragalar (C) calcaneal (D) shape. Abbreviations: Q = quadrupedalism; C = climbing; L = leaping; S = suspension; CC = clawed clinging/climbing. (For interpretation of the references to color in this figure legend, the reader is referred to the web version of this article.)

influences the degree of proximodistal elongation of the tarsus (Moyà-Solà et al., 2012). Most nonprimate generalized mammals, including close relatives of primates such as scandentians and dermopterans, as well as anthropoids and likely plesiadapiforms, possess a metatarsi-fulcrumating foot. This group is characterized by a fulcrum placed distally in the foot, on the heads of metatarsals or even more distally up to the phalanges (Morton, 1924). Conversely, extant strepsirrhines and tarsiers, as well as early

Table 10
Estimated locomotor percentages of the internal nodes representing the last common ancestor (LCA) of euarchontans, primates, euprimates, strepsirrhines, tarsiiforms, and anthropoids.

LCA	Q	C	L	S	CC
Astragalus:					
Euarchonta	39	17	26	13	5
Primates	39	16	27	14	4
Euprimates	37	17	32	12	2
Strepsirrhini	32	16	39	12	1
Tarsiiformes	35	17	43	4	1
Anthropoidea	40	15	38	4	3
Calcaneus:					
Euarchonta	49	15	16	14	6
Primates	49	15	16	15	5
Euprimates	43	17	22	15	3
Strepsirrhini	39	18	24	17	2
Tarsiiformes	31	19	41	8	1
Anthropoidea	39	18	32	9	2

Abbreviations: Q = quadrupedalism; C = climbing; L = leaping; S = suspension; CC = clawed clinging/climbing.

euprimates (adapiforms and omomyiforms), exhibit a tarsi-fulcrumating foot, characterized by a much more proximally placed fulcrum (on the distal tarsal bones). The more proximal placement of the fulcrum provides improved grasping abilities at the cost of losing the part of the lever constituted by the metatarsus. Therefore, tarsi-fulcrumators require further elongation of the tarsal elements to compensate the loss of load arm, even if they are not specialized VCL species (Moyà-Solà et al., 2012). For this reason, small-bodied tarsi-fulcrumating primates are more prone to exhibit proximodistally elongated calcanei, even if they are not specialized leapers. In contrast, metatarsi-fulcrumating habitual leapers, as it is the case of many small platyrrhines and cercopithecoids, do not display a very elongated calcaneus. The results of our analyses concur with previous studies that extreme proximodistal elongation of the mid-tarsal region (including the distal calcaneus) in the case of small-bodied species with a tarsi-fulcrumating foot (e.g., tarsiers, galagids, and some cheirogaleids) is an adaptation for leaping behavior (Hall-Craggs, 1965; Dagosto, 1988; Gebo, 1988; Moyà-Solà et al., 2012; Boyer et al., 2013b; Monclús-Gonzalo et al., 2023) that can be found to different degrees among extinct tarsi-fulcrumating primates, indicating emphasis on leaping (Decker and Szalay, 1974; Dagosto, 1983; Covert, 1988; Gebo, 1988; Godinot, 1991; Gebo et al., 1991, 2001, 2012; Covert and Hamrick, 1993; Dagosto et al., 1999; Seiffert et al., 2015; Dunn et al., 2016; Marigó et al., 2016; Llera Martín et al., 2022). This is further supported by our allometric analyses that indicate significant differences in calcaneal shape (mainly driven by distal calcaneal elongation) between tarsi- and metatarsi-fulcrumating species in relation to body size (Moyà-Solà et al., 2012; Boyer et al., 2013b).

4.2. The locomotor behavior of Paleogene primates

Plesiadapiforms Our locomotor estimates for plesiadapiforms indicate a relatively generalized locomotor repertoire dominated by quadrupedalism, combined with lower percentages of climbing, leaping, and suspensory behaviors, concurring with a relatively mobile ankle, capable of extensive movements of inversion and eversion and adapted to the arboreal milieu (Szalay and Decker, 1974; Chester et al., 2015, 2017, 2019). Compared to most euprimates, plesiadapiforms are reconstructed as more suspensory and less prone to leap (Szalay and Dagosto, 1980; Dagosto, 1988, 2007). Nevertheless, the distinct relative amounts of quadrupedalism, leaping, and suspension predicted for each species, as well as the information provided by other skeletal elements of the postcranium, suggests that plesiadapiforms displayed considerable locomotor diversity (Bloch and Boyer, 2007; Bloch et al., 2007).

Purgatorius, the earliest known plesiadapiform (Van Valen and Sloan, 1965; Clemens, 1974; Wilson Mantilla et al., 2021), is reconstructed as having a locomotor repertoire largely analogous to that of extant arboreal tree shrews (Sargis, 2001, 2002a; Sargis et al., 2007; Chester et al., 2015). However, based on astragalar shape, it exhibits substantial amounts of suspensory behaviors (17%), suggesting a more deliberate type of locomotion for this species than for extant tree shrews. In contrast, calcaneal shape indicates that *Purgatorius* would have been the most quadrupedal plesiadapiform in our sample (69%)—which may be interpreted as a plesiomorphic condition of the ancestral euarchontan locomotor behavior. Extensive quadrupedalism in *Purgatorius* is supported by several calcaneal features, such as the relatively restricted ectal and sustentacular facets, and the dorsoplantarly lower and proximodistally elongated tuber calcanei, resembling those exhibited by tree shrews (Godinot, 2007).

Estimated locomotor percentages for *T. graybulliensis*, solely based on calcaneal shape, suggest a different locomotor behavior to that of *Purgatorius*, emphasizing more suspensory behaviors (19%). This concurs with the view, based on some features at the pelvis resembling those of taxa that frequently engage in suspensory behaviors (such as dermopterans and lorisids), that micromomyids might have been capable of some sort of below-branch suspensory behaviors (Bloch and Boyer, 2007).

We did not find evidence of a 'callitrichid-like' locomotor behavior in paromomyids, which has been inferred due to similarities in body size, exudativory diet, and locomotor repertoire (Garber, 1992; Vinyard et al., 2003; Youlatos and Meldrum, 2011). Our results, based on an astragalus of *Ignacius graybullianus* and a calcaneus of *Phenacolemur*, do not recover percentages of clawed clinging/climbing for these two species, as would be expected from the analysis of the rest of their postcranial skeleton (Bloch and Boyer, 2007; Bloch et al., 2007). In contrast, they are reconstructed as versatile quadrupeds, comparable to the other plesiadapiforms. Nevertheless, given that most features associated with vertical clinging/climbing are found in the trunk and forelimbs, our results do not unambiguously rule out this locomotor behavior and instead, given the less importance of suspensory locomotion (13–15%) inferred for this group, concur with the view that they were also adept pronograde bounders (Bloch and Boyer, 2007; Bloch et al., 2007).

Plesiadapids are consistently reconstructed as generalized arboreal quadrupeds capable of engaging in substantial amounts of suspensory behavior. The results based on the calcaneus of *Pl. cookei* suggest a more frequent use of suspension (26%) and claw clinging/climbing postures (6%), as indicated by the proximodistally long calcaneal ectal facet and dorsoplantarly high tuber calcanei. This result is consistent with its greater inferred BM (Boyer and Gingerich, 2019) as well as with the analysis of other regions of its postcranial skeleton, such as phalangeal proportions and humeral morphology, which resemble those of dermopterans and sloths (Hamrick, 2001; Boyer and Gingerich, 2019).

Calcaneal shape in *C. simpsoni* indicates a marked increase in the utilization of suspensory behaviors (32%) compared to the other plesiadapiforms, supporting the view that this animal had a more deliberate locomotion, which some have analogized to the extant didelphid *Caluromys* (Bloch and Boyer, 2002; Sargis et al., 2007). Similarities between the calcaneal shape of *Carpolestes* and extant suspensory species like dermopterans and lorisids, such as a rounded and oblique ectal facet, a mediolaterally broad and medially oriented sustentacular facet, a more proximally

(compared to other plesiadapiforms) peroneal tubercle, and a proportionally short and a dorsoplantarly high tuber calcanei, are indicative of a very mobile ankle better adapted to accommodate the foot into different postures on differently oriented supports and endure tensile forces during suspension rather than resist large loads derived from a more quadrupedal locomotion. This concurs with other features of the postcranial skeleton, such as the possession of long fingers and an opposable hallux with a nail instead of a claw—which have been related to the ability to grasp small branches and variously interpreted as either homologous or convergent with euprimates (Bloch and Boyer, 2002; Gebo, 2004; Sargis et al., 2007).

Adapiforms Adapiforms are predicted to have exhibited the most diverse locomotor behavior among early euprimates, with species characterized by substantial quadrupedalism accompanied by moderate amounts of leaping, climbing, and suspension; some species inferred to engage more in leaping behavior; and others exhibited a great suspensory component accompanied by climbing, quadrupedalism, and a little leaping behavior. These more extensive locomotor differences may be related with greater differences in body size as well as an occupation of different ecological niches (Godinot, 1998; Gunnell et al., 2008).

Asiadapines, represented by *M. indicus*, are reconstructed as arboreal quadrupeds with less leaping proclivity than in later and more derived adapiforms (Boyer et al., 2013b, 2015; Marigó et al., 2016; Ni et al., 2016). Its predicted low leaping component is explained by many astragalar features (e.g., a proximodistally long trochlea, the lack of a developed PTS, and a mediolaterally expanded and a dorsoplantarly low astragalar head) as well as by its relatively short distal calcaneal region, indicating an abbreviated tarsus, especially when compared with similarly sized adapiforms such as *An. frontanyensis* (Marigó et al., 2016, 2020). Furthermore, locomotor percentages based on calcaneal shape yield substantial suspensory behavior (28%), which is supported by several calcaneal traits resembling lorisids, including a large and more proximally located (compared to other adapiforms) peroneal tubercle, a medially oriented tuber calcanei, a slightly concave calcaneal plantar edge, a rounded ectal facet, and a broad and medially facing sustentacular facet (Gebo, 1988, 1989a). This result is consistent with previous studies that argue for a cautious locomotion with very little leaping behavior for this species (Boyer et al., 2013b), although other suggest a more generalized quadrupedal locomotion (Rose et al., 2009; Dunn et al., 2016; Llera Martín et al., 2022).

Our results do not support the view that notharctines were specialized in VCL like extant indriids and *Lepilemur* (Walker, 1974; Rose and Walker, 1985; Covert, 1995; Schmitt, 1996). This hypothesis has been already contested due to the lack of several key features of the distal tarsus and metatarsus associated with a derived adductor grasping mode (Gebo, 1985), which is at odds with an extensive use of vertical substrates (Gebo et al., 1991). In addition, the relatively long hind limbs, characteristic of notharctines, do not necessarily refer to adaptations for leaping behavior (Preuschoft et al., 1998). Conversely, the notharctines analyzed here (*Cantius*, *Notharctus*, *Smilodectes*, and *Co. tutus*) are reconstructed as above-branch quadrupeds resembling extant lemurids, with substantial amounts of quadrupedalism and leaping in their inferred locomotor repertoire, concurring with previous studies (Gregory, 1920; Decker and Szalay, 1974; Rose and Walker, 1985; Covert, 1988; Gebo, 1988; Gebo et al., 1991). Inferences based on astragalar shape yield higher percentages of leaping behavior (45–52%), whereas calcaneal shape distinguishes *Cantius* and *Notharctus*, characterized by higher suspensory behavior (14–16%), from *Smilodectes* and *Co. tutus*, which are reconstructed as more quadrupedal (45–49%).

Locomotor percentages based on astragalar shape discriminate *L. magnus* from the *Adapis* group because of the more lorisid-like features in the astragalus of the latter (Dagosto, 1983). These results suggest that *L. magnus* was likely an above-branch quadrupedal runner (24%) and leaper (52%), while specimens included in the *Adapis* group displayed more suspensory behaviors (30%), approaching those of extant lorisids (Dagosto, 1983; Gebo, 1988). Conversely, locomotor percentages based on calcaneal shape depict a more homogeneous locomotor behavior for adapines, vastly dominated by quadrupedalism (55%) and convergent to that displayed by anthropoids (Godinot, 1991). This result is explained by the presence of several features in the adapine calcaneus (such as a longer and stouter tuber calcanei, indicating strong plantarflexion) related to quadrupedal locomotion (Godinot, 1991). The overall picture of adapines indicates that these animals moved quadrupedally engaging in less leaping behavior than notharctines, with at least some of the specimens included in the *Adapis* group displaying adaptations for a cautious slow climbing locomotion (Dagosto, 1983; Bacon and Godinot, 1998; Boyer et al., 2013a; Marigó et al., 2019).

As previously suggested by Seiffert et al. (2015), our locomotor estimations based on its calcaneal shape indicate that *Ca. lemuroides* displayed a slow-climbing locomotor repertoire, characterized by considerable amounts of climbing (21%) and suspensory (28%) behaviors. This result is supported by the presence of several adaptations that facilitate rotational movements within the foot (required to habitually hold an inverted foot to navigate across complex arboreal settings), such as concave calcaneal plantar edge, a dorsoplantarly high cuboid facet with a deep cuboid pit, a dorsomedially inclined sustentacular facet, a rounded and oblique ectal facet, and a medially angled and plantarly projecting tuber calcanei. The latter feature is expected to allow for digital flexion because of increasing the mechanical advantage of the flexor digitorum brevis muscle (Sarmiento, 1983).

In agreement with previous studies, our results support marked leaping adaptations in the astragalus and calcaneus of *An. frontanyensis* and *D. martinezi* (43–58%; Marivaux et al., 2013; Marigó et al., 2016, 2020; Monclús-Gonzalo et al., 2023). Features in the astragalus (a dorsoplantarly tall astragalar body, a relatively narrow and proximodistally elongated astragalar neck, and a developed PTS) and the calcaneus (moderate proximodistal elongation of the distal portion, comparable to that of some contemporaneous omomyiforms) are associated with active arboreal locomotion (Gebo, 1988). Nevertheless, other calcaneal features of *An. frontanyensis* (such as a rounded and proximodistally elongated ectal facet, a relatively concave plantar calcaneal edge, and a medially bended tuber calcanei) are indicative of better climbing abilities (21%) and higher mobility of the foot (as suggested by its predicted suspensory locomotion, 14%) than in some omomyiform species with similar distal calcaneal elongation. This concurs with the view that sympatric omomyiforms and adapiforms with similar locomotor profiles may have nevertheless partitioned their niches by substrate preference (Marigó et al., 2020).

Omomyiforms The results for most omomyiforms analyzed here (*Teilhardina belgica*, *Ar. gazini*, *Hemiacodon gracilis*, *Omomys carteri*, *Ourayia uintensis*, *Shoshonius cooperi*, *Washakius insignis*, and *Absarokius*) support an active locomotor behavior dominated by leaping (39–64%) and quadrupedalism (20–39%), in agreement with previous studies (Szalay, 1976; Savage and Waters, 1978; Gebo, 1988; Covert and Hamrick, 1993; Dagosto and Schmid, 1996; Anemone and Covert, 2000; Dunn et al., 2006; Rose et al., 2011; Gebo et al., 2012, 2015). Together with several astragalar features (such as a dorsoplantarly high astragalar body and a narrow and elongated astragalar neck), the moderately elongated calcaneus of omomyiforms, falling within the cheirogaleid range, is the most

prominent feature related with increased leaping behavior. Nevertheless, omomyiforms do not exhibit the extreme elongation displayed by the specialized small VCL species (galagids and tarsiers), suggesting an overall active yet not specialized VCL locomotor behavior for these species (Dagosto, 1988; Gebo, 1988; Boyer et al., 2013b; Monclús-Gonzalo et al., 2023). Only a calcaneus specimen attributed to *Necrolemur*, which is broken distally and could not be included in this study, exhibits a proximodistal elongation comparable to that of galagids and tarsiers (Godinot and Dagosto, 1983).

An astragalus attributed to *V. major* (GU 800) departs from the overall omomyiform locomotor profile discussed earlier. Our locomotor estimates indicate a more generalized locomotor repertoire, dominated by quadrupedal locomotion (41%) and exhibiting less emphasis for leaping behavior (27%). This result concurs with recent studies carried out on the available material attributed to this species (Dunn et al., 2016; Llera Martín et al., 2022).

Early anthropoids Our locomotor estimates concur with previous studies that highlighted the morphological and behavioral shift toward a more quadrupedal locomotion in early anthropoids (Fleagle, 1980; Conroy and Rose, 1983; Gebo and Simons, 1987; Gebo, 1989b; Fleagle and Simons, 1995). However, the Asian taxa (*Eosimias* and *Ganlea*) still retain astragalar and calcaneal features that lack the derived anthropoid condition displayed by the Afro-Arabian taxa, resulting in locomotor repertoires that depart from the latter group and, instead, more closely resemble those of strepsirrhines and tarsiiforms (Gebo et al., 2000, 2001; Marivaux et al., 2003, 2010).

Eosmiids resemble omomyiforms in having a high astragalar body, a reduced PTS (absent from early anthropoids from Afro-Arabia), a shallow trochlea with parallel rims, a mediolaterally narrow astragalar neck, and a moderately long astragalar neck (Gebo et al., 2000, 2001; Gebo and Dagosto, 2004). Our locomotor estimates based on astragalar shape indicate considerable amounts of leaping (42%) and quadrupedalism (43%). Conversely, locomotor estimates based on calcaneal shape yield substantial suspensory (13%) and climbing (20%) components, resembling similar-sized adapiforms like *An. frontanyensis* and *M. indicus*. This is supported by several features (a rounded ectal facet, a moderately concave plantar edge, and a slightly medially bended tuber calcanei) that are associated with relatively mobile ankle (Gebo, 1988). Overall, our locomotor estimates concur with the view that eosimiids fill the morphological and behavioral gap between the earliest euprimates and more derived anthropoids from Afro-Arabia (Gebo, 1986; Dagosto, 1990; Gebo and Dagosto, 2004).

Ganlea is reconstructed as a generalized arboreal quadruped, with substantial amounts of leaping (39%) and quadrupedalism (31%), as well as non-negligible percentages of climbing (19%) and suspensory behaviors (6%). This result is consistent with the mosaic morphology exhibited by its astragalus, displaying features associated with leaping (e.g., a dorsoplantarly high astragalar body, parallel trochlear rims, and a straight and moderately elongated astragalar neck) and others more tightly related to increased mobility at the upper ankle joint (such as a relatively shallow trochlear groove; Marivaux et al., 2003, 2010). Given the purported more basal anthropoid position of eosmiids and amphipithecids in relation to Afro-Arabian parapithecids and proteopithecids (Beard et al., 2009; Coster et al., 2013; Jaeger et al., 2020; Chaimanee et al., 2024), this agrees with the view that a more generalized locomotor behavior with less emphasis on quadrupedalism might be plesiomorphic for anthropoids (Gebo et al., 2000, 2001; Gebo and Dagosto, 2004).

Locomotor estimations based on astragalar and calcaneal shape consistently reconstruct parapithecids and proteopithecids as above-branch arboreal quadrupeds and leapers similar to extant small platyrrhines such as *Cebus* or *Saimiri* (Fleagle, 1980; Gebo and Simons, 1987; Gebo, 1989b; Simons and Seiffert, 1999; Seiffert and Simons, 2001; Gladman et al., 2013). The reconstructed locomotor profile, vastly dominated by quadrupedalism (55–45%) and leaping (35–40%), reflects the presence of many astragalar (a broad trochlear surface with moderate wedging, a marked notch on the astragalar neck, a lack of PTS, and a medial tibial facet forming a small cup-like concavity) and calcaneal features (abbreviated distal calcaneal elongation, a lateral extension of the cuboid facet, and a stout and mediolaterally broad tuber calcanei), indicative of an ankle capable of high degrees of dorsiflexion but less prone to use inverted postures like strepsirrhines or tarsiers (Conroy and Rose, 1983). Compared with the contemporaneous and larger-sized parapithecids, *Pr. sylviae* is reconstructed as a more agile leaper, in agreement with its more proximodistally elongated calcaneal distal region and overall more gracile morphology (Seiffert and Simons, 2001; Gladman et al., 2013).

4.3. Origin and diversification of euprimates in the light of locomotor behavior

Fossil evidence suggests that the emergence of euprimates was marked by profound anatomical modifications, including the acquisition of a complete postorbital bar, convergent orbits, higher encephalization, relatively long digits, opposable hallux and pollex, nails instead of claws, and adaptations for leaping behavior (Cartmill, 1974, 1992; Szalay et al., 1987; Rose, 1994; Silcox et al., 2015). At the hindfoot, several adaptations for strong pedal grasping and leaping behavior (e.g., development of a PTS, a more sloping fibular facet, tarsal elongation) distinguish early euprimates from plesiadapiforms (Dagosto, 1988, 2007; Rose, 1994; Boyer and Seiffert, 2013; Boyer et al., 2013b; Yapuncich et al., 2017, 2019). Our results align with this, as evidenced by the increased evolutionary rates for both astragalar and calcaneal shape along the lineage leading to the first euprimates. However, the lack of any transitional species displaying a mixture of archaic (i.e., plesiadapiform-like) and derived (i.e., euprimate-like) traits hampers testing among competing hypotheses about the original selection pressures that drove the origin and early diversification of euprimates (Silcox et al., 2015). To date, only a single species, *C. simpsoni*, could fill in this 'transitional' gap (Bloch and Boyer, 2002). Based on the features displayed by this species, combining adaptations for strong pedal grasping (opposable hallux with a nail) with the lack of euprimate-like visual or leaping adaptations, Bloch and Boyer (2002) concluded that small-branch specialization would have preceded visual and leaping-related adaptations. Our results provide further support to this hypothesis as our locomotor estimates based on the calcaneus of *C. simpsoni* yielded the highest percentage of suspensory locomotion among plesiadapiforms, concurring with a mobile ankle adapted to a more deliberate type of locomotion, as would be required to engage in the fine branch milieu. Additionally, we also found particularly high evolutionary rates describing plesiadapoid evolution, pinpointing to the substantial morphological changes already occurring prior the emergence of euprimates (Sargis et al., 2007). Altogether, these results are consistent with the terminal branch feeding hypothesis (Rasmussen, 1990), suggesting that adaptation to the fine branch milieu was critical in the early stages of primate evolution.

Of the various locomotor categories investigated here, leaping behavior within the arboreal canopy is the one that most consistently discriminates between plesiadapiforms and euprimates—and, thus, the most relevant for characterizing the locomotor shift that occurred during the plesiadapiform-euprimate

transition. Albeit lacking in some extant euprimates (lorisids and hominids), leaping is widespread and most characteristic of this group (Dagosto, 1988, 2007). This is confirmed by our results as we only obtained substantial percentages of leaping for euprimate specimens. Habitual leaping may be thus considered synapomorphic for euprimates, even though this does not imply that the euprimate LCA was necessarily an adept leaper. These results, in line with previous studies, are consistent with the 'grasp-leaping' hypothesis (Szalay and Dagosto, 1980). The locomotor estimate for the euprimate LCA concurs with only moderate leaping capabilities (22–32%). Indeed, the percentages of leaping inferred for the most basal species in this study, such as *Te. belgica*, *V. major*, and *M. indicus* (Rose et al., 2009, 2011; Dunn et al., 2016; Llera Martín et al., 2022), are substantially lower than those of more derived species, thereby rejecting the existance of specialized leaping behavior during the emergence of euprimates. This view is further supported by a partial skeleton of the basal haplorrhine *Archicebus achilles* described by Ni et al. (2013), which has been reconstructed as a generalized arboreal quadruped instead of a committed leaper—but see Boyer et al.'s (2017a) interpretation of an astragalus of *Donrussellia provincialis* for an alternate view on the importance of leaping among the earliest euprimates. On the other hand, euprimates from various clades (e.g., most omomyiforms and later crown tarsiiforms, galagids, *D. martinezi*, and *An. frontanyensis*) exhibit substantially higher leaping percentages than other members of their respective clades, supporting the independent evolution of specialized leaping adaptations among various extant and extinct euprimate lineages (Boyer et al., 2013b). This is further exemplified by our locomotor estimates (strepsirrhine LCA = 24–39%; tarsiiform LCA = 41–43%; anthropoid LCA = 32–38%) and by the increased evolutionary rates in the branches leading to these groups, suggesting substantial morphological changes associated with the acquisition of more specialized leaping behavior, which probably was absent in the euprimate LCA. Conversely, the low evolutionary rates observed in the branch leading from the euprimate LCA to *Eosimias*, along with the similarity between its locomotor estimates and those of the euprimate LCA, suggest that this early anthropoid could be a reasonably good analogue of the euprimate LCA, even if it already exhibited some derived anthropoid adaptations (Gebo et al., 2000, 2001).

5. Summary and conclusions

We quantitatively analyzed the shape of the astragalus and calcaneus in a broad sample of extant and extinct primates (and close relatives) by means of a high-density sliding semilandmark 3D geometric morphometric approach for the first time. We also investigated the functional relationship between tarsal shape and locomotion using an extensive locomotor dataset of extant species compiled from the literature. Based on the covariation between tarsal shape and locomotion, we made locomotor inferences about early primates and, on this basis, critically evaluated their exhibited locomotor diversity and the potential locomotor changes that might have occurred during the origin and early diversification of euprimates. Concurring with previous studies, our results indicate that the shape of these bones is an excellent predictor of the locomotor repertoire of extant species. In particular, the shape of the facets involved in the mobility at the main joints of the proximal tarsus is indicative of adaptations for different locomotor behaviors. In turn, the elongation of the distal region of the calcaneus is correlated with agile grasp-leaping locomotion in many primates, although biomechanical factors such as BM and foot type may also influence calcaneal proportions.

Plesiadapiforms are reconstructed as generalized arboreal animals with substantial amounts of quadrupedalism and suspensory behaviors. Calcaneal shape further indicates an evolutionary trend toward decreased quadrupedalism and higher reliance on suspensory behaviors in plesiadapoids (*C. simpsoni* and *Pl. cookei*)—supporting the view that locomotor changes were already underway before the LCA of euprimates. Most early euprimates differ from plesiadapiforms in their higher emphasis on leaping. Adapiforms exhibit a diverse locomotor behavior, with some species estimated to have exhibited extensive suspensory behaviors (like extant lorisids, *Daubentonia*, and some cheirogaleids), some characterized as more quadrupedal and resembling anthropoids, and others displaying a more generalized locomotor pattern (similar to extant lemurids and cheirogaleids, depending on their body size). Omomyiforms display moderate percentages of leaping and extensive use of small substrates but lack extreme adaptations for VCL. They rather resemble the most leaping cheirogaleids except for the lack of frequent suspensory behaviors, thus being better envisioned as quadrupedal leapers with less ability to suspend or move deliberately than most strepsirrhines. Finally, early anthropoids are reconstructed as more quadrupedal than both adapiforms and omomyiforms. However, basalmost anthropoids (eosimiids) and *Ganlea* are intermediate in locomotion between omomyiforms and the late Eocene/early Oligocene Afro-Arabian anthropoids.

Overall, our results based on the astragalus and calcaneus indicate that early primates exhibited a very diverse array of locomotor repertoires. Moreover, the estimated locomotor percentages for euprimates differ significantly from those of plesiadapiforms, with the former showing a notably higher predicted leaping behavior. This provides further evidence of a major locomotor shift during the early evolution of euprimates, concurring with the 'grasp-leaping' hypothesis. While no plesiadapiform recovered so far exhibits adaptations for frequent leaping behavior, our results support that some plesiadapoid species displayed a more deliberate locomotion, particularly *C. simpsoni*. We therefore conclude that our results are consistent with the view that the adaptation to the fine branch milieu, as proposed by the terminal branch feeding hypothesis, preceded the leaping specializations exhibited by the earliest euprimates. As suggested by our locomotor estimations, several euprimate lineages further developed these leaping adaptations, some of them reaching very high levels of specialization, for example, extant VCL species. However, leaping behavior, even if not a specialized form, was already present during the origin of euprimates. Future research in other anatomical areas will be required to better determine the original selective pressures underpinning the profound locomotor shift that occurred during the origin and early diversification of euprimates.

Declaration of competing interest

The authors certify that they have no conflict of interest.

Acknowledgments

This article is part R + D + I projects PID2020-116908GB-I00 and PID2020-117289GB-I00 financed by the Agencia Estatal de Investigación (MCIN/AEI/10.13039/501100011033). It has also been supported by CERCA Programme/Generalitat de Catalunya, the Departament de Cultura of the Generalitat de Catalunya (CLT0009_22_000022), the Agència de Gestió d'Ajust Universitaris i de Recerca (AGAUR) of the Generalitat de Catalunya (consolidated research groups 2022 SGR 01188 and 2022 SGR 00620), a Ramón y Cajal grant (RYC2021-034366-I to J.M.) funded by the Agencia

Estatal de Investigación (MCIN/AEI/10.13039/501100011033) and the European Union NextGenerationEU/PRTR, and a Joan Oró FI AGAUR fellowship (2021 FI_B 00524, 2022 FI_B1 00131, and 2023 FI-3 00131 to O.M.G.) funded by the Secretaria d'Universitats i Recerca of the Generalitat de Catalunya and the European Social Fund. We thank the team of the online repository Morphosource, MorphoMuseuM and the following institutions for providing access to specimens: American Museum of Natural History (AMNH), Duke Lemur Center Division of Fossil Primates (DLC), National Museum of Natural History (NMNH), Institut des Sciences de l'Evolution de Montpellier (ISEM), Muséum National d'Histoire Naturelle (MNHN), University of California Museum of Paleontology (UCMP), University of Michigan Museum of Paleontology (MI), Hemvati Nandan Bahuguna Garhwal University (HNBGU), Institut Català de Paleontologia Miquel Crusafont (ICP), United States Geological Survey (USGS), Museum of the Office National des Mines (ONM), Royal Belgian Institute of Natural Sciences (IRSNB), Carnegie Museum of Natural History (CMNH), Museo Argentino de Ciencias Naturales (MACN), Institute of Vertebrate Paleontology and Paleoanthropology (IVPP), National Museum of Myanmar Primates (NMMP), Naturhistorisches Museum Basel (NGiB), University of Colorado (CU), University of Zurich (UZH), San Diego Natural History Museum (SDNH), Caribbean Primate Research Center (CPRC), Harvard Museum Comparative Zoology (MCZ), Field Museum of Natural History (FMNH), Yale Peabody Museum of Natural History (YPM), University of Nebraska State Museum (USNM), and Stony Brook University (SBU). We acknowledge the Magnetic Resonance Imaging (MRI) platform member of the national infrastructure France-BioImaging supported by the French National Research Agency (ANR-10-INBS-04, 'Investments for the future'), the labex Centre Méditerranéen de l'Environnement et de la Biodiversité (CEMEB) (ANR-10-LABX-0004) and Digital and hardware solutions for the environmental and life sciences (NUMEV) (ANR-10-LABX-0020). We also thank James Thostenson (American Museum of Natural History (AMNH)) and Brian Reuther for having scanned the two *Teilhardina belgica* specimens (IRSNB 1235 and IRSNB 26857-01). This article is part of the Ph.D. dissertation of O.M.G. within the Geology Ph.D. Program of the Universitat Autònoma de Barcelona.

Author contributions

Oriol Monclús-Gonzalo: Writing – review & editing, Writing – original draft, Methodology, Investigation, Funding acquisition, Formal analysis, Data curation, Conceptualization. **David M. Alba:** Writing – review & editing, Supervision, Funding acquisition. **Anne-Claire Fabre:** Writing – review & editing. **Judit Marigó:** Writing – review & editing, Supervision, Funding acquisition.

Supplementary online material

Supplementary Online Material related to this article can be found at https://doi.org/10.1016/j.jhevol.2025.103730.

References

Adams, D.C., Otárola-Castillo, E., 2013. Geomorph: An r package for the collection and analysis of geometric morphometric shape data. Methods Ecol. Evol. 4, 393–399.
Adler, D., Murdoch, D., 2020. Rgl: 3D visualization using openGL. https://github.com/dmurdoch/rgl. https://dmurdoch.github.io/rgl/.
Anemone, R.L., Covert, H.H., 2000. New skeletal remains of *Omomys* (Primates, Omomyidae): Functional morphology of the hindlimb and locomotor behavior of a Middle Eocene primate. J. Hum. Evol. 38, 607–633.
Archer, W., Pop, C.M., Rezek, Z., Schlager, S., Lin, S.C., Weiss, M., Dogandžić, T., Desta, D., McPherron, S.P., 2018. A geometric morphometric relationship predicts stone flake shape and size variability. Archaeol. Anthropol. Sci. 10, 1991–2003.
Arnold, C., Matthews, L.J., Nunn, C.L., 2010. The 10kTrees website: A new online resource for primate phylogeny. Evol. Anthropol. 19, 114–118.
Bacon, A.M., Godinot, M., 1998. Analyse morphofonctionnelle des fémurs et des tibias des «*Adapis*» du Quercy: Mise en évidence de cinq types morphologiques. Folia Primatol. 69, 1–21.
Bærentzen, J.A., Aanæs, H., 2002. Generating Signed Distance Fields From Triangle Meshes. Technical University of Denmark. http://www.imm.dtu.dk/pubdb/p.php?1833.
Bardua, C., Felice, R.N., Watanabe, A., Fabre, A.-C., Goswami, A., 2019. A practical guide to sliding and surface semilandmarks in morphometric analyses. Integr. Org. Biol. 1, obz016.
Bastir, M., Torres-Tamayo, N., Palancar, C.A., Lois-Zlolniski, S., García-Martínez, D., Riesco-López, A., Vidal, D., Blanco-Pérez, E., Barash, A., Nalla, S., Martelli, S., 2019. Geometric morphometric studies in the human spine. In: Been, E., Gómez-Olivencia, A., Ann Kramer, P. (Eds.), Spinal Evolution. Springer, Cham, pp. 361–386.
Beard, K.C., 1989. Postcranial anatomy locomotor adaptations and paleoecology of early Cenozoic Plesiadapidae, Paromomyidae and Micromomyidae (Eutheria, Dermoptera). Ph.D. Dissertation, Johns Hopkins University School of Medicine.
Beard, K.C., 2008. The oldest North American primate and mammalian biogeography during the Paleocene–Eocene thermal maximum. Proc. Natl. Acad. Sci. U.S.A. 105, 3815–3818.
Beard, K.C., Wang, J., 2004. The eosimiid primates (Anthropoidea) of the Heti Formation, Yuanqu Basin, Shanxi and Henan Provinces, People's Republic of China. J. Hum. Evol. 46, 401–432.
Beard, K.C., Dagosto, M., Gebo, D.L., Godinot, M., 1988. Interrelationships among primate higher taxa. Nature 331, 712–714.
Beard, K.C., Qi, T., Dawson, M.R., Wang, B., Li, C., 1994. A diverse new primate fauna from middle Eocene fissure-fillings in southeastern China. Nature 368, 604–609.
Beard, K.C., Tong, Y., Dawson, M.R., Wang, J., Huang, X., 1996. Earliest complete dentition of an anthropoid primate from the late middle Eocene of Shanxi Province, China. Science 272, 82–85.
Beard, K.C., Marivaux, L., Chaimanee, Y., Jaeger, J.J., Marandat, B., Tafforeau, P., Soe, A.N., Tun, S.T., Kyaw, A.A., 2009. A new primate from the Eocene Pondaung Formation of Myanmar and the monophyly of Burmese amphipithecids. Proc. R. Soc. B 276, 3285–3294.
Bloch, J.I., Boyer, D.M., 2002. Grasping primate origins. Science 298, 1606–1610.
Bloch, J.I., Boyer, D.M., 2007. New skeletons of Paleocene-Eocene Plesiadapiformes: A diversity of arboreal positional behaviors in early primates. In: Ravosa, M.J., Dagosto, M. (Eds.), Primate Origins: Adaptations and Evolution. Springer, New York, pp. 535–581.
Bloch, J.I., Silcox, M.T., Boyer, D.M., Sargis, E.J., 2007. New Paleocene skeletons and the relationship of plesiadapiforms to crown-clade primates. Proc. Natl. Acad. Sci. U.S.A. 104, 1159–1164.
Blomberg, S.P., Garland Jr, T., Ives, A.R., 2003. Testing for phylogenetic signal in comparative data: Behavioral traits are more labile. Evolution 57, 717–745.
Bock, W.J., Von Wahlert, G., 1965. Adaptation and the form-function complex. Evolution 19, 269–299.
Bookstein, F.L., 1997. Landmark methods for forms without landmarks: Morphometrics of group differences in outline shape. Med. Image Anal. 1, 225–243.
Bookstein, F.L., Gunz, P., Mitteroecker, P., Mitteroecker, P., Prossinger, H., Schaefer, K., Horst, S., 2003. Cranial integration in *Homo*: Singular warps analysis of the midsagittal plane in ontogeny and evolution. J. Hum. Evol. 44, 167–187.
Boyer, D.M., Seiffert, E.R., 2013. Patterns of astragalar fibular facet orientation in extant and fossil primates and their evolutionary implications. Am. J. Phys. Anthropol. 151, 420–447.
Boyer, D.M., Gingerich, P.D., 2019. Skeleton of late Paleocene *Plesiadapis cookei* (Mammalia, Euarchonta): Life history, locomotion, and phylogenetic relationships. Univ. Michigan Pap. Paleontol. 38, 1–269.
Boyer, D.M., Seiffert, E.R., Simons, E.L., 2010. Astragalar morphology of *Afradapis*, a large adapiform primate from the earliest late Eocene of Egypt. Am. J. Phys. Anthropol. 143, 383–402.
Boyer, D.M., Yapuncich, G.S., Chester, S.G., Bloch, J.I., Godinot, M., 2013a. Hands of early primates. Am. J. Phys. Anthropol. 152, 33–78.
Boyer, D.M., Seiffert, E.R., Gladman, J.T., Bloch, J.I., 2013b. Evolution and allometry of calcaneal elongation in living and extinct primates. PLoS One 8, e67792.
Boyer, D.M., Yapuncich, G.S., Butler, J.E., Dunn, R.H., Seiffert, E.R., 2015. Evolution of postural diversity in primates as reflected by the size and shape of the medial tibial facet of the talus. Am. J. Phys. Anthropol. 157, 134–177.
Boyer, D.M., Toussaint, S., Godinot, M., 2017a. Postcrania of the most primitive euprimate and implications for primate origins. J. Hum. Evol. 111, 202–211.
Boyer, D.M., Gunnell, G.F., Kaufman, S., McGeary, T.M., 2017b. Morphosource: Archiving and sharing 3-D digital specimen data. Paleontol. Soc. Pap. 22, 157–181.
Cartmill, M., 1974. Rethinking primate origins. Science 184, 436–443.
Cartmill, M., 1992. New views on primate origins. Evol. Anthropol. 1, 105–111.
Chaimanee, Y., Chavasseau, O., Beard, K.C., Kyaw, A.A., Soe, A.N., Sein, C., Lazzari, V., Marivaux, L., Marandat, B., Swe, M., Rugbumrung, M., 2012. Late Middle Eocene primate from Myanmar and the initial anthropoid colonization of Africa. Proc. Natl. Acad. Sci. U.S.A. 109, 10293–10297.
Chaimanee, Y., Chavasseau, O., Lazzari, V., Soe, A.N., Sein, C., Jaeger, J.-J., 2024. Early anthropoid primates: New data and new questions. Evol. Anthropol. 33, e22022.

Chester, S.G.B., Bloch, J.I., Boyer, D.M., Clemens, W.A., 2015. Oldest known euarchontan tarsals and affinities of Paleocene *Purgatorius* to primates. Proc. Natl. Acad. Sci. U.S.A. 112, 1487–1492.
Chester, S.G.B., Williamson, T.E., Bloch, J.I., Silcox, M.T., Sargis, E.J., 2017. Oldest skeleton of a plesiadapiform provides additional evidence for an exclusively arboreal radiation of stem primates in the Paleocene. R. Soc. Open Sci. 4, 170329.
Chester, S.G., Williamson, T.E., Silcox, M.T., Bloch, J.I., Sargis, E.J., 2019. Skeletal morphology of the early Paleocene plesiadapiform *Torrejonia wilsoni* (Euarchonta, Palaechthonidae). J. Hum. Evol. 128, 76–92.
Chester, S.G., Williamson, T.E., Crowell, J.W., Silcox, M.T., Bloch, J.I., Sargis, E.J., 2025. New remarkably complete skeleton of *Mixodectes* reveals arboreality in a large Paleocene primatomorphan mammal following the Cretaceous-Paleogene mass extinction. Sci. Rep. 15, 8041.
Clavel, J., Escarguel, G., Merceron, G., 2015. mvMORPH: an R package for fitting multivariate evolutionary models to morphometric data. Methods Ecol. Evol. 6, 1311–1319.
Clemens, W.A., 1974. *Purgatorius*, an early paromomyid primate (Mammalia). Science 184, 903–905.
Conroy, G.C., Rose, M.D., 1983. The evolution of the primate foot from the earliest primates to the Miocene hominoids. Foot Ankle 3, 342–364.
Cornette, R., Baylac, M., Souter, T., Herrel, A., 2013. Does shape co-variation between the skull and the mandible have functional consequences? A 3D approach for a 3D problem. J. Anat. 223, 329–336.
Coster, P., Beard, K.C., Soe, A.N., Sein, C., Chaimanee, Y., Lazzari, V., Valentin, X., Jaeger, J.J., 2013. Uniquely derived upper molar morphology of Eocene Amphipithecidae (Primates: Anthropoidea): Homology and phylogeny. J. Hum. Evol. 65, 143–155.
Covert, H.H., 1988. Ankle and foot morphology of *Cantius mckennai*: Adaptations and phylogenetic implications. J. Hum. Evol. 17, 57–70.
Covert, H.H., 1995. Locomotor adaptations of Eocene primates: Adaptive diversity among the earliest prosimians. In: Alterman, L., Doyle, G.A., Izard, M.K. (Eds.), Creatures of the Dark. Springer, Boston, pp. 495–509.
Covert, H.H., Hamrick, M.W., 1993. Description of new skeletal remains of the early Eocene anaptomorphine primate *Absarokius* (Omomyidae) and discussion about its adaptative profile. J. Hum. Evol. 25, 351–362.
Crowell, J.W., Wible, J.R., Chester, S.G., 2024. Basicranial evidence suggests picrodontid mammals are not stem primates. Biol. Lett. 20, 20230335.
Dagosto, M., 1983. Postcranium of *Adapis parisiensis* and *Leptadapis magnus* (Adapiformes, Primates). Adaptational and phylogenetic significance. Folia Primatol. 41, 49–101.
Dagosto, M., 1988. Implications of postcranial evidence for the origin of euprimates. J. Hum. Evol. 17, 35–56.
Dagosto, M., 1990. Models for the origin of the anthropoid postcranium. J. Hum. Evol. 19, 121–139.
Dagosto, M., 2007. The postcranial morphotype of primates. In: Ravosa, M.J., Dagosto, M. (Eds.), Primate Origins: Adaptations and Evolution. Springer, New York, pp. 489–534.
Dagosto, M., Schmid, P., 1996. Proximal femoral anatomy of omomyiform primates. J. Hum. Evol. 30, 29–56.
Dagosto, M., Gebo, D.L., Beard, K.C., 1999. Revision of the Wind River faunas, early Eocene of central Wyoming. Part 14. Postcranium of *Shoshonius cooperi* (Mammalia: Primates). Ann. Carnegie Mus. 68, 175–211.
Decker, R.L., Szalay, F.S., 1974. Origins and function of the pes in the Eocene Adapidae (Lemuriformes, Primates). In: Jenkins, F.A. (Ed.), Primate Locomotion. Academic Press, New York, pp. 261–291.
Demes, B., Günther, M.M., 1989. Biomechanics and allometric scaling in primate locomotion and morphology. Folia Primatol. 53, 125–141.
Demes, B., Jungers, W.L., Fleagle, J.G., Wunderlich, R.E., Richmond, B.G., Lemelin, P., 1996. Body size and leaping kinematics in Malagasy vertical clingers and leapers. J. Hum. Evol. 31, 367–388.
Dunn, R.H., Sybalsky, J.M., Conroy, G.C., Rasmussen, D.T., 2006. Hindlimb adaptations in *Ourayia* and *Chipetaia*, relatively large-bodied omomyine primates from the Middle Eocene of Utah. Am. J. Phys. Anthropol. 131, 303–310.
Dunn, R.H., Rose, K.D., Rana, R.S., Kumar, K., Sahni, A., Smith, T., 2016. New euprimate postcrania from the early Eocene of Gujarat, India, and the strepsirrhine–haplorhine divergence. J. Hum. Evol. 99, 25–51.
Fleagle, J.G., 1980. Locomotor behavior of the earliest anthropoids: A review of the current evidence. Z. Morph. Anthrop. 71, 149–156.
Fleagle, J.G., Mittermeier, R.A., 1980. Locomotor behavior, body size, and comparative ecology of seven Surinam monkeys. Am. J. Phys. Anthropol. 52, 301–314.
Fleagle, J.G., Kay, R.F., 1988. The phyletic position of the Parapithecidae. J. Hum. Evol. 16, 483–532.
Fleagle, J.G., Simons, E.L., 1995. Limb skeleton and locomotor adaptations of *Apidium phiomense*, an Oligocene anthropoid from Egypt. Am. J. Phys. Anthropol. 97, 235–289.
Garber, P.A., 1992. Vertical clinging, small body size, and the evolution of feeding adaptations in the Callitrichinae. Am. J. Phys. Anthropol. 88, 469–482.
Gebo, D.L., 1985. The nature of the primate grasping foot. Am. J. Phys. Anthropol. 67, 269–277.
Gebo, D.L., 1986. Anthropoid origins—The foot evidence. J. Hum. Evol. 15, 421–430.
Gebo, D.L., 1987a. Locomotor diversity in prosimian primates. Am. J. Primatol. 13, 271–281.
Gebo, D.L., 1987b. Functional anatomy of the tarsier foot. Am. J. Phys. Anthropol. 73, 9–31.
Gebo, D.L., 1988. Foot morphology and locomotor adaptation in Eocene primates. Folia Primatol. 50, 3–41.
Gebo, D.L., 1989a. Postcranial adaptation and evolution in Lorisidae. Primates 30, 347–367.
Gebo, D.L., 1989b. Locomotor and phylogenetic considerations in anthropoid evolution. J. Hum. Evol. 18, 201–233.
Gebo, D.L., 2004. A shrew-sized origin for primates. Am. J. Phys. Anthropol. 125, 40–62.
Gebo, D.L., 2011. Vertical clinging and leaping revisited: Vertical support use as the ancestral condition of strepsirrhine primates. Am. J. Phys. Anthropol. 146, 323–335.
Gebo, D.L., Simons, E.L., 1987. Morphology and locomotor adaptations of the foot in early Oligocene anthropoids. Am. J. Phys. Anthropol. 74, 83–101.
Gebo, D.L., Dagosto, M., 1988. Foot anatomy, climbing, and the origin of the Indriidae. J. Hum. Evol. 17, 135–154.
Gebo, D.L., Dagosto, M., 2004. Anthropoid origins: Postcranial evidence from the Eocene of Asia. In: Ross, C.F., Kay, R.F. (Eds.), Anthropoid Origins: New Visions. Kluwer Academic, New York, pp. 369–380.
Gebo, D.L., Dagosto, M., Rose, K.D., 1991. Foot morphology and evolution in early Eocene *Cantius*. Am. J. Phys. Anthropol. 86, 51–73.
Gebo, D.L., Dagosto, M., Beard, K.C., Qi, T., Wang, J., 2000. The oldest known anthropoid postcranial fossils and the early evolution of higher primates. Nature 404, 276–278.
Gebo, D.L., Dagosto, M., Beard, K.C., Qi, T., 2001. Middle Eocene primate tarsals from China: Implications for haplorhine evolution. Am. J. Phys. Anthropol. 116, 83–107.
Gebo, D.L., Smith, T., Dagosto, M., 2012. New postcranial elements for the earliest Eocene fossil primate *Teilhardina belgica*. J. Hum. Evol. 63, 205–218.
Gebo, D.L., Smith, R., Dagosto, M., Smith, T., 2015. Additional postcranial elements of *Teilhardina belgica*: The oldest European primate. Am. J. Phys. Anthropol. 156, 388–406.
Gelman, A., Rubin, D.B., 1992. Inference from iterative simulation using multiple sequences. Stat. Sci. 7, 457–511.
Gladman, J.T., Boyer, D.M., Simons, E.L., Seiffert, E.R., 2013. A calcaneus attributable to the primitive late Eocene anthropoid *Proteopithecus sylviae*: Phenetic affinities and phylogenetic implications. Am. J. Phys. Anthropol. 151, 372–397.
Godinot, M., 1991. Toward the locomotion of two contemporaneous *Adapis* species. Z. Morphol. Anthropol. 78, 387–405.
Godinot, M., 1998. A summary of adapiform systematics and phylogeny. Folia Primatol. 69, 218–249.
Godinot, M., 2007. Primate origins: A reappraisal of historical data favoring tupaiid affinities. In: Ravosa, M.J., Dagosto, M. (Eds.), Primate Origins: Adaptations and Evolution. Springer, New York, pp. 83–142.
Godinot, M., Dagosto, M., 1983. The astragalus of *Necrolemur* (Primates, Microchoerinae). J. Paleontol. 57, 1321–1324.
Godinot, M., Beard, K.C., 1991. Fossil primate hands: A review and an evolutionary inquiry emphasizing early forms. Hum. Evol. 6, 307–354.
Granatosky, M.C., Toussaint, S.L.D., Young, M.W., Panyutina, A., Youlatos, D., 2022. The northern treeshrew (Scandentia: Tupaiidae: *Tupaia belangeri*) in the context of primate locomotor evolution: A comprehensive analysis of gait, positional, and grasping behavior. J. Exp. Zool. A. 337, 645–665.
Gregory, W.K., 1920. On the structure and relations of *Notharctus*, an American Eocene primate. Mem. Am. Mus. Nat. Hist. 3, 49–243.
Gunnell, G.F., Miller, E.R., 2001. Origin of Anthropoidea: Dental evidence and recognition of early anthropoids in the fossil record, with comments on the Asian anthropoid radiation. Am. J. Phys. Anthropol. 114, 177–191.
Gunnell, G.F., Ciochcon, R.L., 2008. Revisiting primate postcrania from the Pondaung Formation of Myanmar: The purported anthropoid astragalus. In: Fleagle, J.G., Gilbert, C.C. (Eds.), Elwyn Simons: A Search for Origins. Springer, New York, pp. 211–228.
Gunnell, G.F., Rose, K.D., Rasmussen, D.T., 2008. Euprimates. In: Janis, C.M., Gunnell, G.F., Uhen, M.D. (Eds.), Evolution of Tertiary Mammals of North America, vol. 2. Cambridge University Press, Cambridge, pp. 239–261.
Gunz, P., Mitteroecker, P., 2013. Semilandmarks: A method for quantifying curves and surfaces. Hystrix 24, 103–109.
Gunz, P., Mitteroecker, P., Bookstein, F.L., 2005. Semilandmarks in three dimensions. In: Slice, E.D. (Ed.), Modern Morphometrics in Physical Anthropology. Kluwer Academic/Plenum Publishers, New York, pp. 73–98.
Hall-Craggs, E.C.B., 1965. An osteometric study of the hind limb of the Galagidae. J. Anat. Lond. 99, 119–126.
Hammer, Ø., Harper, D.A., 2024. Paleontological Data Analysis. John Wiley & Sons, Chichester.
Hamrick, M.W., 2001. Primate origins: Evolutionary change in digital ray patterning and segmentation. J. Hum. Evol. 40, 339–351.
Hoffstetter, R., 1977. Phylogénie des Primates. Confrontation des résultats obtenus par les diverses voies d'approche du problème. Bull. Mem. Soc. Anthropol. Paris 13, 327–346.
Hunt, K.D., Cant, J.H.C., Gebo, D.L., Rose, M.D., Walker, S.E., Youlatos, D., 1996. Standardized descriptions of primate locomotor and postural modes. Primates 37, 363–387.
Jaeger, J.J., Sein, C., Gebo, D.L., Chaimanee, Y., Nyein, M.T., Oo, T.Z., Aung, M.M., Suraprasit, K., Rugbumrung, M., Lazzari, V., Soe, A.N., 2020. Amphipithecine primates are stem anthropoids: Cranial and postcranial evidence. Proc. R. Soc. B 287, 20202129.

Kay, R.F., Ross, C., Williams, B.A., 1997. Anthropoid origins. Science 275, 797–804.
Kay, R.F., Schmitt, D., Vinyard, C.J., Perry, J.M., Shigehara, N., Takai, M., Egi, N., 2004. The paleobiology of Amphipithecidae, south Asian late Eocene primates. J. Hum. Evol. 46, 3–25.
Kemp, A.D., 2024a. Effects of binocular cue availability on leaping performance in *Cheirogaleus medius*: Implications for primate origins. J. Exp. Biol. 227, jeb245434.
Kemp, A.D., 2024b. Effect of binocular visual cue availability on fruit and insect grasping performance in two cheirogaleids: Implications for primate origins hypotheses. J. Hum. Evol. 188, 103456.
Kirk, E.C., Lemelin, P., Hamrick, M.W., Boyer, D.M., Bloch, J.I., 2008. Intrinsic hand proportions of euarchontans and other mammals: Implications for the locomotor behavior of plesiadapiforms. J. Hum. Evol. 55, 278–299.
Konishi, S., Kitagawa, G., 1996. Generalised information criteria in model selection. Biometrika 83, 875–890.
Kuhn, M., Johnson, K., 2013. Over-fitting and model tuning. In: Kuhn, M., Johnson, K. (Eds.), Applied Predictive Modeling. Springer, New York, pp. 61–92.
Lauder, G.V., 1986. Homology, analogy, and the evolution of behavior. In: Nitecki, M., Kitchell, J. (Eds.), The Evolution of Behavior. Oxford University Press, Oxford, pp. 9–40.
Lebrun, R., Orliac, M.J., 2016. MorphoMuseuM: An online platform for publication and storage of virtual specimens. Paleontol. Soc. Pap. 22, 183–195.
Llera Martín, C.J., Rose, K.D., Sylvester, A.D., 2022. A morphometric analysis of early Eocene Euprimate tarsals from Gujarat, India. J. Hum. Evol. 164, 103141.
López-Torres, S., Selig, K.R., Prufrock, K.A., Lin, D., Silcox, M.T., 2017. Dental topographic analysis of paromomyid (Plesiadapiformes, Primates) cheek teeth: More than 15 million years of changing surfaces and shifting ecologies. Hist. Biol. 30, 76–88.
Marigó, J., Roig, I., Seiffert, E.R., Moyà-Solà, S., Boyer, D.M., 2016. Astragalar and calcaneal morphology of the middle Eocene primate *Anchomomys frontanyensis* (Anchomomyini): Implications for early primate evolution. J. Hum. Evol. 91, 122–143.
Marigó, J., Verrière, N., Godinot, M., 2019. Systematic and locomotor diversification of the *Adapis* group (Primates, Adapiformes) in the late Eocene of the Quercy (Southwest France), revealed by humeral remains. J. Hum. Evol. 126, 71–90.
Marigó, J., Minwer-Barakat, R., Moyà-Solà, S., Boyer, D.M., 2020. First navicular remains of a European adapiform (*Anchomomys frontanyensis*) from the Middle Eocene of the Eastern Pyrenees (Catalonia, Spain): Implications for early primate locomotor behavior and navicular evolution. J. Hum. Evol. 139, 102708.
Marivaux, L., Chaimanee, Y., Ducrocq, S., Marandat, B., Sudre, J., Soe, A.N., Tun, S.T., Htoon, W., Jaeger, J.J., 2003. The anthropoid status of a primate from the late middle Eocene Pondaung Formation (Central Myanmar): Tarsal evidence. Proc. Natl. Acad. Sci. U.S.A. 100, 13173–13178.
Marivaux, L., Beard, K.C., Chaimanee, Y., Dagosto, M., Gebo, D.L., Guy, F., Marandat, B., Khaing, K., Kyaw, A.A., Oo, M., Sein, C., Soe, A.N., Swe, M., Jaeger, J.-J., 2010. Talar morphology, phylogenetic affinities, and locomotor adaptation of a large-bodied amphipithecid primate from the late middle Eocene of Myanmar. Am. J. Phys. Anthropol. 143, 208–222.
Marivaux, L., Tabuce, R., Lebrun, R., Ravel, A., Adaci, M., Mahboubi, M., Bensalah, M., 2011. Talar morphology of azibiids, strepsirhine-related primates from the Eocene of Algeria: Phylogenetic affinities and locomotor adaptation. J. Hum. Evol. 61, 447–457.
Marivaux, L., Ramdarshan, A., Essid, E.M., Marzougui, W., Ammar, H.K., Lebrun, R., Marandat, B., Merzeraud, G., Tabuce, R., Vianey-Liaud, M., 2013. *Djebelemur*, a tiny pre-tooth-combed primate from the Eocene of Tunisia: A glimpse into the origin of crown strepsirhines. PLoS One 8, e80778.
Marivaux, L., Lebrun, R., Tabuce, R., 2018. 3D models related to the publication: *Djebelemur*, a tiny pre-tooth-combed primate from the Eocene of Tunisia: A glimpse into the origin of crown strepsirhines. MorphoMuseum 4, e77.
Miller, E.R., Gunnell, G.F., Martin, R.D., 2005. Deep time and the search for anthropoid origins. Am. J. Phys. Anthropol. 128, 60–95.
Monclús-Gonzalo, O., Alba, D.M., Duhamel, A., Fabre, A.-C., Marigó, J., 2023. Early euprimates already had a diverse locomotor repertoire: Evidence from ankle bone morphology. J. Hum. Evol. 181, 103395.
Monclús-Gonzalo, O., Pal, S., Püschel, T.A., Urciuoli, A., Vinuesa, V., Robles, J.M., Almécija, S., Alba, D.M., 2025. A dryopithecine talus from the Late Miocene of the Vallès-Penedès Basin (NE Iberian Peninsula): Morphometric affinities and evolutionary implications for hominoid locomotion. Am. J. Phys. Anthropol. 186, e70043.
Morse, P.E., Chester, S.G., Boyer, D.M., Smith, T., Smith, R., Gigase, P., Bloch, J.I., 2019. New fossils, systematics, and biogeography of the oldest known crown primate *Teilhardina* from the earliest Eocene of Asia, Europe, and North America. J. Hum. Evol. 128, 103–131.
Morton, D.J., 1924. Evolution of the human foot II. Am. J. Phys. Anthropol. 7, 1–52.
Moyà-Solà, S., Köhler, M., Alba, D.M., Roig, I., 2012. Calcaneal proportions in primates and locomotor inferences in *Anchomomys* and other Palaeogene Euprimates. Swiss J. Palaeontol. 131, 147–159.
Ni, X., Gebo, D.L., Dagosto, M., Meng, J., Tafforeau, P., Flynn, J.J., Beard, K.C., 2013. The oldest known primate skeleton and early haplorhine evolution. Nature 498, 60–64.
Ni, X., Li, Q., Li, L., Beard, K.C., 2016. Oligocene primates from China reveal divergence between African and Asian primate evolution. Science 352, 673–677.
Orme, D., Freckleton, R., Thomas, G., Petzoldt, T., Fritz, S., Isaac, N., Pearse, W., 2023. caper: Comparative Analyses of Phylogenetics and Evolution in R. R package version 1.0.3. https://CRAN.R-project.org/package=caper.
Oxnard, C.E., Crompton, R.H., Lieberman, S.S., 1990. Animal Lifestyles and Anatomies. University of Washington Press, Seattle.
Pagel, M., 1999. Inferring the historical patterns of biological evolution. Nature 401, 877–884.
Parr, W.C.H., Soligo, C., Smaers, J., Chatterjee, H.J., Ruto, A., Cornish, L., Wroe, S., 2014. Three-dimensional shape variation of talar surface morphology in hominoid primates. J. Anat. 225, 42–59.
Pina, M., Salesa, M.J., Antón, M., 2011. Functional anatomy of the calcaneum and talus in Cercopithecinae (Mammalia, Primates, Cercopithecidae). Estud. Geol. 67, 385–394.
Plummer, M., Best, N., Cowles, K., Vines, K., 2005. CODA: Convergence diagnosis and output analysis for MCMC. R News 6, 7–11.
Polly, P.D., Lawing, A.M., Fabre, A.C., Goswami, A., 2013. Phylogenetic principal components analysis and geometric morphometrics. Hystrix 24, 33–41.
Preuschoft, H., Witte, H., Christian, A., Fischer, M., 1996. Size influences on primate locomotion and body shape, with special emphasis on the locomotion of 'small mammals'. Folia Primatol. 66, 93–112.
Preuschoft, H., Günther, M.M., Christian, A., 1998. Size dependence in prosimian locomotion and its implications for the distribution of body mass. Folia Primatol. 69, 60–81.
Prufrock, K.A., López-Torres, S., Silcox, M.T., Boyer, D.M., 2016. Surfaces and spaces: Troubleshooting the study of dietary niche space overlap between North American stem primates and rodents. Surf. Topogr. 4, 024005.
Püschel, T.A., Gladman, J.T., Bobe, R., Sellers, W.I., 2017. The evolution of the platyrrhine talus: A comparative analysis of the phenetic affinities of the Miocene platyrrhines with their modern relatives. J. Hum. Evol. 111, 179–201.
Püschel, T.A., Marcé-Nogué, J., Gladman, J.T., Bobe, R., Sellers, W.I., 2018. Inferring locomotor behaviours in Miocene New World monkeys using finite element analysis, geometric morphometrics and machine-learning classification techniques applied to talar morphology. J. R. Soc. Interface 15, 20180520.
Püschel, T.A., Marcé-Nogué, J., Gladman, J., Patel, B.A., Almécija, S., Sellers, W.I., 2020. Getting its feet on the ground: Elucidating *Paralouatta*'s semi-terrestriality using the virtual morpho-functional toolbox. Front. Earth Sci. 8, 79.
R Core Team, 2023. R: A language and environment for statistical computing. R Foundation for Statistical Computing, Vienna.
Rasmussen, D.T., 1990. Primate origins: Lessons from a neotropical marsupial. Am. J. Primatol. 22, 263–277.
Raventós-Izard, G., Monclús-Gonzalo, O., Moyà-Solà, S., Alba, D.M., Arias-Martorell, J., 2025. Ulnar morphology of *Pliobates cataloniae* (Pliopithecoidea: Crouzeliidae): Insights into catarrhine locomotor diversity and forelimb evolution. J. Hum. Evol. 202, 103663.
Revell, L.J., 2009. Size-correction and principal components for interspecific comparative studies. Evolution 63, 3258–3268.
Revell, L.J., 2012. phytools: An R package for phylogenetic comparative biology (and other things). Methods Ecol. Evol. 3, 217–223.
Rohlf, F.J., Slice, D., 1990. Extensions of the Procrustes method for the optimal superimposition of landmarks. Syst. Zool. 39, 40–59.
Rohlf, F.J., Corti, M., 2000. Use of two-block partial least-squares to study covariation in shape. Syst. Biol. 49, 740–753.
Rose, K.D., 1994. The earliest primates. Evol. Anthropol. 3, 159–173.
Rose, K.D., Walker, A., 1985. The skeleton of early Eocene *Cantius*, oldest lemuriform primate. Am. J. Phys. Anthropol. 66, 73–89.
Rose, K.D., Rana, R.S., Sahni, A., Kumar, K., Missiaen, P., Singh, L., Smith, T., 2009. Early Eocene primates from Gujarat, India. J. Hum. Evol. 56, 366–404.
Rose, K.D., Chester, S.G., Dunn, R.H., Boyer, D.M., Bloch, J.I., 2011. New fossils of the oldest North American euprimate *Teilhardina brandti* (Omomyidae) from the Paleocene–Eocene thermal maximum. Am. J. Phys. Anthropol. 146, 281–305.
Rosenberger, A.L., Preuschoft, H., 2012. Evolutionary morphology, cranial biomechanics and the origins of tarsiers and anthropoids. Paleobiodivers. Paleoenviron. 92, 507–525.
Sargis, E.J., 2001. The grasping behaviour, locomotion and substrate use of the tree shrews *Tupaia minor* and *T. tana* (Mammalia, Scandentia). J. Zool. Lond. 253, 485–490.
Sargis, E.J., 2002a. Functional morphology of the hindlimb of tupaiids (Mammalia, Scandentia) and its phylogenetic implications. J. Morphol. 254, 149–185.
Sargis, E.J., 2002b. The postcranial morphology of *Ptilocercus lowii* (Scandentia, Tupaiidae): An analysis of primatomorphan and volitantian characters. J. Mammal. Evol. 9, 137–160.
Sargis, E.J., Boyer, D.M., Bloch, J.I., Silcox, M.T., 2007. Evolution of pedal grasping in Primates. J. Hum. Evol. 53, 103–107.
Sarmiento, E.E., 1983. The significance of the heel process in anthropoids. Int. J. Primatol. 4, 127–152.
Savage, D.E., Waters, B.T., 1978. A new omomyid primate from the Wasatch Formation of southern Wyoming. Folia Primatol. 30, 1–29.
Schlager, S., 2017. Morpho and Rvcg-shape analysis in R. In: Zheng, G., Li, S., Szekely, G. (Eds.), Statistical Shape and Deformation Analysis: Methods, Implementation and Applications. Academic Press, London, pp. 217–256.
Schmitt, D., 1996. Humeral head shape as an indicator of locomotor behavior in extant strepsirhines and Eocene adapids. Folia Primatol. 67, 137–151.
Seiffert, E.R., Simons, E.L., 2001. Astragalar morphology of late Eocene anthropoids from the Fayum Depression (Egypt) and the origin of catarrhine primates. J. Hum. Evol. 41, 577–606.
Seiffert, E.R., Simons, E.L., Fleagle, J.G., 2000. Anthropoid humeri from the late Eocene of Egypt. Proc. Natl. Acad. Sci. U.S.A. 97, 10062–10067.

Seiffert, E.R., Simons, E.L., Simons, C.V., 2004. Phylogenetic, biogeographic, and adaptive implications of new fossil evidence bearing on crown anthropoid origins and early stem catarrhine evolution. In: Ross, C.F., Kay, R.F. (Eds.), Anthropoid Origins: New visions. Kluwer Academic, New York, pp. 157–181.
Seiffert, E.R., Simons, E.L., Clyde, W.C., Rossie, J.B., Attia, Y., Bown, T.M., Chatrath, P., Mathison, M.E., 2005. Basal anthropoids from Egypt and the antiquity of Africa's higher primate radiation. Science 310, 300–304.
Seiffert, E.R., Costeur, L., Boyer, D.M., 2015. Primate tarsal bones from Egerkingen, Switzerland, attributable to the middle Eocene adapiform *Caenopithecus lemuroides*. PeerJ 3, e1036.
Sigé, B., Jaeger, J.-J., Sudre, J., Vianey-Liaud, M., 1990. *Altiatlasius koulchii* n. gen. et sp., primate Omomyidé du Paléocène supérieur du Maroc, et les origines des euprimates. Palaeontographica A 214, 31–56.
Silcox, M.T., López-Torres, S., 2017. Major questions in the study of primate origins. Annu. Rev. Earth Planet Sci. 45, 113–137.
Silcox, M.T., Boyer, D.M., Bloch, J.I., Sargis, E.J., 2007. Revisiting the adaptive origins of primates (again). J. Hum. Evol. 53, 321–324.
Silcox, M.T., Sargis, E.J., Bloch, J.I., Boyer, D.M., 2015. Primate origins and supraordinal relationships: Morphological evidence. In: Henke, W., Tatterstall, I. (Eds.), Handbook of Paleoanthropology, 2nd ed. Springer, Heidelberg, pp. 1053–1081.
Silcox, M.T., Bloch, J.I., Boyer, D.M., Chester, S.G.B., López-Torres, S., 2017. The evolutionary radiation of plesiadapiforms. Evol. Anthropol. 26, 74–94.
Simons, E.L., Seiffert, E.R., 1999. A partial skeleton of *Proteopithecus sylviae* (Primates, Anthropoidea): First associated dental and postcranial remains of an Eocene anthropoidean. C. R. Acad. Sci. Paris 329, 921–927.
Smith, T., Rose, K.D., Gingerich, P.D., 2006. Rapid Asia–Europe–North America geographic dispersal of earliest Eocene primate *Teilhardina* during the Paleocene–Eocene thermal maximum. Proc. Natl. Acad. Sci. U.S.A. 103, 11223–11227.
Sokal, R., Rohlf, F., 1995. Biometry: The Principles and Practice of Statistics in Biological Research, 3rd ed. Freeman, New York.
Strasser, E., 1988. Pedal evidence for the origin and diversification of cercopithecid clades. J. Hum. Evol. 17, 225–245.
Su, A., Zeiniger, A., 2022. The primate ankle and hindfoot. In: Zeiniger, A., Hatala, K. G., Wunderlich, R.E., Schmitt, D. (Eds.), The Evolution of the Primate Foot. Anatomy, Function, and Palaeontological Evidence. Springer, Cham, pp. 21–45.
Sussman, R.W., 1991. Primate origins and the evolution of angiosperms. Am. J. Primatol. 23, 209–223.
Sussman, R.W., Raven, P.H., 1978. Pollination by lemurs and marsupials: An archaic coevolutionary system. Science 200, 731–736.
Sussman, R.W., Rasmussen, D.T., Raven, P.H., 2012. Rethinking primate origins again. Am. J. Primatol. 75, 95–106.
Szalay, F.S., 1976. Systematics of the Omomyidae (Tarsiiformes, Primates): Taxonomy, phylogeny, and adaptations. Bull. Am. Mus. Nat. Hist. 156, 157–450.
Szalay, F.S., Decker, R.L., 1974. Origins, evolution, and function of the tarsus in late Cretaceous Eutheria and Paleocene primates. In: Jenkins, F.A. (Ed.), Primate Locomotion. Academic Press, New York, pp. 223–259.
Szalay, F.S., Delson, E., 1979. Evolutionary History of the Primates. Academic Press, New York.
Szalay, F.S., Dagosto, F.S., 1980. Locomotor adaptations as reflected on the humerus of Paleogene primates. Folia Primatol. 34, 1–45.
Szalay, F.S., Drawhorn, G., 1980. Evolution and diversification of the Archonta in an arboreal milieu. In: Luckett, W.P. (Ed.), Comparative Biology and Evolutionary Relationships of Tree Shrews. Plenum Press, New York, pp. 133–169.
Szalay, F.S., Rosenberger, A.L., Dagosto, M., 1987. Diagnosis and differentiation of the Order Primates. Yearb. Phys. Anthropol. 30, 75–105.
Torres-Tamayo, N., Schlager, S., García-Martínez, D., Sanchis-Gimeno, J.A., Nalla, S., Ogihara, N., Oishi, M., Martelli, S., Bastir, M., 2020. Three-dimensional geometric morphometrics of thorax-pelvis covariation and its potential for predicting the thorax morphology: A case study on Kebara 2 Neandertal. J. Hum. Evol. 147, 102854.
Van Valen, L., Sloan, R.E., 1965. The earliest primates. Science 150, 743–745.
Vinyard, C.J., Wall, C.E., Williams, S.H., Hylander, W.L., 2003. Comparative functional analysis of skull morphology of tree-gouging primates. Am. J. Phys. Anthropol. 120, 153–170.
Walker, A., 1974. Locomotor adaptations in past and present prosimian primates. In: Jenkins, F.A. (Ed.), Primate Locomotion. Academic Press, New York, pp. 349–381.
Wiley, D., 2006. Landmark Editor 3.0. Institute for Data Analysis and Visualization. University of California, Davis.
Willmott, C.J., Matsuura, K., 2005. Advantages of the mean absolute error (MAE) over the root mean square error (RMSE) in assessing average model performance. Clim. Res. 30, 79–82.
Wilson Mantilla, G.P., Chester, S.G., Clemens, W.A., Moore, J.R., Sprain, C.J., Hovatter, B.T., Mitchell, W.S., Mans, W.W., Mundil, R., Renne, P.R., 2021. Earliest Palaeocene purgatoriids and the initial radiation of stem primates. R. Soc. Open Sci. 8, 210050.
Wold, S., Sjöström, M., Eriksson, L., 2001. PLS-regression: A basic tool of chemometrics. Chemometr. Intell. Lab. Syst. 58, 109–130.
Yapuncich, G.S., Granatosky, M.C., 2021. Footloose: Articular surface morphology and joint movement potential in the ankles of lorisids and cheirogaleids. Am. J. Phys. Anthropol. 175, 876–894.
Yapuncich, G.S., Seiffert, E.R., Boyer, D.M., 2017. Quantification of the position and depth of the flexor hallucis longus groove in euarchontans, with implications for the evolution of primate positional behavior. Am. J. Phys. Anthropol. 163, 367–406.
Yapuncich, G.S., Feng, H.F., Dunn, R.H., Seiffert, E.R., Boyer, D.M., 2019. Vertical support use and primate origins. Sci. Rep. 9, 12341.
Yapuncich, G.S., Chester, S.G.B., Bloch, J.I., Boyer, D.M., 2022. The feet of Paleogene primates. In: Zeiniger, A., Hatala, K.G., Wunderlich, R.E., Schmitt, D. (Eds.), The Evolution of the Primate Foot. Anatomy, Function, and Palaeontological Evidence. Springer, Cham, pp. 277–319.
Youlatos, D., 1999. Comparative locomotion of six sympatric primates in Ecuador. Ann. Sci. Nat. 20, 161–168.
Youlatos, D., Meldrum, J., 2011. Locomotor diversification in New World monkeys: Running, climbing, or clawing along evolutionary branches. Anat. Rec. 294, 1991–2012.
Youlatos, D., Karantanis, N.E., Panyutina, A., 2017. Pedal grasping in the northern smooth-tailed treeshrew *Dendrogale murina* (Tupaiidae, Scandentia): Insights for euarchontan pedal evolution. Mammalia 81, 61–70.
Youlatos, D., Widayati, K.A., Tsuji, Y., 2018. Foot postures and grasping of free-ranging Sunda colugos (*Galeopterus variegatus*) in West Java, Indonesia. Mamm. Biol. 95, 164–172.
Zelditch, M.L., Swiderski, D.L., Sheets, H.D., 2012. Geometric Morphometrics for Biologists. A Primer, 2nd ed. Academic Press, Amsterdam.